Origem e evolução dinâmica de algumas populações de pequenos corpos ressonantes no Sistema Solar

Fernando Virgilio Roig

Tese de Doutorado

submetida ao

Departamento de Astronomia

Instituto de Astronomia, Geofísica e Ciêcnias Atmosféricas

Universidade de São Paulo

Orientador: Sylvio Ferraz Mello

São Paulo, Outubro 2001

A mis padres,
Virgilio y Josefina,
por haberme regalado
um pasado maravilloso,
y a Mónica,
por ofrecerme la alegria
de un futuro juntos.

Resumo

Nesta tese estudamos algumas regiões de aparente estabilidade no cinturão de asteróides e no cinturão de Kuiper, analisando a evolução dinâmica dos objetos nessas regiões por intervalos de tempo muito longos, em geral, da ordem da idade do Sistema Solar. Centramos principalmente nossa atenção no estudo das populações de pequenos corpos ressonantes, analisando três exemplos diferentes: a ressonância 2/1 com Júpiter e seu entorno (falha de Hecuba), a ressonância 2/3 com Netuno (Plutinos), e a ressonância 1/1 com Júpiter (Troianos). Atacamos o problema com diferentes ferramentas numéricas e analíticas: integração numérica direta de modelos precisos, modelos estatísticos de caminhada aleatória, modelos semi-analíticos baseados no desenvolvimento assimétrico da função perturbadora, cálculo de expoentes de Lyapunov, análise de freqüências, determinação de elementos próprios e taxas de difusão, etc. Os resultados obtidos permitem elaborar conclusões sobre a possível origem e evolução dinâmica destas populações.

Abstract

In this thesis, we study some regions of regular motion in the asteroid main belt and in the Kuiper belt. We analyze the dynamical evolution in these regions over time scales of the order of the age of the Solar System. We centered our study on the populations of resonant minor bodies, discussing three examples: the 2/1 mean motion resonance with Jupiter (Hecuba gap), the 2/3 resonance with Neptune (Plutinos), and the 1/1 resonance with Jupiter (Trojans). We attack the problem with several different tools, both analytic and numeric: integration of N body models, random-walk statistical models, semi-analytical models based on the assymetric expansion of the disturbing function, calculation of the maximum Lyapunov exponent, frequancy analysis, estimates of the diffusion of proper elements, etc. The results allow to draw conclusions about the possible origin of these populations.

Prólogo

Uno se despide, insensiblemente, de pequeñas cosas,
lo mismo que un árbol que en tiempos de otoño muere por sus hojas.
Al fin, la tristeza es la muerte lenta de las simples cosas,
esas cosas simples que quedan doliendo en el corazón.

Uno vuelve siempre a los viejos sitios en que amó la vida,
y entonces comprende cómo están de ausentes las cosas queridas.
Por eso, muchacho, no partas ahora soñando el regreso,
que el amor es simple y a las cosas simples las devora el tiempo...

César Isella

Esta tese contém os resultados da maioria das pesquisas nas quais estive envolvido ao longo do meu doutoramento. Ela deve ser lida levando em consideração que em muitas destas pesquisas, particularmente as apresentadas nos Capítulos 3 e 4, eu participei apenas como colaborador, e o mérito das mesmas deve ser atribuído não a mim mas aos meus colegas de trabalho: D. Nesvorný, C. Beaugé e Tatiana Michtchenko. No entanto, foi através destas colaborações que eu adquiri a experiência necessária para desenvolver o trabalho de tese proposto originariamente pelo meu orientador. Este

trabalho e seus resultados estão refletidos no Capítulo 2 e, do meu ponto de vista, este capítulo constitui a parte mais relevante da minha tese.

Ao longo de todos estes anos de doutorado, foram muitas as pessoas com as quais fiz amizade, tanto no âmbito profissional quanto pessoal. Seria impossível mencionar todas elas aqui, mas queria, particularmente, expressar minha profunda gratidão às seguintes pessoas e instituições:

A Sylvio Ferraz Mello, não só pela excelente orientação (por default) mas também pela amizade e confiança que me brindou ao longo de todos estes anos.

A David Nesvorný e Cristian Beaugé, que tiveram um papel decisivo no desenvolvimento do meu doutorado, por compartilhar comigo seu conhecimento e sua grande amizade.

A Tatiana Michtchenko, por me oferecer a possibilidade de colaborar com ela, e por ser um exemplo permanente de que "não basta fazer bem, tem que fazer logo".

A Marilia Sartori e Braulo Vitorino, meus colegas de sala durante quase 6 anos, por fazer com que todo dia me sentisse entre verdadeiros amigos.

A Bruno Castilho, Adriano Cerqueira, Jaqueline Vasconcelos, Nelson Callegari, Julio Camargo, Dimitri Gadotti, Marcelo e Dinah Allen, Cristiano Da Rocha, Hector e Amelia Cuevas, Eduardo Cypriano e Lys, Rodrigo Carrasco, Fernando Cachucho, Julio Klafke, Mauro Guimarães e tantos outros amigos e colegas de trabalho que tive a grande sorte de conhecer no IAG.

A Alejandro Dimarco, Gerardo e Paula Goya, Alessandro Simula e Giovanna, Diana Markovsky, Alberto Salcedo, Juan Pablo Neirotti, Horacio e Emilio Moreno, Pedro e Pablo Rodríguez, e todos os muitos amigos que sempre estiveram perto ainda quando estavam longe.

Ao Instituto de Astronomia, Geofísica e Ciências Atmosféricas (IAG) e seus funcionários, por me oferecer condições de trabalho excepcionais para desenvolver minha pesquisa

À Fundação de Amparo a Pesquisa do Estado de São Paulo (FAPESP), que ao longo do doutorado providenciou meu sustento mensal e facilitou a adquisição de material de trabalho e a participação em inúmeras reuniões científicas, através do Processo 97/05806-9.

A Bill Bottke, Hal Levison, e o pessoal do Southwest Research Institute em Boulder,

Colorado, por me hospedar como pesquisador visitante durante os últimos meses do doutorado, fato que contribuiu significativamente para a finalização da tese.

A la familia Vermes, por adoptarme como un miembro más de la misma.

A mi familia, y especialmente a mis padres, por todo el cariño, el apoyo y la comprensión que me brindaron siempre.

A Mónica, por compartir su vida conmigo y por quererme tal como soy.

Conteúdo

1. Introdução

A dinâmica dos pequenos corpos no Sistema Solar apresenta movimentos com graus variáveis de caoticidade. Desde começos dos anos 80, um grande esforço tem sido feito, através de diferentes tipos de pesquisas, para tentar desvendar os mecanismos responsáveis pela caoticidade naqueles casos em que os fenômenos estocásticos são notórios, particularmente no âmbito da dinâmica ressonante. A grande motivação inicial para estes estudos foi o bem conhecido fato de que a distribuição dos objetos do cinturão asteroidal está intimamente vinculada à existência de ressonâncias de movimentos médios entre estes e Júpiter. Mas, a partir da década de 90, com o descobrimento dos primeiros objetos trans-Netunianos, ficou claro que o papel das ressonâncias de movimentos médios na dinâmica dos pequenos corpos no Sistema Solar ultrapassa os limites do cinturão asteroidal e se estende a outras populações como os objetos próximos da Terra (NEOs) e os objetos do cinturão de Kuiper (KBOs). Nesta tese apresentamos resultados sobre a dinâmica e origem de três diferentes grupos de pequenos corpos em ressonâncias de movimentos médios: (i) os Zhongguos, na ressonância 2/1 com Júpiter, (ii) os Plutinos, na ressonância 2/3 com Netuno, e (iii) os Troianos, na ressonância 1/1 com Júpiter.

O primeiro grupo, os Zhongguos, resulta particularmente interessante, já que ele se localiza numa região considerada tradicionalmente como sendo uma falha na distribuição dos objetos no cinturão de asteróides: a falha de Hecuba (Kirkwood 1867). As pesquisas realizadas após o trabalho pioneiro de Wisdom (1982), mostraram que

no cinturão principal ($a < 3.2$ UA), as falhas associadas às ressonâncias 7/3, 5/2, 3/1, 4/1 etc. com Júpiter, são conseqüência da evolução caótica das órbitas no espaço de fase ressonante (Šidlichovský e Melendo 1986; Wisdom 1987; Ferraz-Mello e Klafke 1991; Klafke, Ferraz-Mello e Michtchenko 1992; Moons e Morbidelli 1995). Esta caoticidade já é observada no âmbito do problema restrito de três corpos, e se traduz na aparição de uma série de intermitências na excentricidade dos asteróides, que poderiam eventualmente cruzar as órbitas de Marte ou da Terra, sendo então removidos das ressonâncias pelos encontros próximos com estes planetas. No entanto, no cinturão extreno ($a > 3.3$ UA), o mecanismo dinâmico de depleção é muito mais complexo, envolvendo um número maior de graus de liberdade (Holman e Murray 1996; Murray e Holman 1997). Além disso, as duas principais ressonâncias de movimentos médios com Júpiter não se encontram associadas a falhas, mas a grupos de asteróides (o grupo de Hilda na ressonância 3/2 e o asteróide Thule na ressonância 4/3). Isto significa que, ao contrario do que acontece no cinturão principal, o comportamento ressonante no cinturão externo não pode ser explicado através de um único mecanismo dinâmico.

A falha de Hecuba, centrada em $a = 3.27$ UA e vinculada à ressonância 2/1, ocorre na região de transição entre o cinturão principal e o externo. Recentemente, diversos estudos mostraram que a dinâmica no espaço de fases da ressonância 2/1 está fortemente dominada por uma teia interna de ressonâncias seculares, secundárias, e de três corpos (envolvendo simultaneamente Júpiter e Saturno). Em alguns casos, a superposição de várias destas ressonâncias origina uma forte caoticidade em certas regiões do espaço de fases (Morbidelli e Moons 1993; Michtchenko e Ferraz-Mello 1995, 1996). Em outros casos, o caos é mais fraco, porém suficiente para causar a depleção do espaço de fases ressonante em intervalos de tempo menores do que a idade do Sistema Solar (Michtchenko e Ferraz-Mello 1997; Nesvorný e Ferraz-Mello 1997b; Ferraz-Mello, Michtchenko e Roig 1998). Estes resultados permitiriam então justificar a existência da falha de Hecuba. Mas com os recentes avanços nas técnicas observacionais, foi possível descobrir que a ressonância 2/1 não está totalmente vazia e que atualmente existem mais de 60 asteróides ressonantes com órbitas bem determinadas. Quase a metade deles possui órbitas muito regulares (ver Morbidelli 1996), podendo sobreviver na ressonância por intervalos de tempo maiores do que a idade do Sistema Solar. Estes constituem o grupo de Zhongguo, chamado assim a partir do seu membro mais importante, o

asteróide 3789 Zhongguo. Como conseqüência disto, surgem duas perguntas: (i) como estes asteróides conseguiriam sobreviver à estocasticidade global do espaço de fases?, e (ii) qual seria a sua origem? O primeiro objetivo desta tese é achar uma resposta plausível para estas perguntas.

O segundo grupo mencionado no início deste capítulo, os Plutinos, suscita interesse por tratar-se do mais numeroso grupo de objetos trans-Netunianos em ressonância de movimentos médios. Centrada em $a = 39.45$ UA, a ressonância 2/3 com Netuno concentra de 15 a 20% da população total de cometas do cinturão de Kuiper, e é a única ressonância trans-Netuniana com uma população relevante de objetos (as ressonâncias 1/2 e 3/4 concentram apenas 2% do total de KBOs, respectivamente), entre os quais se encontra o próprio planeta Plutão: daí o nome de Plutinos.

Já na década de 80 foi reconhecido que o cinturão de Kuiper poderia constituir um reservatório dos chamados cometas da família de Júpiter (JFCs), isto é, cometas de curto período com inclinações particularmente baixas (Fernández 1980; Duncan, Quinn e Tremaine 1988). Mas foi só na decada seguinte, após o descobrimento do primeiro KBO (Jewitt e Luu 1993), que surgiram os primeiros trabalhos tentando explicar como isto aconteceria (Levison e Duncan 1993; Holman e Wisdom 1993; Duncan, Levison e Budd 1995). Atualmente, sabemos que as ressonâncias de movimentos médios cumprem um papel fundamental na transferência de material cometário do cinturão de Kuiper para o Sistema Solar interior e deveriamos esperar, portanto, que os Plutinos sejam um dos principais reservatórios de JFCs.

A dinâmica das ressonâncias trans-Netunianas, e particularmente sua estrutura interna, ainda não foi estudada com muito detalhe. Diferentemente do que acontece no cinturão asteroidal, existe pouca evidência observacional sobre a estrutura do cinturão de Kuiper, o que dificulta a interpretação de qualquer resultado sobre a dinâmica ressonante. Só no caso da ressonância 2/3 existem alguns trabalhos detalhados (Morbidelli, Thomas e Moons 1995; Malhotra 1996; Morbidelli 1997), que mostram que os Plutinos, localizados na região central da ressonância, seriam estáveis por tempos da ordem da idade do Sistema Solar, enquanto que o caos seria importante só nas bordas da ressonância. Ha também alguns trabalhos sobre a possível origem dos Plutinos (Malhotra 1995; Gomes 2000), normalmente atribuída à migração planetária (Fernández e Ip 1984). Mas por outro lado, quase não existem estudos sobre as demais ressonâncias

trans-Netunianas. Assim, um segundo objetivo desta tese é o de apresentar os resultados de uma pesquisa detalhada sobre a dinâmica destas ressonâncias. A ênfase é colocada especialmente nas ressonâncias 1/2, 2/3 e 3/4 com Netuno. Basicamente, tentamos explicar: (i) por que existem cometas na ressonância 2/3 ao passo que quase não há objetos nas 1/2 e 3/4; (ii) qual é a eficiência da ressonância 2/3 para transferir cometas para o Sistema Solar interior; e (iii) qual é o papel das perturbações gravitacionais de Plutão na dinâmica dos Plutinos.

O último grupo a ser estudado são os Troianos de Júpiter, na ressonância 1/1. Estes asteróides formam o maior grupo observado de objetos ressonantes no Sistema Solar, contabilizando atualmente mais de 600 membros. Sua existência é conhecida de longa data, e é explicada pela estabilidade dos pontos Lagrangeanos L_4 e L_5 de Júpiter. Existem muitos trabalhos, tanto analíticos quanto numéricos, sobre a evolução dinâmica e colisional, a origem e as características espectroscópicas destes objetos (ver referências em Beaugé e Roig 2001). Em termos gerais, todos estes trabalhos mostram que os Troianos possuem órbitas estáveis ao longo da idade do Sistema Solar, e que tratar-se-ia de uma população primordial de objetos, isto é, ou se formaram na ressonância ou foram capturados nela ainda nas etapas finais da formação do Sistema Solar (Levison, Shoemaker e Shoemaker 1997; Marzari e Scholl 1998). Os trabalhos também mostram que os Troianos sofreram uma evolução colisional ativa (Marzari et al. 1997) e, como resultado dessa evolução, deveríamos observar na atualidade as famílias de asteróides (Milani 1993).

Tanto a sua estabilidade a longo prazo quanto a eventual existência de famílias, fazem dos Troianos um verdadeiro "laboratório" para testar e colocar limites aos diferentes processos dinâmicos que podem ter acontecido ao longo da idade do Sistema Solar. Assim, um terceiro objetivo desta tese é: (i) apresentar os resultados relativos à construção de um modelo semi-analítico da dinâmica na ressonância 1/1, e o uso do mesmo para determinar elementos próprios e famílias; e (ii) analisar os efeitos da migração planetária (Gomes 1998) sobre a estabilidade dos Troianos reais.

Tanto os Zhongguos quanto os Plutinos e Troianos possuem uma característica em comum: trata-se de objetos cujas órbitas são estáveis ao longo da idade do Sistema Solar. Portanto, os estudos que apresentamos nesta tese estão orientados à descrição da dinâmica a longo prazo destas populações e das respectivas ressonâncias de movimentos

médios. Na maioria dos casos, o problema é tratado através da integração numérica direta das equações do problema de N corpos, incluindo as perturbações dos quatro planetas Jovianos, por intervalos de tempo da ordem da idade do Sistema Solar. Os resultados destas simulações são analisados utilizando diferentes ferramentas, que permitem quantificar o grau de caoticidade das trajetórias no espaço de fases. A principal delas é a determinação dos elementos próprios e o cálculo da sua variação temporal, o que usualmente é conhecido como difusão. Para levar adiante as simulações utilizamos, em quase todos os casos, o integrador simplético SWIFT (Levison e Duncan 1994), devidamente adaptado para estudar diferentes modelos de perturbações (ex., incluindo efeito Yarkovsky, migração planetária, etc.). Em alguns casos, as integrações numéricas são substituídas por modelos de caminhada aleatória ou por métodos perturbativos semi-analíticos baseados no desenvolvimento assimétrico da função perturbadora (Roig et al. 1998).

Os capítulos 2, 3 e 4 desta tese são dedicados, respectivamente, a cada uma das três populações referidas acima. Como a maioria dos resultados já se encontram publicados ou em vias de publicação, cada capítulo possui uma ou várias seções introdutórias seguida dos "preprints" ou "reprints" dos artigos, em anexo. Na introdução de cada capítulo é feita uma descrição geral dos objetivos da pesquisa e dos procedimentos utilizados, assim como uma discusão dos resultados obtidos, deixando os detalhes para serem consultados diretamente nos artigos. Finalmente, o capítulo 5 é dedicado às conclusões gerais e à discussão das perspectivas futuras.

2. A ressonância 2/1 com Júpiter

2.1. Introdução

A ressonância 2/1 ocorre numa região de aproximadamente 0.2 UA de largura, centrada em $a = 3.27$ UA. Historicamente, esta ressonância é associada a uma falha na distribuição dos asteróides: a falha de Hecuba. Nos últimos anos, surgiram várias pesquisas detalhadas sobre a origem desta falha (Ferraz-Mello 1994; Morbidelli 1996; Nesvorný e Ferraz-Mello 1997a, Ferraz-Mello, Michtchenko e Roig 1998), motivadas não só pela necessidade de explicar a ausência de asteróides na ressonância 2/1, como também a existência de um grupo de asteróides na ressonância 3/2 ($a = 3.96$ UA): o grupo de Hilda. A idéia por trás destas pesquisas é que, sendo as ressonâncias 2/1 e 3/2 ambas de primeira ordem, sua topologia é muito similar e, portanto, não haveria razão evidente para as mesmas estarem associadas a fenômenos observacionais tão diferentes.

A partir destas pesquisas, foi possível explicar a existência da falha de Hecuba e do grupo de Hilda sobre a base de que a difusão caótica é maior na ressonância 2/1 do que na 3/2 (Michtchenko e Ferraz-Mello 1995, 1996; Nesvorný e Ferraz-Mello 1997b; Ferraz-Mello et al. 1998; Roig e Ferraz-Mello 1999). A idéia é que o espaço de fases das duas ressonâncias é globalmente estocástico, no sentido de que qualquer condição inicial dentro das ressonâncias irá evoluir caoticamente. Porém, no caso da ressonância 3/2, esta estocasticidade é suficientemente fraca como para permitir que o grupo de Hilda possa sobreviver na ressonância por intervalos de tempo maiores do que a idade do Sistema Solar. Já no caso da ressonância 2/1, a estocasticidade é suficientemente

forte como para esvaziar a mesma em intervalos de tempo menores do que idade do Sistema Solar: daí a existência da falha.

No entanto, os recentes avanços nas técnicas observacionais levaram a descobrir vários asteróides ressonantes dentro da falha de Hecuba, formando uma população que atualmente conta com mais de 60 membros com órbitas bem conhecidas. Ainda que este número continue contrastando com os mais de 280 asteróides observados no grupo de Hilda, a presença desta população asteroidal na ressonância 2/1 não pode ser totalmente explicada com base nos mecanismos de difusão caótica conhecidos.

Neste capítulo, analisamos as características dinâmicas dos asteróides observados na ressonância 2/1, determinamos a estabilidade a longo prazo dos mesmos, e discutimos diferentes hipóteses sobre a sua origem, particularmente do ponto de vista dinâmico.

2.2. Asteróides observados na falha de Hecuba

Para identificar os asteróides observados atualmente na falha de Hecuba, analisamos o comportamento do ângulo ressonante, $\sigma_{2/1} = 2\lambda_{\rm J} - \lambda - \varpi$, de 2600 asteróides numerados e multi-oposicionais tirados do catálogo de elementos orbitais do Lowell Observatory, atualizado em abril de 2001. Achamos 421 objetos tais que $\sigma_{2/1}$ libra ou alterna entre libração e circulação. Estes objetos foram classificados da seguinte forma:

1. ressonantes: 61 asteróides para os quais $\sigma_{2/1}$ libra em torno de 0, com semi-amplitudes da ordem de 60° ou maiores. A maioria destes asteróides possui $0.2 < e < 0.4$. Só 1 possui diâmetro conhecido (1362 Griqua), da ordem de 30 km.

2. alternadores pericêntricos: 305 objetos para os quais $\sigma_{2/1}$ alterna entre libração em torno de 0 e circulação. Localizam-se nas excentricidades muito baixas, à esquerda da ressonância 2/1. Ainda, alguns deles apresentam as chamadas "librações paradoxais", isto é, circulações de amplitude muito pequena que aparecem como se fossem librações. Apenas 6 possuem diâmetros conhecidos, da ordem de 50 km.

3. alternadores apocêntricos: 55 asteróides para os quais $\sigma_{2/1}$ alterna entre libração em torno de 180° e circulação. Localizam-se nas excentricidades muito baixas, à direita da ressonância 2/1. Estes objetos estão associados a um regime dinâmico

conhecido como libração apocêntrica (Greenberg e Franklin 1976; Henrard et al. 1983). Apenas doze possuem diâmetros conhecidos, entre 70 e 250 km. O principal membro é 168 Sybilla.

Neste capítulo só estudamos o grupo dos asteróides ressonantes. De acordo com a sua estabilidade, estes podem ser subdivididos em três grupos: (i) estáveis, ou grupo de Zhongguo; (ii) marginalmente instáveis, ou grupo de Griqua; e (iii) fortemente instáveis.

2.3. O grupo de Zhongguo

Os asteróides estáveis são 27 objetos localizados entre $0.2 < e < 0.3$, com inclinações menores que $5°$ e amplitudes de libração entre $\sim 60°$. O principal representante deste grupo é 3789 Zhongguo. Analisando a distribuição destes asteróides no espaço de elementos próprios, a_p, e_p, I_p, verificamos que a maioria deles forma um aglomerado entre $3.22 \leq a_p \leq 3.24$ UA, $0.25 \leq e_p \leq 0.28$, e $I_p \leq 5°$. Destaquemos que, neste caso, os elementos próprios são definidos, em primeira aproximação, como o mínimo de a e o máximo de e e I sobre 10 milhões de anos. Segundo as simulações de Morbidelli (1996) e nossas próprias simulações, estes objetos podem sobreviver dentro da ressonância 2/1 por intervalos de tempo de, no mínimo, 500 milhões de anos.

A estabilidade a longo prazo desta população de asteróides é analisada integrando numericamente uma grade de 100 partículas de teste na ressonância, por 4 bilhões de anos e incluindo as perturbações gravitacionais dos quatro planetas Jovianos. Observamos que aproximadamente 20% das condições iniciais sobreviviem até o final da simulação. A partir dos nossos resultados, montamos um mapa das regiões de estabilidade e caos dentro da ressonância. Para isto, o espaço dos elementos próprios é subdividido num conjunto de células, formando uma grade, e a estabilidade é quantificada através do tempo de residência das várias trajetórias em cada célula. Este mapa mostra que o grupo de Zhongguo reside na região mais estável do espaço de fases ressonante, onde os asteróides podem sobreviver por intervalos de tempo da ordem da idade do Sistema Solar. Isto é verificado mais tarde através de simulações com modelos de caminhada aleatória, que indicam que o grupo de Zhongguo poderia ser o remanescente de uma população primordial de asteróides ressonantes, que sobreviveu à depleção global do espaço de fases da ressonância 2/1.

No entanto, a distribuição de tamanhos do grupo de Zhongguo apresenta as características típicas de uma distribuição vinculada a um fenômeno colisional muito recente. O ajuste da distribuição segundo uma lei de potências (Petit e Farinella 1993) fornece um expoente entre 1.5 e 2 vezes maior do que no caso das distribuições do grupo de Hilda ou da família de Themis. Além disso, todos os membros conhecidos do grupo de Zhongguo possuem diâmetros menores do que 20 km, o que se traduz num tempo de vida média colisional menor do que a idade do Sistema Solar ($\sim 2 \times 10^9$ anos). Toda esta evidência entra em conflito com a idéia de uma origem primordial destes asteróides.

Se o grupo de Zhongguo não for primordial, ele deve ter sido "injetado" na ressonância há menos de 4 bilhões de anos através de algum mecanismo dinâmico. Nós analisamos quatro possibilidades diferentes. A primeira está relacionada à difusão caótica na região à esquerda da ressonância 2/1, onde se localiza a família de Themis. Esta difusão caótica é favorecida pela teia de ressonâncias fracas de três corpos (Nesvorný e Morbidelli 1998), envolvendo simultaneamente o período de Júpiter e Saturno. Através de simulações numéricas de condições iniciais fictícias no intervalo $3.12 \lesssim a \lesssim 3.22$ UA, por tempos da ordem de 200 milhões de anos, nós mostramos que estas ressonâncias fracas, e particularmente a superposição das mesmas nas altas excentricidades ($e > 0.3$), podem contribuir para injetar asteróides dentro da ressonância 2/1. Porém, os objetos entram na ressonância cruzando a separatriz onde o movimento é extremamente caótico, e não conseguem ficar capturados nas regiões mais estáveis da ressonância.

Uma segunda alternativa analisada é o efeito Yarkovsky. Este efeito está vinculado à dissipação de energia que ocorre na re-emisão de radição quando o asteróide está girando. Na verdade, existem duas versões deste efeito: a diurna, vinculada à rotação do asteróide (ex., Vokrouhlický, Milani e Chesley 2000) e a estacional, vinculada ao movimento orbital do asteróide (Rubincam 1995). O efeito diurno pode fazer o semi-eixo do asteróide aumentar ou diminuir dependendo do sentido da rotação do corpo, enquanto o estacional só faz o semi-eixo diminuir. O efeito Yarkovsky depende de vários parâmetros relacionados à composição química e tamanho dos corpos. Nossas simulações mostram que, para asteróides do tipo C (característico da família de Themis), e com diâmetro de 6 km (limite inferior da maioria dos Zhongguos observados), o efeito Yarkovsky não consegue transportar objetos desde fora da ressonância 2/1 até a região do grupo de Zhongguo. O problema é o forte caos na região da separatriz e das ressonâncias se-

cundárias ($e \sim 0.15$, ver Michtchenko e Ferraz-Mello 1996), que forma uma barreira impedindo que os asteróides possam cruzar por ela sem excitar significativamente as inclinações, o que acaba sendo incompatível com as baixas inclinações observadas dos Zhongguos.

A terceira alternativa analisada é a captura em ressonância devido à migração planetária. A migração planetária (Fernández e Ip 1984) teria causado uma diminuição do semi-eixo de Júpiter da ordem de 0.2 UA em intervalos de tempo da ordem de 10 a 100 milhões de anos (Hahn e Malhotra 1999). Como conseqüência disto, a ressonância 2/1 teria se deslocado umas 0.12 UA, possibilitando a captura de asteróides não ressonantes. Nossas simulações utilizando um modelo simples de migração exponencial (Malhotra 1995) mostram que é possível capturar objetos com caraterísticas dinâmicas semelhantes aos Zhongguos. Porém a migração planetária é um mecanismo ainda pouco conhecido: não sabemos quando aconteceu extamente, o quanto durou, e como fez variar o semi-eixo dos planetas na realidade. Portanto, precisamos de simulações mais detalhadas e realistas antes de poder tirar conclusões definitivas sobre a eficiência deste mecanismo para capturar asteróides na ressonância 2/1.

Finalmente, analisamos a possível origem dos Zhongguos a partir da fragmentação que deu origem à família de Themis. Este mecanismo já foi proposto por Morbidelli et al (1995) e Moons, Morbidelli e Migliorini (1998). Utilizando um modelo simples de fragmentação isotrópica com velocidades de ejeção independentes da massa dos fragmentos, nós achamos que resulta difícil reproduzir as velocidades de ejeção necessárias para injetar fragmentos na região que os Zhongguos ocupam atualmente. Estas velocidades de ejeção baixas são consistentes com os modelos de fragmentação baseados em códigos hidrodinâmicos (Benz e Asphaug 1999). Ainda que este mecanismo não possa ser desconsiderado como possível origem dos Zhongguos, achamos que ele seria pouco provável, tanto em função do nosso conhecimento presente sobre os processos de fragmentação, como da distribuição espacial dos Zhongguos em relação à família de Themis.

2.4. O grupo de Griqua e a população instável

O grupo de Griqua está constituído por 13 asteróides observados, cujos tempos de sobrevivência na ressonância são da ordem de 100 a 500 milhões de anos. Estes objetos

localizam-se numa região de transição entre a região ocupada pelo grupo de Zhongguo e a região de forte caoticidade perto da separatriz. A origem destes asteróides não é muito clara. De acordo com as nossas simulações de caminhada aleatória, é provável que estes objetos tenham atingido a região onde se encontram atualmente difundindo-se lentamente a partir de regiões mais estáveis. Portanto, poderiam estar vinculados dinamicamente ao grupo de Zhongguo. Mas por outro lado, alguns deles possuem inclinações particularmente altas ($\sim 20°$) o que faz pensar na possibilidade de terem sido injetados desde fora da ressonância 2/1, atravesando a separatriz ou a região das ressonâncias secundárias.

Por sua vez, os asteróides instáveis são cerca de 20 objetos que se distribuem nas regiões mais caóticas do espaço de fases ressonante, perto da separatriz, e não sobrevivem na ressonância 2/1 além de 10 milhões de anos. O fato de observar atualmente esta população ressonante com tempos de vida tão curtos, significa que a mesma deve estar sendo re-alimentada continuamente. A partir dos nossos resultados, podemos concluir que tanto a difusão pelas ressonâncias fracas à esquerda da ressonância 2/1 quanto o efeito Yarkovsky poderiam dar conta deste mecanismo de re-alimentação, pelo menos em parte. Existem outros mecanismos, que nós não analisamos com detalhe, mas que poderiam contribuir para o fluxo de novos asteróides instáveis na ressonância 2/1. É o caso do "scattering" gravitacional devido à interação com os grandes asteróides do cinturão principal (especialmente Ceres e Pallas), e também do "sticking" em ressonância, ou captura temporária em ressonância, que pode ocorrer no caso dos asteróides que cruzam as órbitas dos planetas Terrestres com excentricidade muito alta.

Para finalizar, destacamos que a região central da ressonância, no intervalo $0.3 < e < 0.4$, possui níveis de estabilidade comparáveis ou ainda maiores do que a região onde se localiza o grupo de Griqua. No entanto, nenhum asteróide foi observado nesta região até agora. De acordo com Ferraz-Mello, Michtchenko e Roig (1998), a depleção na região central da ressonância está vinculada a pequenas variações no período da Grande Desigualdade (comensurabilidade 5/2) entre Júpiter e Saturno, que poderiam ocorrer no âmbito da migração planetária. Porém, não fica claro se estas variações poderiam afetar da mesma forma a região ocupada pelo grupo de Zhongguo, causando uma depleção semelhante desta população. Por enquanto, a ausência de asteróides na região central da ressonância 2/1 não pode ser justificada através dos modelos que

apresentamos aqui.

2.5. Conclusões

Nossos resultados não permitem elaborar uma conclusão definitiva sobre a origem dos asteróides observados na ressonância 2/1 com Júpiter. Por um lado, fica claro que há mecanismos dinâmicos que conseguem justificar a existência de uma população de asteróides instáveis na ressonância. Mas estes mecanismos são insuficientes para explicar a presença do grupo de Zhongguo. Do ponto de vista dinâmico, os Zhongguos poderiam ser os remanescentes de uma população primordial de asteróides ressonantes, capturada, por exemplo, na época da migração planetária. No entanto, esta idéia não pode ser sustentada levando em conta a distribuição de tamanhos dos Zhongguos. Acreditamos que a solução mais plausível, porém quase impossível de verificar do ponto de vista dinâmico, é que os Zhongguos sejam o resultado da fragmentação recente de um asteróide da ordem de 50 a 100 km de diâmetro, que poderia ter existido na ressonância desde os primórdios do Sistema Solar. Esta fragmetação teria sido causada pela colisão com um objeto do cinturão principal, provavelmente da família de Themis. Pensamos que a única forma de desvendar este problema seja através de observações espectroscópicas, que revelem a composição química e a taxonomia dos Zhongguos.

Anexo:

The asteroidal population in the Hecuba gap.
Part I: Dynamics and size distribution of the resonant asteroids

The Asteroidal Population in the Hecuba Gap. Part I: Dynamics and size distribution of the resonant asteroids

F. Roig

Instituto Astronômico e Geofísico, Universidade de São Paulo.

Av. Miguel Stefano 4200, (04301-904) São Paulo, SP, Brasil.

D. Nesvorný

Department of Space Studies, Southwest Research Institute.

1050 Walnut St., Suite 426, Boulder, CO 80302, USA

and

S. Ferraz-Mello

Instituto Astronômico e Geofísico, Universidade de São Paulo

Av. Miguel Stefano 4200, (04301-904) São Paulo, SP, Brasil.

1. Introduction

The Hecuba gap is a region of about 0.2 AU in width, located at the outermost edge of the main asteroid belt. It is related to the 2:1 mean motion resonance with Jupiter, centered at 3.27 AU, and it is characterized by an extremely low density of observed asteroids when compared with its immediate neighborhoods. At the left side of the gap, for values of $3.1 < a < 3.2$ AU, a huge amount of asteroids is observed, most of them related to Themis family[1]. At the right side of the gap, for $3.35 < a < 3.45$ AU, the density of objects slightly rises due to the presence of Cybele's group (see for example, Figs. 7 and 8 of Knežević and Milani, 2001). The Hecuba gap marks the limit between the main asteroid belt, dominated by the presence of asteroidal families, and the outer asteroid belt, dominated by the presence of groups of asteroids with no evidence of an active collisional history.

For many years, it was believed that the Hecuba gap was depleted of asteroids. By the middle of the XXth century, only one asteroid, (1362) Griqua, was known to reside in the 2:1 resonance. The population began to grow from the '70s on, when the asteroids (1921) Pala and (1922) Zulu were added to the list. During the next 20 years, the number increased slowly and reached the modest value of some 10 objects by the beginning of the '90s. This figures contrasted with the large

[1]This family has at present $\sim$ 1850 members.

number of asteroids of the Hilda group, located at the 3:2 resonance with Jupiter, which by the same epoch accounts for more than 80 objects. Moreover, the Hilda group seems to form a well defined cluster inside the 3:2 resonance, and has several large asteroids ($D > 100$ km) among its members. On the other hand, most of the 2:1 resonant objects appeared spread throughout the resonant space, having quite irregular orbits and small sizes ($D < 20$ km). This remarkable observational difference between the two most important first order resonances in the asteroid belt led several authors during the '90s to work on its explanation. The answer arrived in different pieces (Ferraz-Mello, 1994; Morbidelli, 1996; Nesvorný and Ferraz-Mello, 1997a,b; Ferraz-Mello et al., 1998a) that joined together allowed to mount a global portrait of the dynamics at both resonances. The main conclusion was that the resonant space is globally chaotic in both cases, but the chaos at the 3:2 resonance is weak enough to allow a population like the Hildas to survive there over the age of the Solar System. The same assertion cannot be made for the 2:1 resonance, and one should expect that any possibly primordial resonant population have been depleted over the age of the Solar System (Ferraz-Mello et al., 1998b).

The surprise arrived when during the last decade new asteroids at the 2:1 resonance began to be discovered at a really astonishing rate. The 10 objects known in 1990 grew to 25 in 1996, and to more than 60 in 2001. This latter value does not take into account objects with poorly determined orbits, which can roughly duplicate it. Of course, many new objects were also discovered in the Hilda group, which now accounts for more than 280 asteroids. But even when the observational difference between both resonances is still remarkable, we cannot continue claiming that the Hecuba gap is "depleted". Since we should not expect to find such a large number of asteroids at the 2:1 resonance, their presence there requires an explanation. The main question is: would these asteroids be the lucky survivors of a primordial resonant population, or have they arrived to the resonance in a more recent time? In any case, the answer to this question could help not only to better understand the internal dynamics of the 2:1 resonance, but also to put constrains to the different dynamical mechanisms that dominated the evolution of main belt asteroids over the age of the Solar System (formation of families, planetary migration, etc.)

This is the first of two papers where we intend to provide some insight into the problem of the asteroidal population in the Hecuba gap. We do not expect to give a definitive answer to it, but rather to present a set of evidences that could help to find this answer, and also to rise up some open problems which could deserve more detailed studies in the future. This paper will be devoted to describe the dynamical characteristics of the asteroids inside the 2:1 resonance and their size distribution. The discussion about their origin will be reserved for an upcomming paper. This paper is organized as follows: in Sect. 2 we describe the population of presently observed resonant objects, analyzing their spatial distribution and stability. In Sect. 3 we study the long term dynamics inside the 2:1 resonance, trying to quantify the chaotic diffusion and its effect on the evolution of a hypothetical primordial population of asteroids. We also discuss the possible role of perturbations other than planetary ones in enhancing this diffusion., like Yarkovsky orbital drift and mutual scattering. Section 4 is devoted to analyze and discuss the size distribution of the

resonant asteroids. Finally, Sect. 5 contains the conclusions.

2. The resonant population

The first step in our study was to identify the presently observed population of resonant asteroids in the Hecuba gap. In order to do this, we proceeded as follows. We considered all the numbered and unnumbered multi-oppositional[2] asteroids contained in the asteroid database of Lowell Observatory (ftp://ftp.lowell.edu/pub/elgb) as to April 2001, and we took apart those having osculating semi-major axis and eccentricity between the limits indicated by dotted-dashed lines in Fig. 1. These "osculating limits" were defined empirically based on a trial-and-error approach, and are such that almost any possible resonant asteroid will be contained within them. We ended up with a list of about 2600 asteroids which we then propagated numerically over 10,000 yr, and we proceeded to identify those dynamically related to the 2:1 resonance by visually inspecting the behavior of the critical argument, given by:

$$\sigma = 2\lambda_{\rm J} - \lambda - \varpi. \tag{1}$$

where λ and ϖ represent the mean longitude and the longitude of perihelion, respectively, and the subindex J refers to Jupiter. We considered an asteroid to be related to the resonance whenever σ librated around 0, or alternated between libration and circulation, even if this behavior lasted for a short interval of time.

We found 421 asteroids showing some kind of resonant behavior. Their present osculating elements are shown in Fig. 1, and they can be divided in three main groups:

1. Resonant (triangles in Fig. 1): 61 asteroids for which σ librates around 0 in a high-eccentricity regime For a few of them, σ alternates between libration with a large amplitude and circulation, thus jumping outside and inside the resonance alternately.

2. Apocentric alternators (stars in Fig. 1): 55 objects with σ alternating between circulation and libration around 180°, in a low-eccentricity regime. This behavior is also known as apocentric libration (Greenberg and Franklin, 1976; Henrard et al., 1983). The motion is, in fact, a circulation with a forced term and a modulated amplitude that, at times, becomes smaller than the forced term itself. When this happens, σ does not take all the values in the interval $[0, 360°]$ but shows what is usually known as a "paradoxal libration".

3. Pericentric alternators (crosses in Fig. 1): 305 asteroids were found in a low-eccentricity regime, with σ alternating between circulation and libration around 0. This behavior is the analogous of the apocentric alternation, and we identified several paradoxal librators.

[2] An asteroid at about 3.2-3.3 AU is multi-oppositional if their observations span a time interval larger than 440 days.

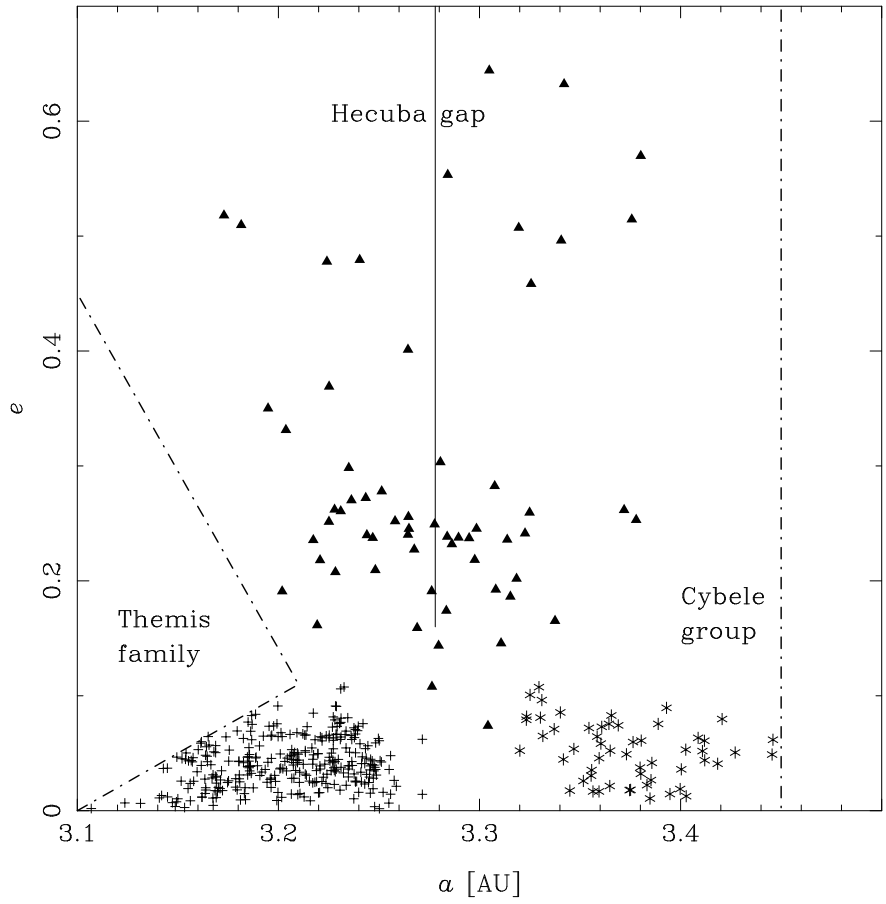

Fig. 1.— The asteroidal populations in the Hecuba gap, projected in the space of osculating orbital elements. Triangles are resonant asteroids, stars represent apocentric alternators and crosses are apocentric librators (see text). The full vertical line marks the approximate location of the exact resonance. The dashed-dotted lines are the boundaries of our searching criteria to identify the members of each population.

This paper is mainly devoted to study the dynamics of the resonant asteroids. A detailed analysis of the other two groups is beyond its scope, and will be eventually left for a future paper.

2.1. Spatial distribution and typical lifetimes

Once we had identified the resonant asteroids, the next step was to determine their location inside the resonant phase space and their typical lifetimes. The first task was accomplished through the determination of proper elements, while the second required a long term numerical simulation. We detail both in the following.

2.1.1. Resonant proper elements

Proper elements are invariants of motion of the given dynamical system, and they only exist if the system is integrable. However, even for non integrable systems it is still possible to define "proper elements", which of course will not be constant during the evolution of the system. In these cases, we can only assure that these proper elements will vary very little over long intervals of time, provided the system is weakly chaotic. The time variation of the proper elements is sometimes (improperly) referred to as diffusion[3], and it can be used to quantify the chaoticity of an orbit. Moreover, the location of a given body in the space of proper elements has a well defined dynamical meaning, and is useful to identify clusters or families.

Now, our problem is how to determine a good set of proper elements for our population of resonant bodies. In the non resonant case, proper elements are associated to the time averages of the orbital elements a, e and I. Then, a practical way to estimate the "diffusion" of these proper elements is to calculate running averages of the time signals of a, e, I, using a suitable window-shift combination (Press et al., 1996; see also Morbidelli and Nesvorný, 1999). However, this definition is useless in the resonant case, because all the resonant trajectories will have the same averaged semi-major axis, namely the critical semi-major axis $a_{\rm res}$ of the resonance. In these cases, the average over a can be replaced with advantage by the average over the amplitude of libration A_σ, which is an invariant of motion in the integrable approximation of the resonant dynamics, and so has the desirable properties of a proper element (Schubart, 1982; Bien and Schubart, 1987).

An alternative to the use of running averages is to determine the successive intersections of a given trajectory with a suitable "surface of section". We know that periodic orbits are represented by fixed points on the surface of section. Then, any stable (weakly chaotic) trajectory around the periodic orbit will successively intersect the surface of section at about the same place. The average

[3]The word "diffusion" should not be understood in the strict physical sense. Any quantity giving information about the change of the proper elements can be considered as a diffusion parameter, although it could have no direct relation with the usual concept of diffusion arising from the solution of the heat equation.

value of these intersections can be used as an estimate of the proper element, and their dispersion (r.m.s.) as an approximate measure of the diffusion.

Based on the particular topology of the 2:1 resonance, a suitable surface of section could be defined by the following simultaneous conditions for the angles:

$$\sigma = 0; \quad \varpi - \varpi_{\rm J} = 0; \quad \Omega - \Omega_{\rm J} = 0 \tag{2}$$

where Ω represents the longitude of node. However, these conditions can hold simultaneously only in an approximate way, mainly because the motion of ϖ is uncoupled with the motion of Ω. Moreover, depending on the chaoticity of the given trajectory, the simultaneous condition does not hold approximately either. Then, a possible solution is to define a less restrictive surface of section, for example considering only the first two conditions

$$\sigma = 0; \quad \varpi - \varpi_{\rm J} = 0 \tag{3}$$

and leaving the longitude of node free. For most resonant asteroids, the frequency of libration of σ is much faster than the frequency of circulation of ϖ, and we can assure that Eq. (3) is approximately satisfied in most cases within an interval of $\pm 3^\circ$ in both angles. To compute the proper elements in this surface of section, we first propagated the osculating elements of the 61 resonant asteroids over 2×10^5 yr. The propagator was the symplectic integrator Swift (Levison and Duncan, 1994), with a time step of 0.01 yr, and we took into account planetary perturbations from Venus to Neptune. The osculating orbital elements were sampled every 5 yr, and we stored apart the values of a, e, I whenever $|\sigma| \leq 5^\circ$ and $|\varpi - \varpi_{\rm J}| \leq 5^\circ$. These stored values of a, e, I were further divided into two different sets: (i) a set corresponding to values of a, e located at the left side of the center of the resonance, which are related to the condition $\dot{\sigma} < 0$, and (ii) a set such that $\dot{\sigma} > 0$, which corresponds to values of a, e located at the right side of the resonance center. It is worth noting that, whenever $\varpi - \varpi_{\rm J} \simeq 0$, the first set is associated to a condition where a is minimum while e is maximum, and the second set is such that a is maximum while e is minimum. Moreover, for weakly chaotic trajectories at intermediate eccentricities ($0.2 < e < 0.3$), the condition $\Omega - \Omega_{\rm J} \simeq 0$ is normally associated to a maximum of I. Then, among the various intersections of a given trajectory with the surface of section (Eq. 3), we chose the one corresponding to the pair $a_{\rm min}, e_{\rm max}$ nearest to some maximum of the inclination. These latter values were considered the *resonant proper elements*: a_p, e_p, I_p, and the remaining intersections (those for other values of I, not necessary close to a maximum) were used to estimate their r.m.s.

The location of the resonant asteroids in the space of resonant proper elements is shown in Fig. 2. The panels show the projections in the a_p, e_p and a_p, I_p spaces, respectively. Gray and black dots were used to distinguish the asteroids according to their typical lifetimes: the darker the dot, the shorter the lifetime (see Sect. 2.1.2). The left panel also shows the location of the resonance centers (full vertical line) and the left separatrix (bold line marked Sx). The distance of each asteroid to the resonance center, i.e. $\delta a = a_p - a_{\rm res}$, is roughly proportional to its amplitude of libration A_σ. We have also plot in this panel the approximate location of the ν_{16} secular resonance (dashed line

marked ν_{16}), and the instability border (dotted-dashed line marked IB), both computed numerically. The phase space above the IB line and between the IB and Sx lines is dominated by the overlap of ν_5, ν_6 secular resonances and Kozai resonance (Morbidelli and Moons, 1993), which generates a strong chaos (Nesvorný and Ferraz-Mello, 1997a).

In Fig. 2, the error bars of each point represent the standard deviations $\sigma_a, \sigma_e, \sigma_I$ of the proper elements[4]. We can see that, even when no condition was imposed over the longitude of node to define the surface of section (Eq. 3), the resonant proper elements are quite well determined for most of the asteroids. Some exceptions are related to strongly chaotic objects, mainly between the IB and Sx lines, for which the proper elements vary significantly in short time-scales. Moreover, there are some of these chaotic asteroids for which only one or two intersection could be determined, so they are shown with no error bars or with a viciously small error bar. In order to remove any possible noise related to the short period perturbations of Jupiter's mean motion, we re-calculated the proper elements using filtered elements, instead of osculating, but the differences detected were well inside the σ_E confidence interval in all cases. In spite of their pretty good accuracy, we must bear in mind that the resonant proper elements shown in Fig. 2 should be considered reliable only for a time scale of the order of the integration time span used to calculate them, that is, some 0.1 Myr. Since this is a short time scale compared to the age of the Solar System, we can say that Fig. 2 is a portrait of the "present" distribution of the resonant population.

Other interesting features can be appreciated in Fig. 2, for example:

- Almost all asteroids are located at the left side of the ν_{16} resonance, and the central region (between the ν_{16} and IB lines) is not populated. This feature is already known from the works of Michtchenko and Ferraz-Mello (1995,1996), Morbidelli (1996) and Moons et al. (1998), and has been explained on the basis that the central region is extremely sensitive to the presence of three body mean motion resonances involving the 5:2 Great Inequality between Jupiter and Saturn (Ferraz-Mello et al., 1998a).

- There seems to be a quite well defined cluster of some 15 objects at about $a_p \simeq 3.23$ AU, $e_p \simeq 0.28$ and $I_p \simeq 1°$. Their σ_E are very small, and we could expect a quite regular behavior of these objects over time-scales of at least some Myr. The lowest numbered asteroid of this cluster is (11097) 1994 UD1. However, the first asteroid with a quite regular behavior that was identified near that region of the phase space, was (3789) Zhongguo (Morbidelli, 1996). Then, one is tempted to call this cluster "the Zhongguos" to continue the tradition, although it is clear that Zhongguo itself does not seem to be a member of the cluster.

- Other old-known resonant asteroids, like (1362) Griqua, (1921) Pala, (1922) Zulu and (3688) Navajo, lie far away form the region of the Zhongguos, and in some cases their motion is remarkable chaotic.

[4]Do not confuse these σ_E with the resonant angle σ!

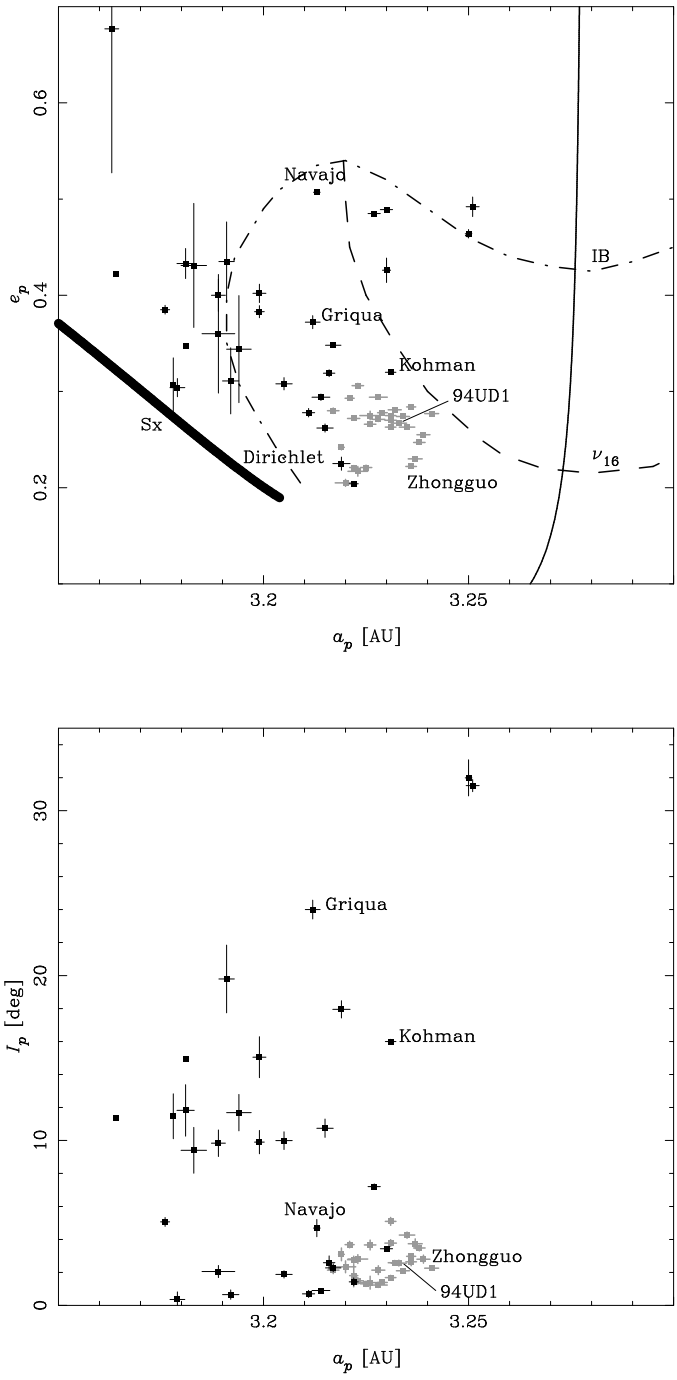

Fig. 2.— The spatial distribution of resonant asteroids in the Hecuba gap, projected in the space of proper a, e (left panel) and proper a, I (right). Gray and black dots distinguish the asteroids according to their typical lifetimes (see Fig. 4). The error bars correspond to the standard deviations of the proper elements. The left panel also shows the location of the resonance centers (full vertical line), leftmost separatrix (Sx), ν_{16} secular resonance and instability border (IB).

- Another small cluster of 5 objects seems to exist at about $a_p \simeq 3.22$ AU, $e_p \simeq 0.22$ and $I_p \simeq 2^\circ$ (gray dots). The main member of this cluster is an unnumbered object, 1975 SX. The cluster seems to be nearby to the asteroid (11665) Dirichlet (black dot), but this latter has a much higher proper inclination.

To close this section, we want to address a final comment concerning the determination of resonant proper elements. The method of surface of section described here is quite accurate, but requires a lot of user manipulation and cannot be applied in a large a scale to huge sets of data. Fortunately, the method gives a hint for a more automated process, which resembles the method of running averages. Since the conditions of the surface of section are related to maxima and/or minima of a, e and I, we can calculate running maxima and/or minima over the time series of the osculating elements, and consider the resulting values as the time series of the proper elements. In fact, some authors have already applied this method to similar problems, and it is sometimes referred to as the "sup-map" method (e.g., Morbidelli, 1996, 1997). Figure 3 shows a comparison between the proper elements determined through the surface of section (in the abscissas) against those determined through running minima for a and running maxima for e, I (in the ordinates). The dashed lines have slope $= 1$. In this figure we only show the minima/maxima determined over the first 10 Myr of evolution, and we can see that in most cases the agreement between both sets is very good. Exceptions are some chaotic objects for which the use of maxima over a large time interval overestimates the value of the proper element over shorter time-scales.

2.1.2. Lifetimes

Having determined the location of the resonant population in the proper elements space, we proceeded to analyze their stability. We integrated the 61 resonant asteroids over 520 Myr, taking into account perturbations of four major planets only. The propagator was Swift, with a time step of 0.08 yr. Each asteroid was followed until the end of the simulation or until it became discarded because: (i) reached a value of $q < 0.01$, (ii) reached a value of $a > 20$ AU, or (iii) had a planetary encounter within 0.01 Hill's sphere. Then, the lifetime of a given asteroid was defined as the time interval it remained active during the simulation. It is worth noting that this definition is not directly related to the lifetime "inside the resonance", because in most cases, the asteroids had already escaped from the resonance some Myr before being discarded.

The lifetime of the resonant asteroids is shown in Fig. 4 in dependence of their proper semi-major axis. As expected, the objects located near the separatrix and near the instability border have the shortest lifetimes, escaping in many cases in less than 20 Myr. Table 1 lists all the asteroids with lifetimes shorter than 100 Myr. We will refer to this short lived population as the "unstable" resonant population. The shortest lived object is the asteroid (5201) Ferraz-Mello, which escaped in less than 20,000 yr.

Another group of asteroids, having typical lifetimes between 100 and 500 Myr, is listed in Table

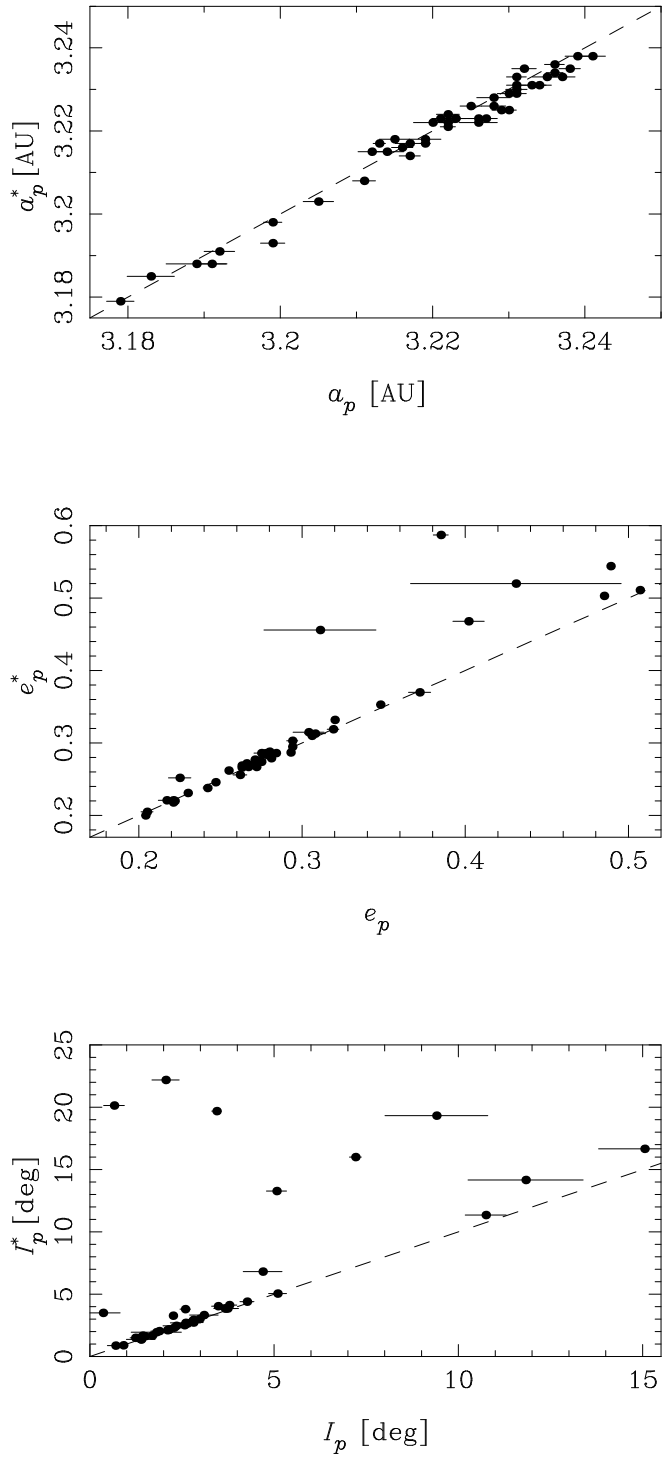

Fig. 3.— Comparison between resonant proper elements a_p, e_p, I_p determined using the surface of section method, and proper elements a^*_p, e^*_p, I^*_p computed as minimum of a and maxima of e and I over 10 Myr.

2. This group includes (1362) Griqua, (3688) Navajo and (11665) Dirichlet. Most of them seem to lie in a transition region between the IB line and the region of the Zhongguos, and some have proper inclinations larger than 10°. A particular case is the asteroid (4177) Kohman, that is captured in the ν_{16} secular resonance. We will refer to this set of asteroids as the "marginally unstable" population, or simply "the Griquas".

Finally, 27 asteroids survived up to 520 Myr. This group is listed in Table 3, and includes (3789) Zhongguo and all the Zhongguos (i.e., the cluster of 1994 UD1). We will call this population the "stable" one. The transition between the stable and marginally unstable populations is not clear enough, mainly because the limit of 520 Myr is quite arbitrary. It is difficult to say how many asteroids would escape if we push our simulation up to 1 Byr or more. For example, simulations carried out by Morbidelli (1996) showed that Zhongguo itself is not able to survive in the resonance for more than 1 Byr. We will discuss this problem with more detail in the next section.

3. Long term stability

The existence of a possible long-lived population of resonant objects raises the question about their actual long term stability. Would these asteroids have lifetimes shorter than the age of the Solar System? Or would they be able to survive in their present location over 4.5 Byr?

To answer these questions, we performed a series of simulations aiming to analyze the stability in the resonant space between $0.2 \leq e \leq 0.5$. We chose a grid of 100 initial conditions distributed in the range $3.205 \leq a \leq 3.286$ AU; $\Delta a = 0.009$ AU, and $0.22 \leq e \leq 0.40$; $\Delta e = 0.02$. The initial inclinations were set equal to 0, and the remaining initial angles were chosen such that $\sigma = 0$; $\varpi - \varpi_{\rm J} = 0$ and $\Omega - \Omega_{\rm J} = 0$ for all particles. This grid of particles was integrated over 4 Byr using Swift, with a time step of 0.08 yr. We considered perturbation of four major planets, and the resulting osculating elements were sampled every 5,000 yr.

The first result of this simulation is presented in Fig. 5, where each initial condition is represented by a rectangle, shaded according to its survival time. The gray-scale is such that darker rectangles are initial conditions that escaped faster, while blank rectangles correspond to particles that survived the whole simulation inside the resonance. By "escape" we mean that the particle was discarded from the simulation due to any of the three criteria mentioned in Sect. 2.1.2. The figure also shows four dotted curves, denoted $N_1, \ldots, N_4$, which correspond to four different constant levels of the invariant

$$N = \sqrt{a}\left(-2 + \sqrt{1-e^2}\cos I\right). \qquad (4)$$

This quantity is an integral of motion of the averaged circular restricted three body problem, and the resonant motion is approximately symmetric with respect to the resonance center along these lines.

Figure 5 provides a clear evidence that, in spite of the dynamical diffusion, some particles could

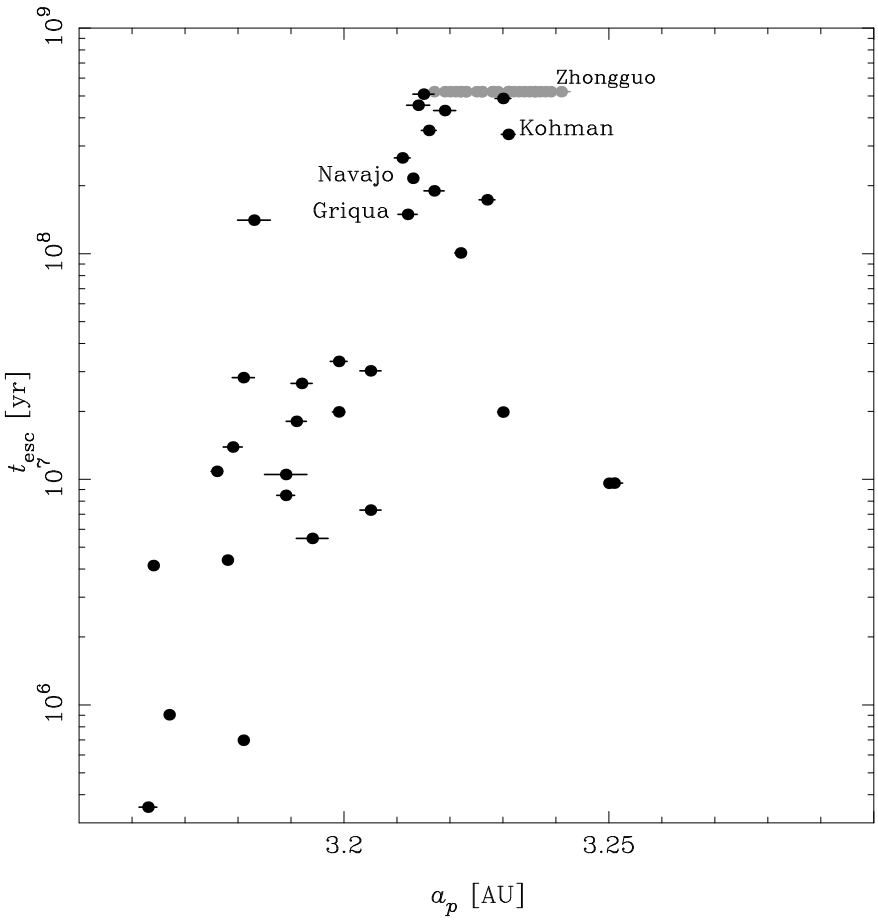

Fig. 4.— The typical lifetimes of resonant asteroids in the Hecuba gap. Gray dots are objects that survived over the 520 Myr simulation (compare with Fig. 2). For the escaping asteroids (black dots), the actual lifetimes inside the 2:1 resonance could actually be smaller than the values shown here.

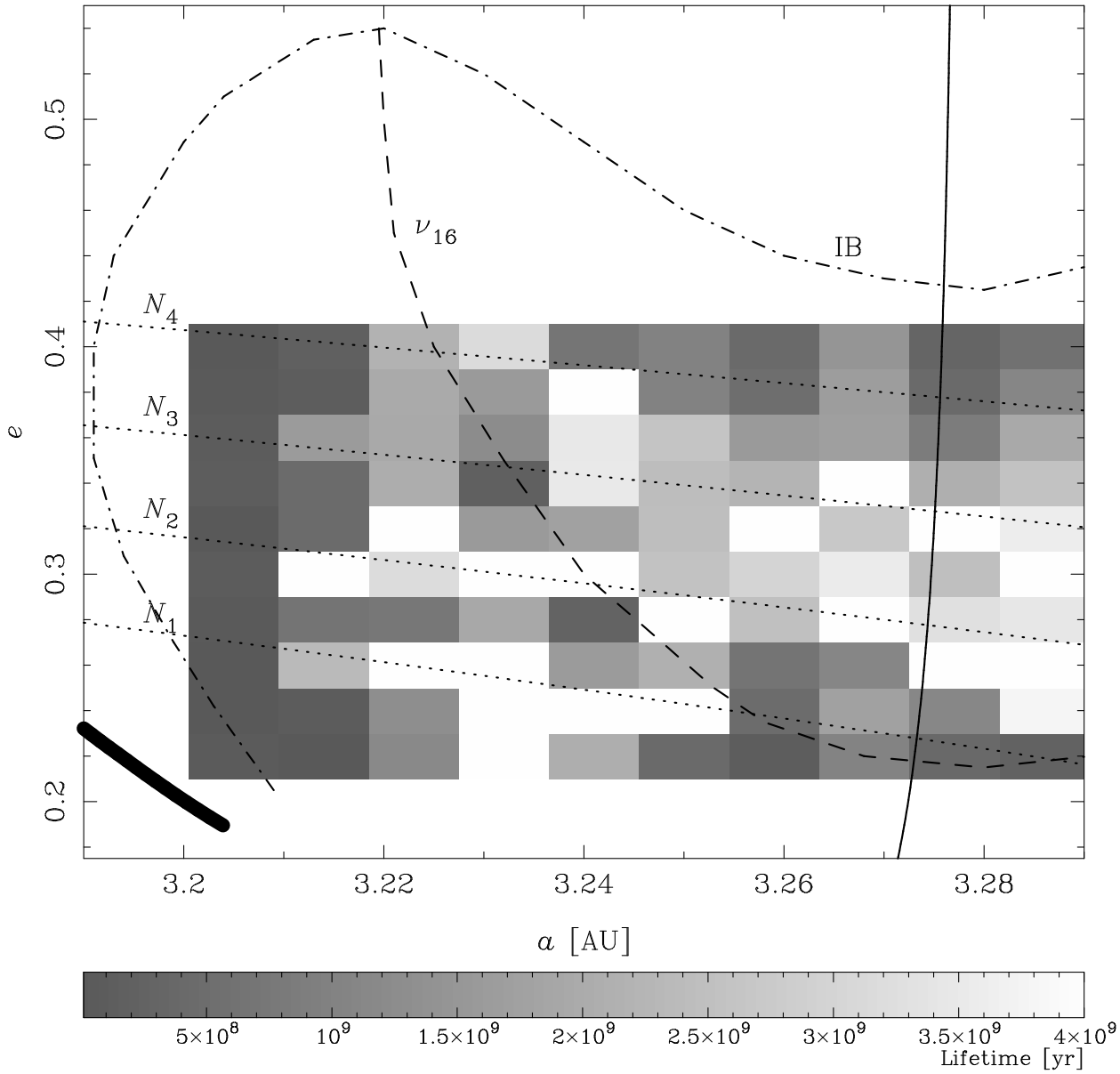

Fig. 5.— Initial conditions of the 4 Byr simulation (shaded rectangles) and their lifetimes. The darkest conditions have the shortest lifetimes. The dotted lines marked N_i correspond to different levels of the invariant Eq. (4).

survive inside the resonance over the age of the Solar System. It is worth noting that about 36% of the initial conditions in the region $3.21 < a < 3.25$ AU and $0.20 < e < 0.33$ survived after 4 Byr, and it is in this region where almost all the stable asteroids are located. This cannot be so by mere chance, and it opens the possibility for the stable population having been in the resonance from the very early times. In such case, the Zhongguos could be the few lucky survivors of a primordial resonant population, captured during the last stages of the formation of the Solar System. However, about 25% of the initial conditions between $3.25 < a < 3.29$ AU and $0.20 < e < 0.34$ also survived after 4 Byr, although no real asteroid is observed in that region. Then, it is clear that the information provided by Fig. 5 is not sufficient, and a deeper analysis of the dynamics in those regions is necessary before trying to conclude anything about the origin of the Zhongguos.

In order to carry out such deeper study, we proceeded to construct a map of the diffusion in the region of the phase space covered by our simulations. This was accomplished by the following procedure:

1. We took each initial condition of our simulation and determined their proper elements using running maxima and minima. The minimum of a and the maxima of e and I where calculated every 0.1 Myr using a running window of 10 Myr in width.

2. We considered the region of the phase space in the interval $3.19 \leq a \leq 3.28$ AU, $0.175 \leq e \leq 0.550$ and $0 \leq I \leq 10°$, and divided it in $18 \times 15 \times 1 = 270$ equal cells of dimension $\Delta a = 0.005$ AU, $\Delta e = 0.025$ and $\Delta I = 10°$ each.

3. We proceeded to determine the time of residence of the different trajectories in each cell, according to the following recipe: Let $(a_p, e_p, I_p)^n = (a_p(n\tau), e_p(n\tau), I_p(n\tau))$ be the discrete time series of proper elements for a given particle, where n is an integer and $\tau = 0.1$ Myr. Then, the time of residence, T_{ij}, of this particle in the cell (a_i, e_j) was computed as

$$T_{ij} = \sum_k (r_k - s_k)\tau, \tag{5}$$

for every $s_k \leq n \leq r_k$ such that

$$\begin{aligned} a_i &\leq a_p^n < a_i + \Delta a \\ e_j &\leq e_p^n < e_j + \Delta e \\ 0 &\leq I_p^n \leq \Delta I \end{aligned} \tag{6}$$

Note that we are considering a unique cell along the inclinations, i.e. the trajectories do not contribute to the residence time whenever $I_p > 10°$.

4. In most cases, different trajectories provided different values of T_{ij} for the same cell. Then, in the end we took the average over all the values of T_{ij} we got. On the other hand, some cells were never occupied by any trajectory, and were arbitrary assumed to have $T_{ij} = 0$.

The whole procedure can be visualized in Fig, 6. We show there the evolution of the proper elements of five particles in our simulation, three of them at the left side of the ν_{16} line, and the other two at the right side. The grid of cells is indicated by the dotted lines. The proper elements are sampled every 0.1 Myr, and the time of residence should be roughly proportional to the density of points of each trajectory in each cell. Since T_{ij} can be considered as a measure of the average dynamical diffusion in the i, j cell, we ended up with a bi-dimensional map of the diffusion inside the 2:1 resonance. This map is shown in Fig. 7. In this figure, the color scale is such that green/reddish cells have the shortest residence times, blue/dark ones have the longest, and blank cells have zero residence time. For the sake of comparison, we have superimposed the location of the stable asteroids (yellow dots) and the marginally unstable ones (red dots), with their corresponding error bars. It is worth recalling that this map is a portrait of the diffusion only for $I_p \leq 10°$.

Several features can be appreciated in Fig. 7: (i) The residence time is relatively short ($\sim 10-20$ Myr) along a strip that follows the line of the ν_{16} secular resonance (recall that the dashed line only indicates the approximate location of this resonance). (ii) The residence time is large at both sides of the ν_{16} line, but the longest times (~ 1 Byr) are observed in the region between $3.22 < a_p < 3.24$ AU and below the υ_{16} line. This region matches very well the present location of the stable asteroids (yellow dots), and we will refer to it as Region Z (after Zhongguo). (iii) The marginally unstable asteroids are located in the region $3.205 < a_p < 3.22$ AU where the average residence time is compatible with their typical lifetimes ($\sim 100 - 500$ Myr). However, we must note that some of these asteroids have inclinations larger than 10°, and the red dots are only their projections on the map. We will call this, Region G (after Griqua). (iv) The lower right region of the map is covered by blank cells. This is because the initial conditions in that region have their inclinations and amplitudes of libration excited to larger values in relatively short time-scales ($\ll 10$ Myr). This behavior could be related to the ν_{16} resonance. (v) The upper and lower left corners of the plot are also empty, because trajectories reaching those regions are fastly driven to higher eccentricities, and escape in time-scales $\ll 10$ Myr. Since this is the region of strong chaos, we will call it Region C. (vi) Finally, there is a large region at the right side of the ν_{16} resonance, between $3.225 < a_p < 3.26$ AU, $e_p > 0.32$, and below the IB line, where the average residence time is about 1/4 of that in Region Z. However, no asteroid is observed there, exception made of two asteroids at $e_p \simeq 0.48$ (2000 CM67 and 1032 T-1), which do not lie in the most stable place. Following the same convention applied in other papers (Ferraz-Mello et al., 1998a,b; Nesvorný and Ferraz-Mello, 1997a,b), we will refer to this region as Region A[5]. It is worth noting that, in Fig. 7, we are showing the "present" location of the real asteroids (proper elements over 0.1 Myr), but the time of residence in each cell has been estimated over the whole age of the Solar System (4 Byr). Then, due to the intrinsic diffusion of the proper elements, we should not expect to see a perfect matching between the location of the stable asteroids and the most stable cells. This is why in Fig. 7 some red dots seem to lie in more stable cells than some yellow dots.

[5]In those papers, Regions Z+G are referred to as Region B.

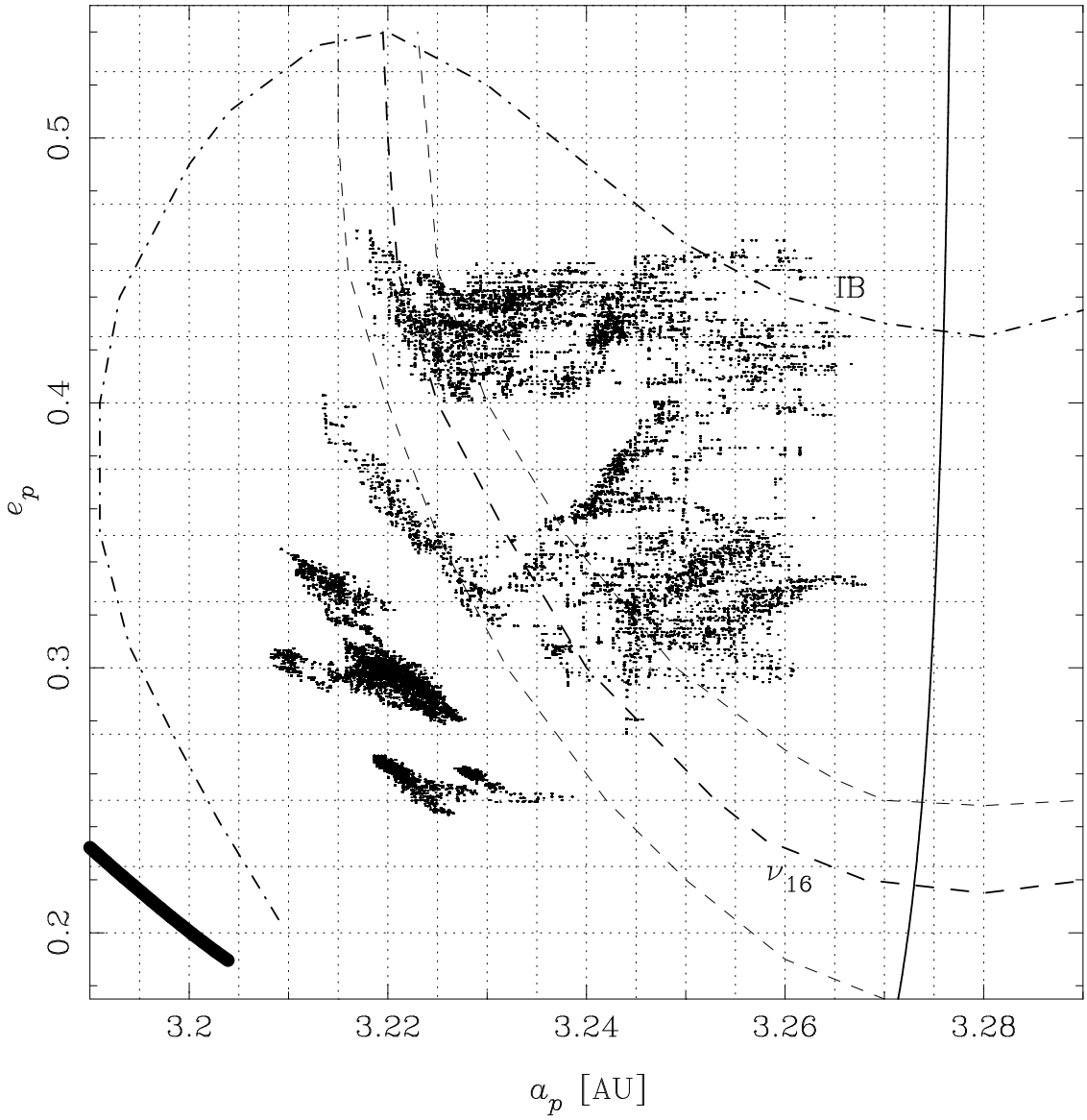

Fig. 6.— The evolution of resonant proper elements for some particles in our simulation. The ν_{16} resonance is marked by three dashed lines representing its center and separatrices. Three particles are located initially at the left side of the ν_{16} resonance, at about $e = 0.25$, 0.30 and 0.33 respectively. Two particles are initially at the right side of the ν_{16} line, above and below $e = 0.40$, respectively. This latter one shows a clear diffusion path along the ν_{16} resonance between $0.33 < e < 0.40$. The density of points in each cell (dotted lines) is proportional to the residence time in that cell.

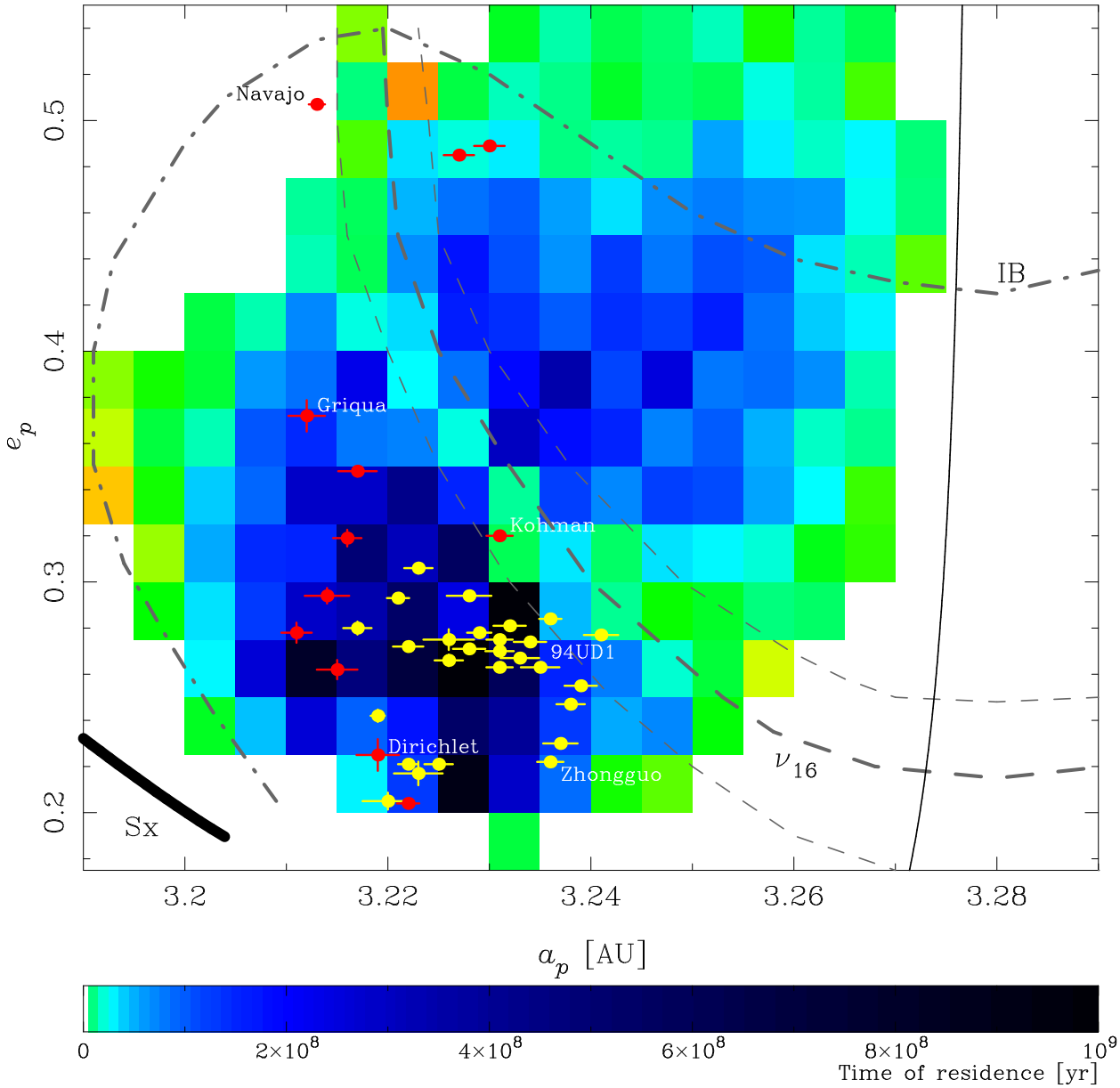

Fig. 7.— Map of the diffusion (residence time) inside the 2:1 resonance. Blue/dark cells have the longest residence times, and green/reddish ones have the shortest ($\ll 50$ Myr). Blank areas are not mapped ($\equiv$ zero residence time). The stable and marginally unstable asteroids are shown in yellow and red dots, respectively. The ν_{16} resonance is marked by three dashed lines corresponding to its center and separatrices.

Comparing Figs. 6 and 7, it is easy to understand why the residence times in Regions Z and G are larger than in Region A. However, the actual difference is not too big. Table 4 lists the average residence times, $\overline{T}$, in the different regions. The first column gives the values of $\overline{T}$ computed from the values of T_{ij} in a grid with $\Delta I = 10^\circ$ (i.e., the same used to mount Fig. 7). The second column gives the same values, but using a grid with $\Delta I = 5^\circ$, that is, neglecting the contribution of trajectories with $I_p > 5^\circ$. Note that in Region A, $\overline{T}$ is quite sensitive to the upper cutoff in inclinations, which means that many trajectories in that region have their inclinations significantly excited. On the other hand, in Region Z, $\overline{T}$ increases for the lower cutoff in I_p. This means that trajectories in that region do not have their inclinations excited, and for larger cutoffs in I_p the region receives the contribution of highly-inclined orbits from the neighboring regions. In any case, the values of $\overline{T}$ in Region A are only some 50% smaller than those in Region G, and this is not enough to justify the almost absence of objects in Region A. In the following, we will try to give some insight into this problem, using a statistical approach.

3.1. A random-walk model of the long term dynamics

The map of residence times computed in the previous section can be used to mount a model of bi-dimensional random-walk to describe the resonant dynamics. The basic idea underneath this approach is that the long term dynamical diffusion can be roughly modeled by a statistical process. We know that this is not quite true, because the resonant motion is far from being "Brownian". However, a model of random-walk with carefully chosen boundary conditions can provide a rough description of the dynamics at a very low computational cost. The statistical validity of the model relies in its application to a huge set of test particles.

We mounted a very simple model of random-walk where a particle in the cell (a_i, e_j), at time t, is randomly moved to one of its eight neighboring cells after a time $t + T_{ij}$. The process starts at $t = 0$ and is repeated until $t = 4.5$ Byr, when the final location of the particle is recorded. The jumping probability is not the same along a_p and e_p. In fact, we know from our simulations that most orbits in the space of proper elements tend to have an elongated shape along the lines of $N = \text{const.}$ (Eq. 4), which are related to levels of $e \sim \text{const}$. This is more or less evident in the examples shown in Fig. 6. Then, in order to account for this and other properties of the resonant motion, we adopted the following boundary conditions: (i) The particles always jump along a_p to one neighboring cell. The jumps have equal probabilities in both directions (left/right). (ii) The particles jump along e_p following a given probability $p_e \leq 1$. The jumps have equal probabilities in both directions (up/down). (iii) Due to the symmetry of the resonant motion with respect to the resonance center, the particles that reach a blank cell with $a_p > 3.25$ AU are "reflected" by putting them back in their previous (non bank) cell. (iv) Particles reaching any other blank cell are deactivated from the simulation.

Using this model of random-walk, we simulated the evolution of a hypothetical primordial population of resonant asteroids. The initial conditions were set assuming that the particles were

randomly distributed in a, e and σ, and that all had $I \leq 10^\circ$. It is worth recalling that a uniform distribution in a, σ translates into a non uniform distribution in A_σ. This is because trajectories with large amplitudes of libration occupy larger volumes in the phase space, due to the natural topology of the resonant problem[6]. The area $V(a_p, e_p)$ enclosed by a resonant trajectory in the plane a, σ, can be easily estimated from the averaged circular-planar restricted three body problem as follows: (i) for different levels of the invariant N (Eq. 4), we calculate the integral

$$V(a_p, e_p) = \int_0^{\tau_\sigma} (a(t) - a_{\rm res})\ \dot{\sigma}\ dt \tag{7}$$

where $a(0) = a_p$, and τ_σ is the libration period of the trajectory; (ii) assuming a uniform density of particles, δ, throughout the resonant space, the number of particles between a' and $a' + \Delta a'$ at a given e' can be determined approximately as:

$$\Delta N(a', e') = \delta \times \frac{dV(a', e')}{da_p} \times \frac{\Delta a'}{\Delta V^*} \tag{8}$$

where $\Delta V^* = \Delta V(a_p^*, e_p^*)$ is a normalization factor, corresponding, for example, to the largest possible area occupied by the trajectories. ΔN grows with increasing amplitude of libration, as dV/da_p also does. It also has a weak dependence with the eccentricity since, for constant a_p, the area $V(a_p, e_p)$ is smaller at larger e_p. Then, we started the simulation with a uniform density $\delta = 1000$ particles per cell, and evolved them over the age of the Solar System. The simulation was repeated several times, using different values of the probability p_e. Figure 8 shows the results of a simulation using $p_e = 0.35$. This value was inferred from the average ratio of dispersion along e_p and a_p that is observed in Fig. 6. Each panel in Fig. 8 shows the number of particles per cell at different times during the evolution of the system: (a) $t = 0$, (b) $t = 1$ Byr, (c) $t = 2$ Byr, (d) $t = 3$ Byr, (e) $t = 4$ Byr and (f) $t = 4.5$ Byr. The darker the cell the larger the number of particles. Panel (a) reflects the initial distribution of the particles, according to Eq. (8). In panel (f) we also plot the location of the stable (white dots) and marginally unstable asteroids (black dots). In all panels but (a), we can appreciate a difference in the overall number of survivors between Regions A and Z. According to this simulation, the largest number of surviving particles occurs in Region Z. Figure 9 shows the final states, at $t = 4.5$ Byr, from two other simulations: (a) using $p_e = 0$, and (b) using $p_e = 1$. In the former case, the particles never jump along e_p. We can see that the overall number of survivors is smaller in the latter case.

Table 5 summarizes the results of these simulations. The first six rows give the number of survivors per cell in Regions A and G, normalized to the number of survivors per cell in Region Z. The last row gives the observed values. According to these results, our random-walk model gives reasonable estimates of the ratio between the number of asteroids in Regions G and Z. However, the ratio between the amount of asteroids in Regions A and Z is an order of magnitude overestimated.

[6]In other words, a uniform distribution in the space of osculating elements implies a non uniform distribution in the space of proper elements

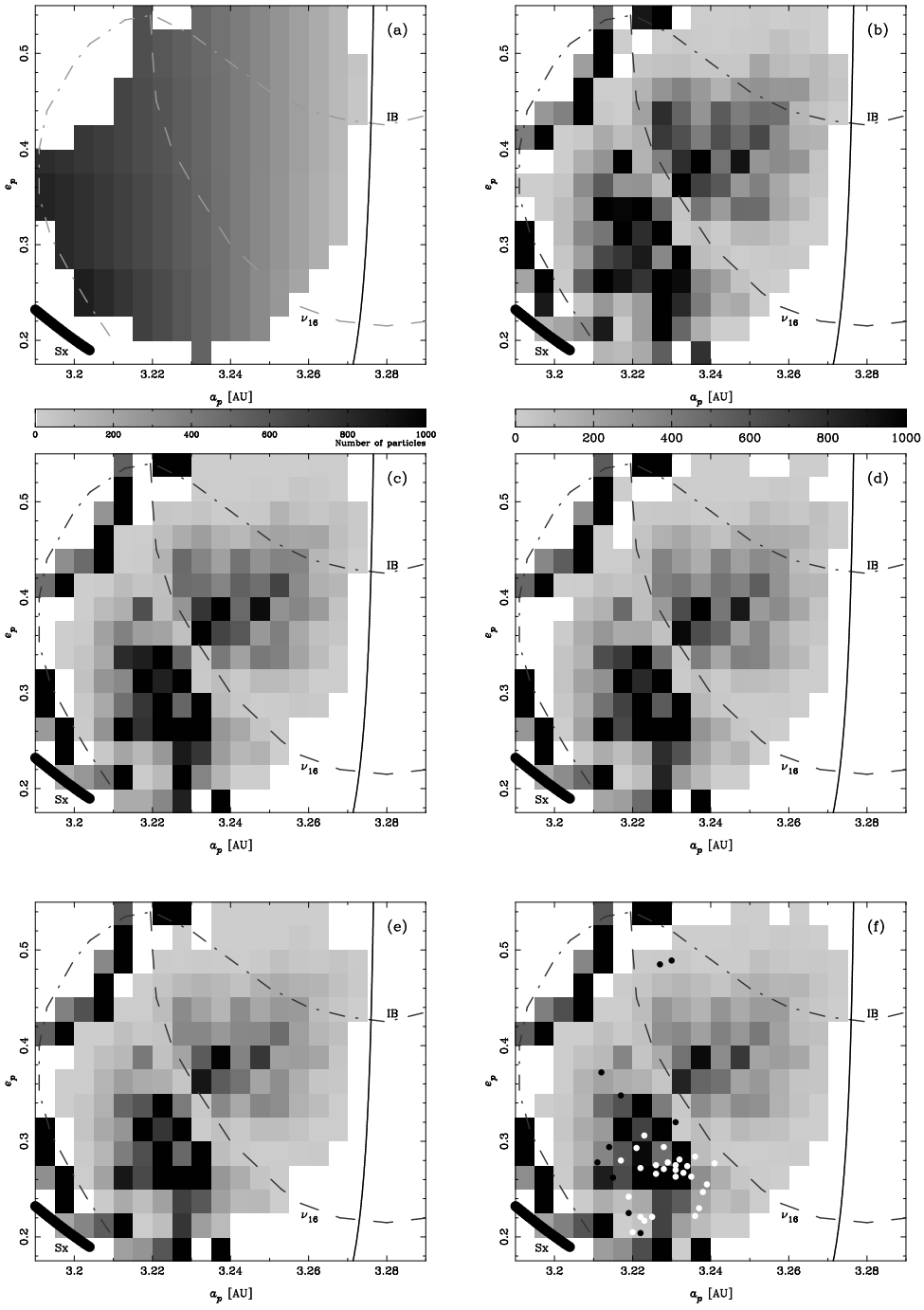

Fig. 8.— Six stages in the evolution of fictitious test particles using a random-walk model with $p_e = 0.35$: (a) $t = 0$, (b) 1 Byr, (c) 2 Byr, (d) 3 Byr, (e) 4 Byr and (f) 4.5 Byr. The panels show the number of particles per cell. The darker regions concentrates the largest number of particles. The last panel also shows the location of stable and marginally unstable asteroids (white and black dots, respectively).

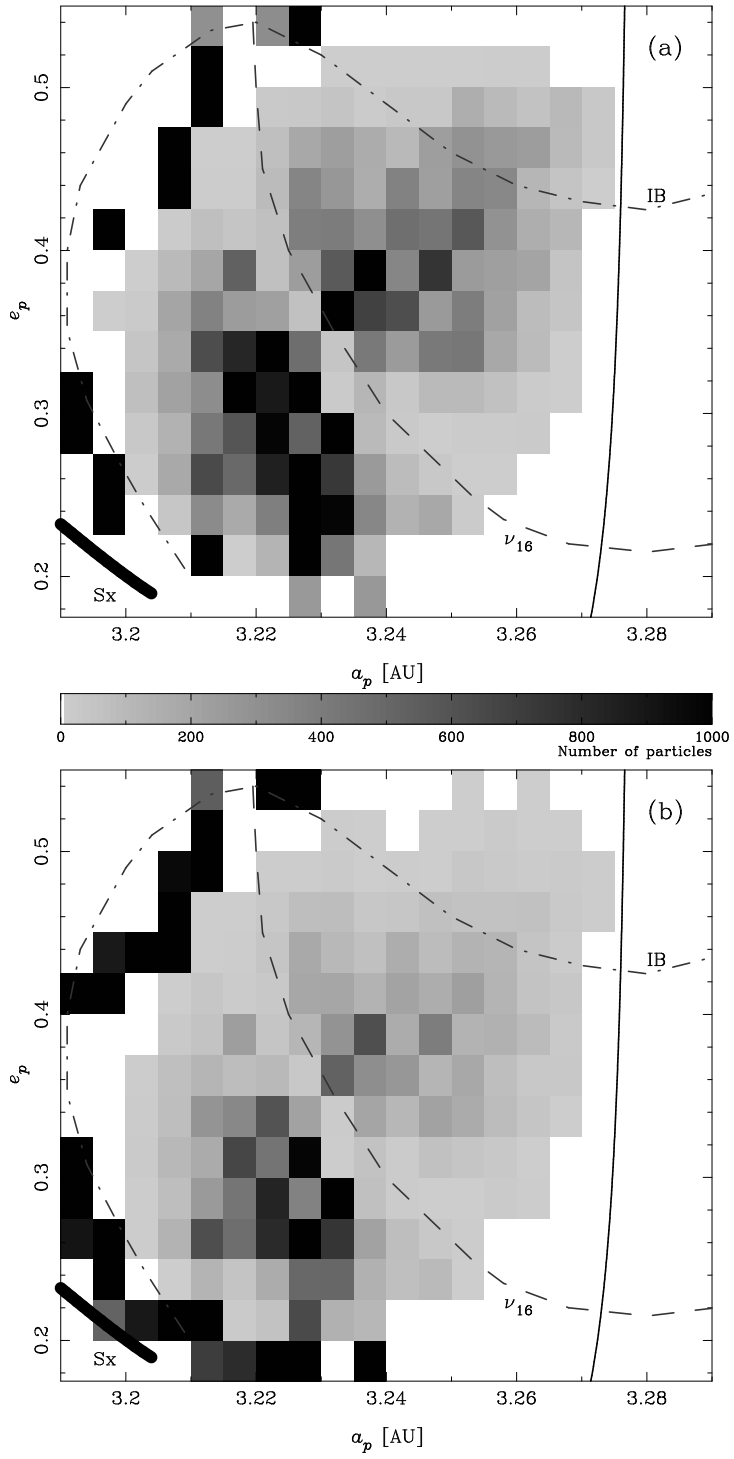

Fig. 9.— Final stage ($t = 4.5$ Byr) in the evolution of fictitious test particles using two random-walk models: (a) $p_e = 0$, and (b) $p_e = 1$.

This could indicate that there is some dynamical mechanism operating in Region A that we are not taking into account in our simplified model. Otherwise, we should expect to observe about 10 asteroids in that Region, which up to know were not yet discovered.

We cannot forget that our model has several limitations: it is bi-dimensional only, it has quite forced boundary conditions, it simulates a quasi-random behavior, and the definitions of the limits of each Region are quite arbitrary. Moreover, it assumes that the planets have been in their present orbits over the age of the Solar System, without taking into account the possible effects of the planetary migration (e.g., Ferraz-Mello et al., 1998) But in spite of these limitations, the most important result of the model is that it provides a strong evidence that the Zhongguos (and particularly the cluster of 1994 UD1) could have survived in their present location over the age of the Solar System. Our conclusion is that, *from the dynamical point of view, the Zhongguos could be the remnants of a primordial resonant population*. We will return to this subject later in Sect. 4.

To close this section, let us note that, as a by-product of our random-walk simulations, we can obtain some interesting information about the unstable asteroids. Looking at Figs. 8 and 9, we can see that a large amount of particles accumulates in Region S (near the IB line). This is because the particles are deactivated whenever they reach a cell with zero residence time, remaining in that cell until the end of the simulation. Since Region C coincides with the region where the unstable asteroids are located, we can assume that the deactivated particles contribute to resupply the population of unstable asteroids. According to our random-walk models, we can estimate that $\sim 1.2\%$ of the particles in Region Z at $t = 4.5$ Byr, were able to reach Region C in the last 100 Myr of evolution (i.e., between 4.4 and 4.5 Byr). Since at present we observe some 20 Zhongguos, we can conclude that about 0.2 of these objects arrived to Region C in the last 100 Myr. Now, the population of unstable asteroids has typical lifetimes smaller than 100 Myr, and at present we observe some 20 of such asteroids. Then, this population should be resupplied at a rate of about 0.2 objects per Myr. Since this rate is two orders of magnitude larger than that provided by the Zhongguos, we conclude that the unstable asteroids are unlikely to come from inside the 2:1 resonance, and their origin should be searched for on some extra-resonance source. We will leave a detailed analysis of this problem to a future paper.

3.2. The effect of Yarkovsky forces on the resonant diffusion

In the previous sections, we have analyzed the long term dynamics of the 2:1 resonance considering only gravitational perturbations from the major planets. However, we neglected other kind of perturbations that could contribute to enhance the diffusion in the most stable places of the resonant phase space. In this context, it would be interesting to discuss the effect of non conservative forces, such as Yarkovsky effect.

Yarkovsky effect, hereinafter YE, is a relatively new subject in celestial mechanics. The effect

arises from the thermal recoil suffered by a rotating object, and translates into an increase or decrease of the energy of the body (Afonso et al., 1995). In fact, two variants of the effect have been identified: the diurnal effect, related to the period of rotation, and the seasonal effect, related to the orbital period of the body (Rubincam, 1995). While the former can cause an increase or decrease of the energy depending on the rotation being prograde or retrograde, the latter always causes a decrease of the energy. Each one can be dominant over the other, depending on the values of the various parameters involved (Farinella and Vokrouhlický, 1999). The most critical parameters are the distance to the Sun r, the diameter of the object D, its rotational period τ_d and the thermal conductivity of its surface K. Both effects decrease with increasing r and D. The diurnal effect also decreases with increasing τ_d. For very low values of K, as in the case of regolith-covered and stony bodies, the diurnal effect is dominant, while for larger values, typical of basalts and irons, the seasonal effect dominates.

For a typical non resonant asteroid, the energy balance between both variants of YE translates into a net drift in semi-major axis, while e and I remain almost unchanged. This drift has proved to play an important role in enhancing the dynamical diffusion of the members of asteroidal families in the main belt (Nesvorný et al., 2001), and we could expect to find a similar result in the case of the resonant asteroids in the Hecuba gap.

In order to accomplish this study, we modified Swift to include the components of the acceleration due to YE. Our Yarkovsky model closely follows the formulas of Vokrouhlický et al. (2000), where the body is assumed to have spherical symmetry, so the heat equation that describes the surface thermal conduction has an explicit analytical solution by series.

Using our Swift+YE code we re-integrated the 50 leftmost initial conditions in Fig. 5 ($3.20 < a < 3.245$ AU), taking into account both components of YE. The Yarkovsky parameters were chosen similar to those corresponding to typical regolith-covered bodies (see Farinella et al., 1998), that is: $K = 0.0015$ W m^{-1} K^{-1}, $C = 680$ J kg^{-1} K^{-1} (specific heat), $\rho = 3500$ kg m^{-3}(core density), and $\rho_s = 1500$ kg m^{-3} (surface density). We also set $A = 0.05$ (albedo), and $\varepsilon = 1$ (infrared emissivity). The direction of the spin components (s_x, s_y, s_z) of each particle were chosen at random, with $s_z > 0$ (prograde rotation). With this choice of parameters, the diurnal effect should dominate over the seasonal one, causing a net gain of energy in the particle. We assumed all particles having a diameter $D = 6$ km, which is compatible with the observed sizes of the stable resonant asteroids (see Sect. 4). Following Farinella et al. (1998), we further assumed a size dependent rotational period, such that $\tau_d = 10^5$ sec. The total integration time spanned 1 Byr with a time step of 0.08 yr.

The first result of our YE simulation is presented in Fig. 10, where the (percentual) number of surviving particles is plotted against the time. By the end of the YE simulation, 48% of the particles had escaped, while only 42% did it in the simulation without YE. However, the two curves in Fig. 10 show more or less the same trend, which could means that YE does not actually play a significant role in the overall diffusion. In any case, it is difficult to elaborate some definite conclusion from the results shown in this figure.

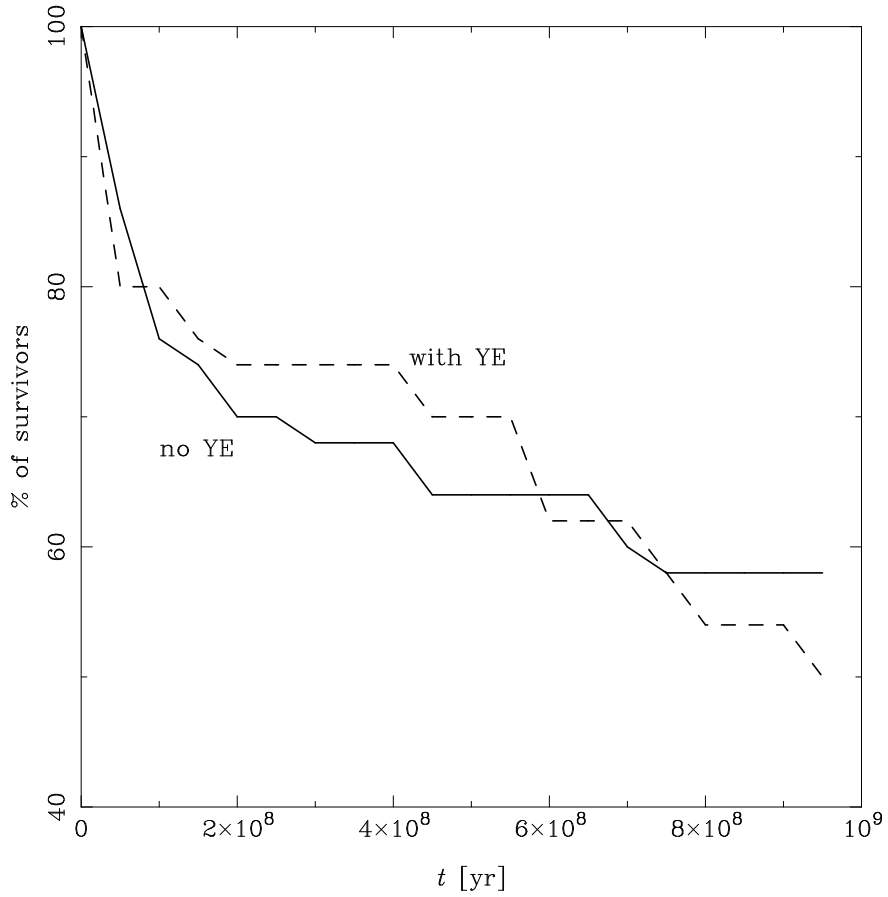

Fig. 10.— Percent of surviving particles as a function of time, for two simulations: (i) not including Yarkovsky effect (full line), and (ii) including it (dashed line).

In order to make a deeper analysis of our simulations, we proceeded to compute diffusion parameters. *A diffusion parameter can be considered as any quantity able to provide information about the chaotic change of the proper elements with time*[7]. In our case, we defined two different parameters:

1. If $\overline{E}_n$ is the time average of the proper element over the interval $n\tau$, the first parameter will be its standard deviation:
$$\sigma_E = \sqrt{\sum_{k=1}^{n} \frac{\left(E(k\tau) - \overline{E}_n\right)^2}{n-1}} \tag{9}$$
This is related to the average dispersion of the proper element in the phase space.

2. The second parameter is obtained by fitting the time series of the proper element to a straight line. The slope of this fit, β_E, (in absolute value) gives the average rate of change of the proper element.

The values of σ_E and β_E for a_p, e_p, I_p, over $t = 1$ Byr, are shown in Fig. 11. We plot in the abscissas the diffusion parameters from the simulation without YE, and in the ordinates, those from the simulation with YE. We do not plot the parameters of the particles that escaped before 1 Byr, because these are biased by the strong variation that the proper elements suffer during the stages previous to the escape. It is interesting to note a trend to larger values of the parameters for e_p in the simulation with YE, and also, although less evident, a similar trend for I_p. On the other hand, no trend at all is observed for a_p. These results indicate that YE would enhance the diffusion mainly in eccentricity and inclination, rather than in semi-major axis. This behavior is not surprising, and can be easily understood in the framework of the theory of adiabatic invariants. The main idea underlying this theory is that a non conservative force outside the resonance will cause an increase/decrease of the averaged semi-major axis. However, inside the resonance the averaged semi-major axis is locked, and the gain/loss of energy is transferred to the other momenta (e and I), while the amplitude of libration behaves as an adiabatic invariant of the system. This mechanism can be described using very simple analytical models (e.g., Gomes, 1995,1997), and has been applied to explain the resonant capture in the context of drag forces (e.g., Beaugé and Ferraz-Mello, 1993,1994). According to these models, we should expect that a particle drifting outwards and encountering an inner mean motion resonance, will be captured by the resonance, will stop to drift in semi-major axis, and start to continuously increase its eccentricity. This would be the scenario in our simulation, since the YE parameters were chosen such that it always induced a gain of energy in the particles (prograde rotation and diurnal effect dominant),

---

[7] A particular case is the diffusion coefficient which comes from the solution of the diffusion equation, and it is usually defined as
$$\mathcal{D}_t = \frac{\langle \Delta x^2 \rangle}{t}$$
where $\langle \Delta x^2 \rangle$ is the average quadratic spatial dispersion over time t.

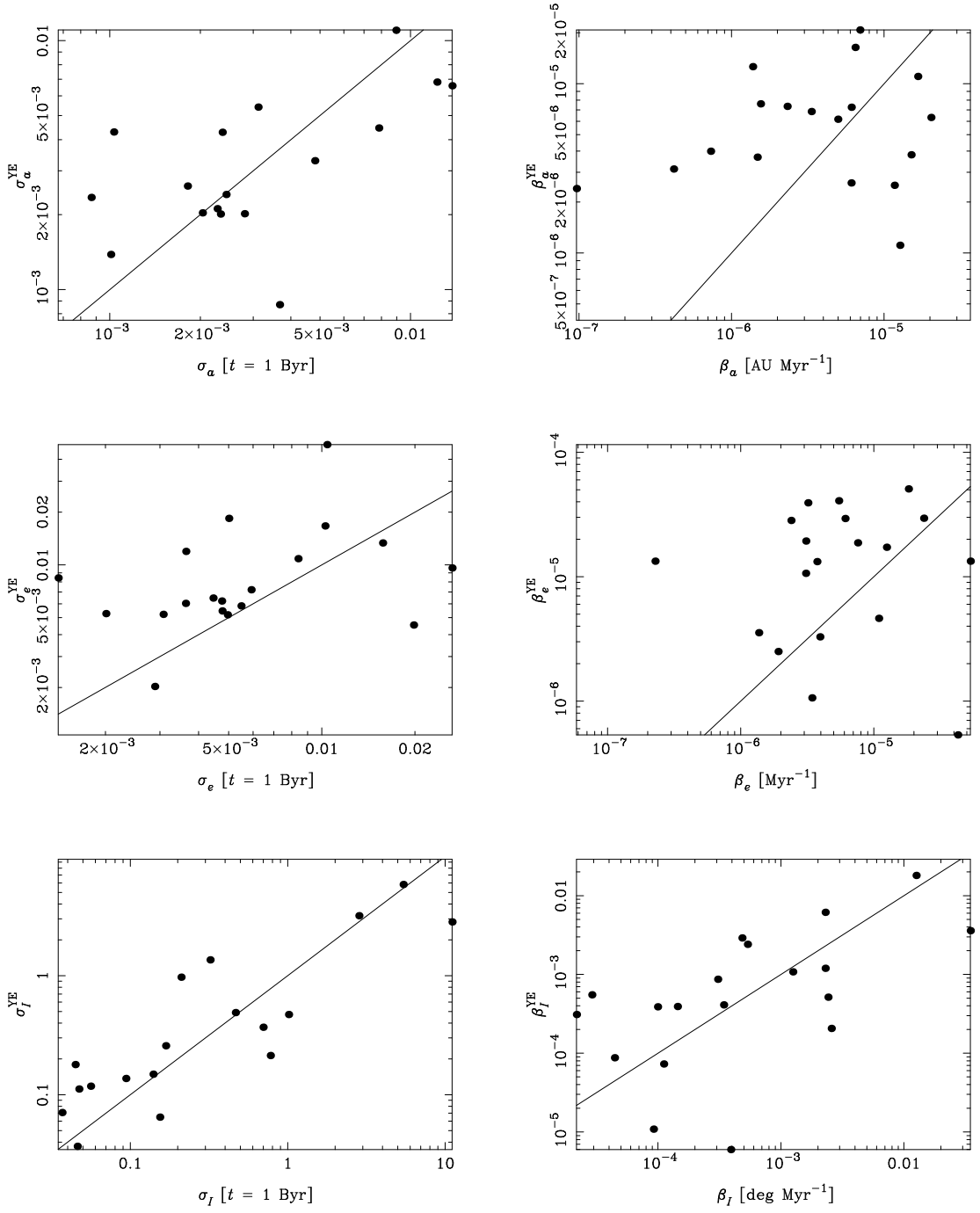

Fig. 11.— Diffusion parameters σ_E and β_E for each proper element in the simulation without YE (in the abscissas), and comparison with the same quantities in the simulation with YE (in the ordinates). Each dot corresponds to one particle in the simulations. Only particles that survived over 1 Byr in both simulations are shown. The solid lines correspond to the identity function.

Of course the above picture is a very simplified approach to the real problem. In fact, the interaction of a weak non conservative force, like YE, with the inner dynamical structure of a mean motion resonance, could be much more complex than we can imagine. Although our results do not provide much insight on this subject, our conclusion is that Yarkovsky forces do not seem to cause any significant enhancing of the diffusion inside the 2:1 resonance. This would be true at least for asteroids larger than 6 km in diameter, but we could expect that smaller objects would be more affected. In any case, the results presented in Fig. 11 needs to be verified by further simulations, using several different values of the YE parameters and a much larger set of test particles. Meanwhile, the mechanisms of interaction between YE and mean motion resonances still remain an open problem for future studies, both analytic and numeric.

3.3. The role of mutual scattering

We will try in this section to briefly discuss the possible role of mutual scattering in enhancing the diffusion of the stable resonant asteroids. By mutual scattering we understand the perturbations caused by close encounters with other asteroids, disregarding the possibility of impacts and fragmentation.

According to their typical eccentricities, both the stable and marginally unstable asteroids are potentially able to have close encounters with main belt asteroids. The Zhongguos can reach values of q as smaller as 2.35-2.50 AU, which put them in crossing orbits not only with the largest asteroids (Ceres and Pallas) but also with most of the large asteroidal families. They can also reach values of Q as large as 4.15 AU, allowing them to have close encounters even with the Hilda group. This means that the intrinsic collision probability of the Zhongguos would not be too different from the typical collision probability estimated by Farinella and Davis (1992) for main belt asteroids.

Which could be the actual effect of a large number of close encounters on the long term stability of the 2:1 resonant bodies? An answer to this question would require a deep analysis of the collisional evolution of the Zhongguos, that is well beyond the scope of the present paper. It would be quite difficult to quantify the actual diffusion induced by mutual scattering without performing a large set of accurate simulations. However, recent studies (Carruba et al., 2000) indicate that mutual scattering could contribute to the semi-major axis mobility of main belt asteroids, although only the largest asteroids (Ceres, Pallas and Vesta) seem to have a dominant scattering effect throughout the main belt. According to Monte Carlo simulations (Bottke, personal comm.), the close encounters between Ceres and a small body at $\sim$ 3.27 AU could be responsible for an overall dispersion of about 1/100 AU per Byr in proper semi-major axis, or maybe less. Then, we conclude that it is rather improbable that mutual scattering can significantly destabilize the Zhongguos, although this possibility cannot be ruled out without a previous, more detailed, study.

On the other hand, we have no reason to ignore the possible effect of actual collisions, i.e. fragmentation. In the next section we will discuss this problem in the context of the size distribution

of the resonant population.

4. Size distribution

The last topic we will analyze and discuss in this paper concerns the size distribution of the resonant asteroids in the Hecuba gap. This, together with the results of the previous sections, will provide the necessary background for the future discussion about the origin of these objects.

The size distribution of a given population gives information about its collisional evolution. For example, we know that the outcomes of a breakup event will have a quite steep size distribution, and their subsequent collisional evolution will make this distribution more shallow. Unfortunately, in the case of the 2:1 resonant asteroids we do not know their actual size. In fact, there is only one object, (1362) Griqua, with known IRAS albedo (= 0.0667). Then, the sizes of the remaining asteroids have to be estimated by arbitrarily assuming a mean albedo. This estimation was accomplished by the following formula

$$\log D = 3.1296 - 0.2H - 0.5 \log A \tag{10}$$

(Muinonen et al., 1995), where D is the diameter, A the albedo, and H is the absolute magnitude, which is normally provided in most asteroids' databases. We assumed a mean albedo $A = 0.05$. This value seems to be a good compromise between the typical albedos of C-type and D-type asteroids, which are the most frequent types in the outer asteroid belt ($a > 2.8$ AU).

The estimated diameters of the resonant asteroids are listed in the last column of Tables 1, 2 and 3. We can see that all of them but Griqua have a sizes smaller than 22 km. Then, their typical collisional lifetimes should be between 1 and 2 Byr, (Farinella and Davis, 1992) which would imply that they are unlikely to be primordial in the resonance. However, we must recall that the collisional lifetime is rather a sufficient condition for primordiality, but not a necessary one[8]. A deeper insight in this problem can be achieved by analyzing the size distribution itself.

The cumulative size distributions of the resonant asteroids are shown in Fig. 12a. The full line (marked Z) is the size distribution of the Zhongguos, while the dashed line (marked G+U) is the joint distribution of the marginally unstable (Griquas) and unstable populations. The dotted lines are the power-law best fits of the distributions (the so-called *Pareto* distributions, see Petit and Farinella, 1993), in the range where we assume they are complete, that is, $D \geq 10$ km. The power-law exponent, α, is indicated in each case. Fig, 12b shows a comparison between the Zhongguos' distribution and the distribution of Themis family (dashed line marked T)[9]. The mean IRAS albedo

[8]In other words, large asteroids are certainly primordial but primordial asteroids are not necessaryly large

[9]To identify the present members of this family, we have applied the Hierarchical Clustering Method (Zappalà et al. 1990) to the 66089 proper elements database of Milani and Knezevic (http://hamilton.dm.unipi.it/astdys). We have used the d_1 metric with a cutoff of 100 m s^{-1}.

of this family is 0.08 ± 0.03, but we used here a value 0.05, compatible with our previous assumption. The power-law, in this case, was fitted in the range $10 \leq D \leq 60$ km.

The most remarkable feature observed in Fig. 12 is the rather high steepness of the Zhongguos' distribution. According to the simplest collisional models, the distribution of a collisionally relaxed population should tend to a power-law with coefficient $\alpha \sim -2.5$ (Dohnanyi, 1969). Then, the steepness of the Zhongguos could indicate that they are a "fresh" population, in the sense that they could have been formed very recently, and still have not had enough time to evolve to a more shallow distribution. On the other hand, the steepness could actually be the consequence of other mechanisms. In the following, we will discuss different approaches to this problem.

Observational bias

The sizes of both Zhongguos and Griquas are below the limit of observational completeness for that region of the asteroid belt. According to Jedicke and Metcalfe (1998), this limit is about 24 km in diameter. However, since all these objects are concentrated in the same small region of the belt, it is difficult to attribute the steepness of the Zhongguos to an observational bias. In any case, such bias would affect the low-sizes tail of the distribution, rather than large-sizes end, and the discovery of new smaller objects will tend to make it even steeper. It is worth noting that about 2/3 of the Zhongguos have been discovered in the last 5 years, all of them having diameters smaller than 14 km (see last column of Table 3). Then, it seems unlikely to discover a Zhongguo-type asteroid larger than 20 km in the future, although this possibility cannot be ruled out.

Concerning a wrong assumption on the albedo, this would not change the slope of the distribution, but rather shift it along the abscissas, since all asteroids are assumed to have the same albedo. Different albedos for each object could actually change the slope of the size distribution, and make it more shallow (or steeper), but we have no means to actually quantify this. On the other hand, we cannot rule out the possibility that the absolute magnitudes be poorly, or even badly, estimated.

Finally it could be possible that the steepness be simply due to a statistical bias, from the fact of being looking at a quite small sample of objects.

Dynamical bias

According to the results in Sect. 3, we can assume that the Zhongguos are the actual survivors of a hypothetical primordial population of resonant bodies. Then, the smallest objects of this primordial population, being initially more numerous, would have a statistically larger chance to become trapped in the most stable places of the resonance, surviving there over the age of the Solar System. This chance can be easily quantified by comparing the size distribution of the 2:1 resonant objects with that of the Hilda group, in the 3:2 resonance. We know that the Hildas should be

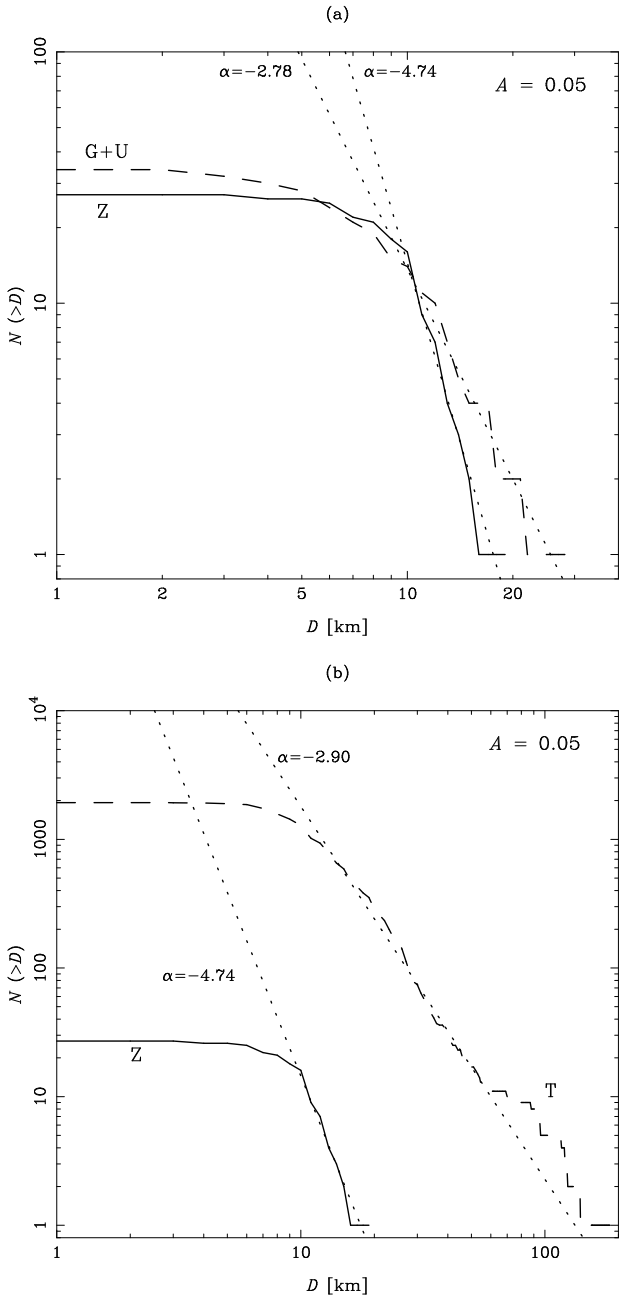

Fig. 12.— (a) Size distributions of the resonant asteroids in the Hecuba gap. Full line correspond to the Zhongguos and dashed line are the joint distributions of Griquas and unstable asteroids. The dotted lines are the fits of power-laws (*Pareto* distributions) with exponent α, in the range $D \geq 10$ km. (b) Comparison between the size distribution of Zhongguos (full line) and Themis family (dashed line). In this latter, the power-law was fitted in the range $10 \leq D \leq 60$ km. In all cases, we assumed a mean albedo $A = 0.05$ to compute the unknown sizes

primordial in the 3:2 resonance, because of the sizes of their largest members (> 100 km) and their typical taxonomy (D-type), In order to compare the two populations, we will make the following assumptions: (i) the initial primordial populations in the 2:1 and 3:2 resonances had similar size distributions; (ii) the primordial populations had initially low inclinations, and were randomly distributed in a, e and σ; (iii) the collisional evolution of both 2:1 and 3:2 resonant populations were more or less the same over the age of the Solar System; (iv) the present size distribution of the Hildas is similar to the primordial one. Under these assumptions, if $N_z(D)$ and $N_h(D)$ are the cumulative size distributions of Zhongguos and Hildas, respectively, then we can write down the following relation:

$$N_z(D) = \frac{n_z\,\Delta V_z}{n_h\,\Delta V_h} N_h(D) \tag{11}$$

where n_z, n_h are the total number of presently observed Zhongguos and Hildas, respectively, and

$$\Delta V = \frac{dV}{da_p} \Delta a_p \Delta e_p \Delta I_p \tag{12}$$

is the volume occupied by each population in the space of proper elements, which is computed with the aid of Eq. (7). Equation (11) can be used to predict the present size distribution of the Zhongguos from the observed distribution of the Hildas.

Table 6 shows the assumed values for the different quantities in Eqs. (11) and (12). The result is shown in Fig. 13. The size distribution of the Hildas (dashed line marked H) was computed assuming a mean albedo 0.05 (which is, in fact, the mean IRAS albedo of this population). A power-law distribution (dotted line) was fitted in the range $40 \leq D \leq 126$ km. This power-law was extrapolated to the Zhongguos' case (dotted-dashed line) according to $N_z(D) = 0.055\, N_h(D)$.

Form Fig. 13 it is evident that the actual distribution of Zhongguos cannot be reproduced from that of the Hildas. This would indicate that the Zhongguos are not primordial in the resonance. Otherwise we should expect to find at least a couple of Zhongguos larger than 40-50 km. It could be argued that Griqua is, indeed, one of this objects, and actually, in Sect. 3.1, we established a possible dynamical link between Zhongguos and Griquas. However, we must recall that Griqua has a rather high inclination, and from our long term simulations it seems highly improbable that a typical Zhongguo with $I_p < 5^\circ$ can have its inclination excited to $I_p > 20^\circ$ over the age of the Solar System.

On the other hand, it should be noted that the approach given by Eq. (11) is very rough, and involves some assumptions that are not realistic. For example, the collisional evolution at the 2:1 and 3:2 resonance has been actually very different. The 3:2 resonance remained relatively isolated from the main belt over the age of the Solar System, and the collisional history of the Hildas has been mainly dictated by their mutual collisions (Dell'Oro et al., 2001). Meanwhile, the objects in the 2:1 resonance have certainly had a much more active collisional interaction with main belt asteroids, as we discussed in Sect. 3.3. Paradoxally, this should have made the size distribution of the Zhongguos more shallow than that of the Hildas, while in Fig. 13 we have exactly the opposite situation. Another unrealistic assumption is to consider that both populations had the same initial

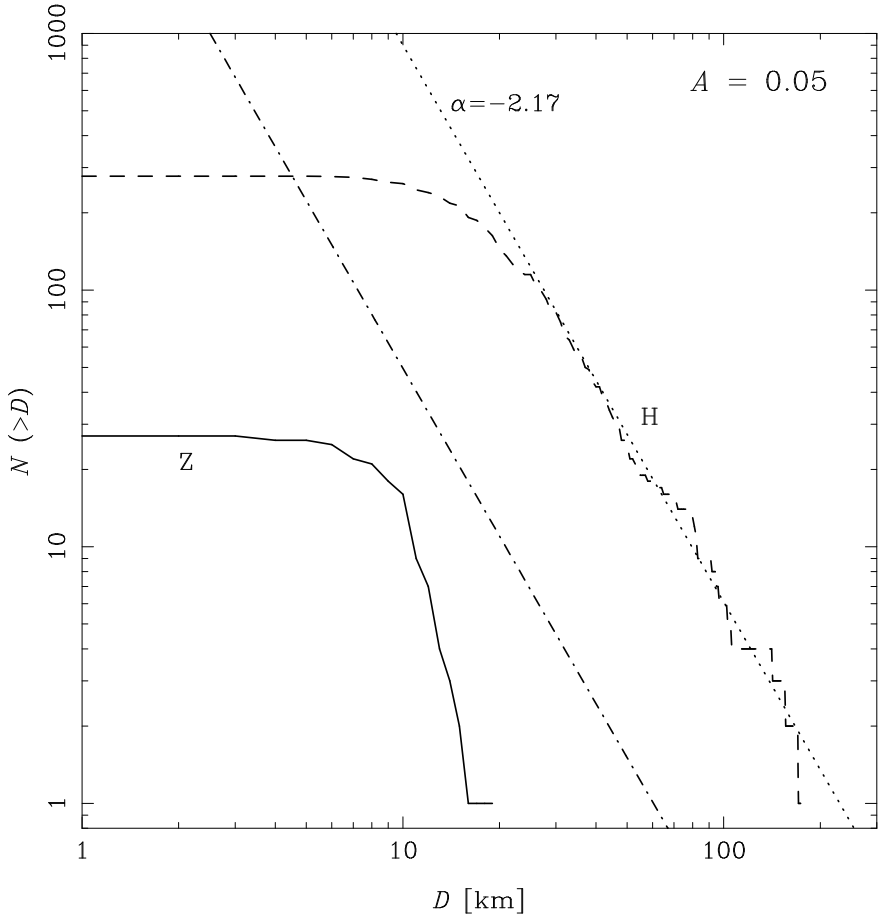

Fig. 13.— Size distributions $N_z(D)$ (full line) and $N_h(D)$ (dashed line) for the Zhongguos and Hildas, respectively. The $\alpha = -2.17$ power-law for the Hildas was fitted in the range $40 \leq D \leq 126$ km. The dotted-dashed line is the extrapolation of this power-law to the case of the Zhongguos, according to Eq. (11).

size distribution, since this strongly depends on the size distribution of the primordial asteroid belt. This distribution is unknown, and maybe it was different in the main belt and in the outer belt.

Finally, we could imagine that the steep size distribution of the Zhongguos is a consequence of the chaotic diffusion in the resonance. In such case, we should find some "perverse" dynamical mechanism that makes the large objects to be more unstable. Chaotic diffusion by planetary perturbations does not have any preference for sizes, and its only effect would be to shift the size distributions in Figs. 12-13 along the abscissas, eventually reducing the total amount of bodies. The same should be applicable for other gravitational perturbations, like mutual scattering, excitation by a swarm of planetesimals (Petit et al., 1999), and planetary migration. Yarkovsky effect do actually depend on the size, but unfortunately, it destabilizes the smallest bodies rather than the large ones.

Breakup event

Another possibility is to assume that the Zhongguos are actually the outcomes of a recent breakup event. In this context, it is easy to understand their steep size distribution, and we believe that this could be the most plausible explanation. However, there are still some open questions: when did this breakup happen, and where is the parent body. None of these questions have a simple answer. Since the distribution is quite steep, one would be tempted to think in a very recent breakup event. On the other hand, the steepness could be the consequence of a particular process of breakup, not necessaryly recent. A good example is the case of the Vesta family, where all the members but Vesta distribute according to a power-law with exponent $\alpha \sim -5.3$.

Concerning the parent body, there are no large asteroids among the Zhongguos. In fact, the largest one is Zhongguo itself, with some 20 km, and it seems less probable that this can be the parent body. Actually, we can think of two possibilities:

1. The parent body was in the most stable place of the resonance (where the cluster of 1994 UD1 is found) from the very primordial times, until it collided with some main belt asteroid. Then, it broke up in several fragments, none of them larger than 20 km. Some of these fragments remained in the region where the parent body was. The remaining ones were ejected outside that island of stability, and were later depleted by the chaotic diffusion of the resonance.

2. The parent body was a main belt asteroid that became temporarily captured in the resonance. It collided with some other main belt asteroid and spread several fragments in the resonant space. Some of these fragments stayed captured in the most stable place of the resonance, where we observe them today. The remaining ones, including the parent body, were depleted by the diffusion.

The problem of any of these scenarios is that the breakup inside the resonance would inject fragments

not only in the region of Zhongguos, but also in other regions (like Regions A and G). This puts an important constraint to the time of the breakup: it should be old enough to allow fragments other than Zhongguos to be depleted from the resonance. According to the stability time-scales of Regions A and G, we have to conclude that this hypothetical breakup must be older than 500 Myr (probably much older). The question is if the resulting fragments would maintain a steep size distribution over such time-scales. Unfortunately, we have no answer to it.

A last possibility could be to assume that the Zhongguos were fragments of the breakup of Themis, as Morbidelli et al. (1995) and Moons et al. (1998) have proposed. In this case, their size distribution would be at the tail of the distribution of Themis family. However, it is not clear whether or not such breakup event can produce the large ejection velocities which are necessary for the fragments to reach the region of Zhongguos. A better discussion of this problem is left to an upcoming paper.

5. Conclusions

In this work, we have studied the dynamical properties and analyzed the size distribution of the asteroids in the 2:1 resonance with Jupiter (Hecuba gap). We have found a presently observed population of about 60 resonant objects that can be divided into three sub-populations:

1. the Zhongguos or stable asteroids, which are able to survive in the resonance for more than 500 Myr
2. the Griquas or marginally unstable asteroids, which escape from the resonance in time scales of the order of some 100 Myr
3. the unstable asteroids, which escape from the resonance in much less than 100 Myr

The Zhongguos account for about 50% of the observed population and are located in the most stable place of the resonant phase space, having a very low inclination ($< 5°$). Most of them form a well defined cluster in the space of proper elements, whose main member is the asteroid (11097) 1994 UD1. According to our simulations, the memebers of this cluster would be able to survive in the resonance over the age of the Solar System, when pure gravitational perturbations of the four major planets are considered. We have further analyzed the possible effect of non planetary perturbations, like Yarkovsky effect and mutual scattering by main belt asteroids. We have found that none of these perturbations is relevant to the evolution of the Zhongguos. Then, we conclude that, from the dynamical point of view, the Zhongguos could be the remnants of a primordial population of asteroids, that survived the depletion of the resonant phase space.

The Griquas lie in a region of transition between the most stable and the most unstable regions of the resonant phase space. According to our simulations, these objects could be the fugitives from

the Zhongguo group, that arrived to their present location due to the natural chaotic diffusion inside the 2:1 resonance.

The unstable asteroids are characterized for their large amplitude of libration. They lie in the most unstable place of the resonant phase space, near the borders of the resonance. Due to their short lifetimes, it is necessary to continously re-supply them, in order to keep their numbers in a steady state. Our simulations showed that the population of unstable asteroids can be re-supplied only from outside the 2:1 resonance, so we need to search for the dynamical mechanisms responsible for this.

We have analyzed the size distribution of the resonant asteroids, and found that the Zhongguos have a quite steep distribution, which is not compatible with the idea of a collisionally evolved population. This implies that the Zhongguos would be a relatively new population, related to a recent breakup event.

While the dynamical properties of the Zhongguos point towards a primordial origin of these objects, their size distribution seems to contradict this idea. Then, the problem of the actual origin of the asteroids in the 2:1 resonance is far from being solved. However, we believe that it is possible to bound it by making a detailed analysis of the several hypothesis we have at hand. At least, this would allow to keep the most plausible ones and discard the others. We will try to give some insight to this problem in an upcomming paper.

F. Roig wish to thank the São Paulo State Science Foundation (FAPESP) for giving financial support to this work through PhD scholarship 97/5806-9. The Department of Space Studies of the Southwest Research Institute at Boulder, Colorado, is highly acknowledge for hosting the four month visit of F. Roig during the final stages of this work. Fruitful discussions with W. Bottke, A. Morbidelli and D. Durda helped to improve the contents of this paper, and are highly appreciated.

REFERENCES

Afonso, G., Gomes, R., and Florczak, M.: 1995. Asteroid fragments in Earth-crossing orbits. *Planet. Space Sci.* **43**, 787–795.

Beaugé, C., and Ferraz-Mello, S.: 1993. Resonance trapping in the primordial solar nebula: The case of a Stokes drag dissipation. *Icarus* **103**, 301–318.

Beaugé, C., and Ferraz-Mello, S.: 1994. Capture in exterior mean motion resonances due to Poynting-Robertson drag. *Icarus* **110**, 239–260.

Bien, R., and Schubart, J.: 1987. Three characteristic orbital parameters for the Trojan group of asteroids. *Astron. Astrophys.* **175**, 292–298.

Carruba, V., Burns, J., Bottke, W., and Morbidelli, A.: 2000. Asteroid mobility due to encounters with Ceres, Vesta, Pallas: Monte Carlo codes *vs.* direct numerical integrations. *DPS Meeting #32*, 14.06

Dell'Oro, A., Marzari, F., Paolicchi, P., and Vanzani, V.: 2001. Updated collisional probabilities of minor body populations. *Astron. Astrophys.* **366**, 1053–1060.

Dohnanyi, J.: 1969. Collisional model of asteroids and their debris. *J. Geophys. Res.* **74**, 2531–2554.

Farinella, P., and Davis, D.: 1992. Collision rates and impact velocities in the Main Asteroid Belt. *Icarus* **97**, 111–123.

Farinella, P., and Vokrouhlický, D.: 1999. Semi-major axis mobility of asteroidal fragments. *Sci.* **283**, 1507–1510.

Farinella, P., Vokrouhlický, D., and Hartmann, W.K.: 1998. Meteorite delivery via Yarkovsky orbital drift. *Icarus* **132**, 378–387.

Ferraz-Mello, S.: 1994. Dynamics of the asteroidal 2/1 resonance. *Astron. J.* **108**, 2330–2337.

Ferraz-Mello, S., Michtchenko, T.A., and Roig, F.: 1998a. The determinant role of Jupiter's Great Inequality in the depletion of the Hecuba gap. *Astron. J.* **116**, 1491–1500.

Ferraz-Mello, S., Michtchenko, T.A., Nesvorný, D., Roig, F., and Simula, A.: 1998b. The depletion of the Hecuba gap *vs.* the long lasting Hilda group. *Planet. Space Sci.* **46**, 1425–1432.

Gomes, R.: 1995. The effect of non-conservative forces on resonance lock: Stability and instability. *Icarus* **115**, 47–59.

Gomes, R.: 1997. Orbital evolution in resonance lock I. The restricted 3-body problem. *Astron. J.* **114**, 2166–2176.

Greenberg, R., and Franklin, F.: 1976. Coupled librations in the motion of asteroids near the 2:1 resonance. *MNRAS* **173**, 1–8.

Henrard, J., Milani, A., Murray, C.D., and Lemaitre, A.: 1983. The reducing transformation and apocentric librators. *Celest. Mech.* **38**, 335–344.

Jedicke, R., and Metcalfe, T.S.: 1998. The orbital and absolute magnitude distributions of main belt asteroids. *Icarus* **131**, 245–260.

Knežević, Z., and Milani, A.: 2001. Synthetic proper elements for outer main belt asteroids. Submitted to *Cel. Mech. Dyn. Astr.*

Levison, H.F., and Duncan, M.J.: 1994. The long-term dynamical behavior of short-period comets. *Icarus* **108**, 18–36.

Michtchenko, T.A., and Ferraz-Mello, S.: 1995. Comparative study of the asteroidal motion in the 3:2 and 2:1 resonances with Jupiter I. Planar model. *Astron. Astrophys.* **303**, 945–963.

Michtchenko, T.A., and Ferraz-Mello, S.: 1996. Comparative study of the asteroidal motion in the 3:2 and 2:1 resonances with Jupiter II. Three-dimensional model. *Astron. Astrophys.* **310**, 1021–1035.

Moons, M., Morbidelli, A., and Migliorini, F.: 1998. Dynamical structure of the 2/1 commensurability with Jupiter and the origin of the resonant asteroids. *Icarus* **135**, 458–468.

Morbidelli, A.: 1996. The Kirkwood gap at the 2/1 commensurability with Jupiter: New numerical results. *Astron. J.* **111**, 2453–2461.

Morbidelli, A.: 1997. Chaotic diffusion and the origin of comets from the 2/3 resonance in the Kuiper belt. *Icarus* **127**, 1–2.

Morbidelli, A., and Moons, M.: 1993. Secular resonances inside mean motion commensurabilities. The 2/1 and 3/2 cases. *Icarus* **103**, 99–108.

Morbidelli, A., and Nesvorný, D.: 1999. Numerous weak resonances drive asteroids toward Terrestrial planets orbits. *Icarus* **139**, 295–308.

Morbidelli, A., Zappalà, V., Moons, M., Cellino, A., and Gonczi, R.: 1995. Asteroid families close to mean motion resonances: Dynamical effects and physical implications. *Icarus* **118**, 132–154.

Muinonen, K., Bowell, E. and Lumme, K.: 1995. Interrelating asteroid size, albedo and magnitude distributions. *Astron. Astrophys.* **293**, 948–952.

Nesvorný, D., and Ferraz-Mello, S.: 1997a. Chaotic diffusion in the 2/1 asteroidal resonance: An application of the frequency map analysis. *Astron. Astrophys.* **320**, 672–680.

Nesvorný, D., and Ferraz-Mello, S.: 1997b. On the asteroidal population of the first-order Jovian resonances. *Icarus* **130**, 247–258.

Nesvorný, D., Morbidelli, A., Vokrouhlický, D., and Brož, M.: 2001. The Flora family: A case of the dynamically dispersed collisional swarm? Submitted to *Icarus*.

Petit, J.M., and Farinella, P.: 1993. Modeling the outcomes of high-velocity impacts between small solar system bodies. *Cel. Mech. Dyn. Astr.* **57**, 1–28.

Petit,J.M., Morbidelli, A., and Valsecchi, G.: 1999. Large scattered planetesimals and the excitation of the small body belts. *Icarus* **141**, 367–387.

Press, W., Teukolsky, S., Vetterling, W., and Flannery, B.: 1996. Numerical recipes in Fortran 77, 2nd. Edition. Cambridge University Press, Cambridge, MA.

Rubincam, D.P.: 1995. Asteroid orbit evolution due to thermal drag. *J. Geophys. Res.* **100**, 1585–1594.

Schubart, J.: 1982.Three characteristic parameters of orbits of Hilda-type asteroids. *Astron. Astrophys.* **114**, 200–204.

Vokrouhlický, D., Milani, A., and Chesley, S.: 2000. Yarkovsky effect on small near-Earth asteroids: Mathematical formulation and examples. *Icarus* **148**, 118–138.

Zappalà, V., Cellino, A., Farinella, P., and Knežević, Z.: 1990. Asteroid families I. Identification by hierarchical clustering and reliability assessment. *Astron. J.* **100**, 2030–2046.

No.	Name	a_p [AU]	e_p	I_p [deg]	σ_a [AU]	σ_e	σ_I [deg]	$t_{\rm life}$ [$\times 10^4$ yr]	Other	D [km]
1921	Pala	3.191	0.435	19.793	0.0019	0.0413	2.0576	1807.5		8.3
1922	Zulu	3.230	0.426	37.900	0.0010	0.0127	0.3078	1985.9		21.9
5201	Ferraz-Mello	3.100	0.531	4.984	—	—	—	1.8	SC	6.6
5370	Taranis	3.205	0.703	9.989	0.0020	0.0015	0.5432	730.4	ν_5	4.4
8373	Stephengould	3.251	0.492	31.518	0.0016	0.0102	0.3687	962.3		10.5
9767	Midsomer Norton	3.167	0.784	64.981	0.0006	0.0588	3.7424	90.4	K, SC	3.2
	1977 OX	3.181	0.347	14.943	—	—	—	69.8	ν_5	5.5
	1994 JC	3.163	0.677	67.844	0.0017	0.1497	19.4343	35.2	K, SC	5.8
	1995 QN3	3.250	0.464	31.992	0.0008	0.0044	1.0954	959.5		2.4
	1995 DY8	3.205	0.308	1.880	0.0020	0.0064	0.2239	3025.7		8.7
	1998 BM24	3.192	0.311	0.655	0.0020	0.0343	0.2820	2661.9	ν_5, SC	8.7
	1998 KY30	3.194	0.344	11.687	0.0030	0.0557	1.1027	547.5	ν_5, SC	12.0
	1998 XH21	3.179	0.304	0.356	0.0018	0.0095	0.4663	1390.8	SC	5.8
	1999 XY223	3.176	0.385	5.064	0.0011	0.0046	0.2726	1084.0	ν_5	7.2
	2000 ER4	3.189	0.360	2.054	0.0040	0.0617	0.3696	1049.8	ν_5	3.5
	2000 EU170	3.199	0.383	9.903	0.0012	0.0063	0.7103	1989.0		11.5
	2000 JV60	3.181	0.433	11.824	0.0021	0.0157	1.5629	2822.3	ν_5	2.2
	2000 WZ161	3.178	0.307	11.463	—	0.0280	1.3630	438.0		12.0
	9593 P-L	3.189	0.400	9.836	0.0017	0.0167	0.8051	848.2	K	13.2
	3260 T-1	3.164	0.422	11.368	—	—	—	414.9		5.8
	2406 T-2	3.199	0.402	15.049	0.0016	0.0096	1.2469	3333.5		13.8

Table 1: The population of unstable asteroids in the 2:1 resonance, as to April 2001. Columns 1 and 2 identify the object. Columns 3 to 5 are the values of the proper elements, determined in the surface $\sigma = 0, \quad \dot{\sigma} > 0$ and $\varpi - \varpi_J = 0$. Columns 6 to 8 are the standard deviation of each proper element, determined from several intersections of the trajectory with the above surface, whenever possible (it could not be estimated for some highly chaotic asteroids). Column 9 is the typical lifetime over a 520 Myr time span. In all cases this is shorter than 100 Myr. Column 10 indicates if the asteroid is captured or ratherly near to some secular resonance inside the 2:1 resonance. K means Kozai, and SC means that the asteroid behaves as a separatrix crosser. Column 11 gives the estimated diameter, assuming a mean albedo 0.05.

No.	Name	a_p [AU]	e_p	I_p [deg]	σ_a [AU]	σ_e	σ_I [deg]	$t_{\rm life}$ [$\times 10^6$ yr]	Other	D [km]
1362	Griqua	3.212	0.372	24.005	0.0018	0.0068	0.5716	149.5		29.9‡
3688	Navajo	3.213	0.507	4.688	0.0008	0.0009	0.5251	216.1	ν_{16}	6.3
4177	Kohman	3.231	0.320	15.997	0.0013	0.0011	0.1379	337.7	ν_{16}	17.4
11665	Dirichlet	3.219	0.225	17.953	0.0021	0.0069	0.5259	431.0		9.1
13963	1991 PT4	3.216	0.319	2.592	0.0014	0.0036	0.4092	352.2		11.0
	1998 AE	3.215	0.262	10.742	0.0020	0.0042	0.5550	509.1		12.0
	1999 NF10	3.211	0.278	0.696	0.0015	0.0044	0.2199	265.8	ν_{16}	8.3
	1999 XB143	3.183	0.431	9.403	0.0031	0.0645	1.3933	140.8	ν_5	17.4
	2000 AW144	3.217	0.348	2.278	0.0019	0.0023	0.2412	190.0		11.0
	2000 CM67	3.230	0.489	3.437	0.0015	0.0012	0.1282	487.3	ν_{16}	7.6
	2000 HY9	3.214	0.294	0.905	0.0022	0.0034	0.1175	455.0	ν_{16}	6.9
	2000 YT123	3.222	0.204	1.430	0.0011	0.0022	0.2415	100.8		14.5
	1032 T-1	3.227	0.485	7.205	0.0015	0.0013	0.1603	173.3	ν_{16}	4.8

‡ IRAS diameter.

Table 2: The population of marginally unstable asteroids (Griquas) in the 2:1 resonance, as to April 2001. The typical lifetime of these objects is between 100–500 Myr. See Table 1 for the explanation of each column.

No.	Name	a_p [AU]	e_p	I_p [deg]	σ_a [AU]	σ_e	σ_I [deg]	$t_{\rm life}$ [$\times 10^6$ yr]	Other	D [km]
3789	Zhongguo	3.236	0.222	2.642	0.0013	0.0015	0.2357	> 520		20.0
11097	1994 UD1	3.233	0.267	2.564	0.0019	0.0013	0.1809	> 520		12.6
11266	1981 ES41	3.222	0.272	2.770	0.0015	0.0018	0.2145	> 520		11.0
11573	Helmholtz	3.221	0.293	3.688	0.0011	0.0019	0.1954	> 520		15.8
14871	1990 TH7	3.217	0.280	2.137	0.0014	0.0028	0.2163	> 520		11.0
16882	1998 BO13	3.228	0.271	2.138	0.0016	0.0022	0.2648	> 520		11.0
18888	2000 AV246	3.231	0.263	1.689	0.0013	0.0013	0.1339	> 520		11.5
22740	1998 SX146	3.237	0.230	3.735	0.0017	0.0009	0.2998	> 520		13.8
	1975 SX	3.223	0.217	2.808	0.0024	0.0051	0.2646	> 520		8.3
	1991 PG18	3.238	0.247	3.478	0.0014	0.0009	0.1738	> 520		14.5
	1997 BT4	3.231	0.270	3.779	0.0014	0.0013	0.2097	> 520		3.2
	1998 DF14	3.223	0.306	1.490	0.0014	0.0024	0.1996	> 520	ν_{16}	6.3
	1998 FP70	3.236	0.284	2.976	0.0011	0.0008	0.1039	> 520	ν_{16}	10.0
	1998 KZ5	3.226	0.266	3.663	0.0014	0.0025	0.2988	> 520		10.0
	1998 RO49	3.226	0.275	1.379	0.0025	0.0045	0.3900	> 520	ν_{16}	7.2
	1999 RC168	3.225	0.221	1.312	0.0014	0.0024	0.1619	> 520		9.1
	1999 XT23	3.234	0.274	2.098	0.0016	0.0009	0.0867	> 520	ν_{16}	9.1
	1999 XZ55	3.222	0.221	1.802	0.0010	0.0020	0.6800	> 520		10.5
	1999 XZ56	3.239	0.255	2.804	0.0016	0.0010	0.2460	> 520		10.0
	2000 BC23	3.220	0.205	2.340	0.0025	0.0037	0.3565	> 520		12.6
	2000 EF60	3.241	0.277	2.256	0.0017	0.0007	0.0282	> 520	ν_{16}	5.0
	2000 FN44	3.219	0.242	3.093	0.0007	0.0027	0.3857	> 520		12.0
	2000 SF206	3.235	0.263	4.261	0.0019	0.0013	0.1897	> 520		6.0
	2000 UZ4	3.228	0.294	1.233	0.0022	0.0022	0.1427	> 520	ν_{16}	8.3
	2000 UM53	3.231	0.275	5.093	0.0013	0.0011	0.2417	> 520		8.7
	2001 AO22	3.232	0.281	2.586	0.0016	0.0007	0.1431	> 520	ν_{16}	6.6
	2001 BB58	3.229	0.278	1.392	0.0012	0.0018	0.1035	> 520	ν_{16}	11.5

Table 3: The population of stable asteroids (Zhongguos) in the 2:1 resonance, as to April 2001. Their lifetime is based on a 520 Myr simulation. Asteroids marked ν_{16} are very close to this resonance, but they are not actually captured in it. See Table 1 for the explanation of each column.

	$\overline{T}$ [Myr] $I_p \leq 10°$	$\overline{T}$ [Myr] $I_p \leq 5°$
Region Z	500	550
Region G	250	230
Region A	130	90

Table 4: The average residence time $\overline{T}$ in the different regions of the resonance, for two cutoff levels of I_p (see text).

	Model $p_e = 1$		Model $p_e = 0.35$		Model $p_e = 0$	
	Region A	Region G	Region A	Region G	Region A	Region G
Initial	0.71	1.25	0.71	1.25	0.71	1.25
1.0 Byr	0.57	0.70	0.58	0.71	0.49	0.68
2.0 Byr	0.43	0.49	0.52	0.54	0.48	0.56
3.0 Byr	0.37	0.42	0.47	0.49	0.47	0.48
4.0 Byr	0.33	0.40	0.42	0.45	0.47	0.47
4.5 Byr	0.32	0.38	0.40	0.45	0.47	0.46
Actual	0.04	0.36	0.04	0.36	0.04	0.36

Table 5: The number of surviving test particles vs. time in Regions A and G, for three different models of random walk (see text). The values are normalized to the surviving particles in Region Z, The last row shows the presently observed values.

	Δa_p [AU]	Δe_p	ΔI_p [deg]	dV/da_p [rad]	n
Zhongguos	0.035	0.1	5	2.70	30
Hildas	0.040	0.2	10	1.23	260

Table 6: Approximate values of the parameters used in Eqs. (11) and (12). The values of dV/da_p were computed form Eq. (7), for $I_p = 0$ and a_p, e_p equal to the mean proper a and e of each population, respectively. The value of n_h does not take into account some 20 Hildas having $e_p < 0.05$, which are σ-alternators.

Anexo:

The asteroidal population in the Hecuba gap. Part II: Origin of the resonant asteroids

The Asteroidal Population in the Hecuba Gap. Part II: Origin of the resonant asteroids

F. Roig

Instituto Astronômico e Geofísico, Universidade de São Paulo.

Av. Miguel Stefano 4200, (04301-904) São Paulo, SP, Brasil.

D. Nesvorný

Department of Space Studies, Southwest Research Institute.

1050 Walnut St., Suite 426, Boulder, CO 80302, USA

S. Ferraz-Mello

and

T.A. Michtchenko

Instituto Astronômico e Geofísico, Universidade de São Paulo

Av. Miguel Stefano 4200, (04301-904) São Paulo, SP, Brasil.

1. Introduction

This paper is the continuation of our work about the population of asteroids in the Hecuba gap. In our previous paper (Roig et al. 2001), hereinafter RNF-I, we studied the dynamical characteristics of the real asteroids in the 2:1 resonance with Jupiter. We identified 61 resonant asteroids known at April 2001, both numbered and unnumbered multi-oppositional, and divided them in three sub-populations: (i) stable objects, that are able to survive in the resonance for more than 500 Myr, (ii) marginally unstable, with typical lifetimes between 100 and 500 Myr, and (iii) unstable objects, with lifetimes smaller than 100 Myr (in most cases much smaller). The main members of the stable and marginally unstable populations are the asteroids (3789) Zhongguo and (11362) Griqua, respectively. Then, throughout this paper we will usually refer to these two populations simply as "the Zhongguos" and "the Griquas".

In RNF-I we have shown that the Zhongguos are about 30 asteroids located in the most stable region inside the 2:1 resonance, where they would be able to survive over the age of the Solar System. We have also discussed the role of Yarkovsky effect and of mutual scattering in enhancing the chaotic diffusion in this region, concluding that these processes do not affect significantly the long term stability of the Zhongguos. Then, the open problem is to determine if these objects have actually been in the resonance from the very primordial times, or if they arrived to their

present location in more recent times. As we discussed in RNF-I, the main argument against the primordiality of these resonant asteroids in the resonance is their steep size distribution and their rather small sizes (less than 20 km in diameter).

We have also shown in RNF-I that there is a possible dynamical link between the Griquas and the Zhongguos, supported by the natural chaotic diffusion in the resonant phase space. Concerning the unstable population, their members lie in the most unstable regions of the resonance, and we concluded that such asteroids should be continuously resupplied from outside the resonance in order to keep the population in steady state, as we presently observe it.

However, in RNF-I we did not do a detailed analysis and discussion of the specific mechanisms that could "inject" asteroids in the resonance, both in stable or unstable regions. The aim of this paper is to complete this analysis, presenting the main outlines of the most interesting alternatives. We do not intend to draw definitive conclusions about the origin of the resonant asteroids in the Hecuba gap, but rather to provide the necessary evidence that could allow to either support or discard any of these alternatives.

The mechanisms we will study here are basically three: (i) dynamical diffusion at the left side of the Hecuba gap (Sect. 2), (ii) resonant capture due to planetary migration (Sect. 3), and (iii) breakup of Themis and formation of Themis family (Sect. 4). In Sect. 2, we will also discuss the role of different sources of diffusion, like weak mean motion resonances, Yarkovsky effect, and mutual scattering. Most of the definitions and techniques applied in this section were already described in detail in RNF-I, and we will avoid to repeat their description here. Then, we will frequently refer the reader to that paper. Finally, Sect. 5 is devoted to the conclusions.

2. Diffusion in the neighborhood of the Hecuba gap

If we are looking for a reservoir of asteroids able to supply or resupply the population of resonant objects at the 2:1 resonance, then we have to look first at the left side of the resonance. The large density of background asteroids observed there is even enhanced by the presence of Themis family, which accounts for some 2000 asteroids. Moreover, the asteroidal density in the region shows a clear cutoff at the border of the 2:1 resonance, which means that a lot of asteroids lie very close to the separatrix and could be able to be injected somehow in the resonance. We will discuss in the following, how could this injection be favored by the chaotic diffusion at the left side of the Hecuba gap.

The first step was to mount a map of the diffusive structure near the separatrix of the 2:1 resonance. This map is shown in Fig. 1. The darker areas correspond to regions where the motion is very stable, while the lighter ones are associated to regions of strong chaos. The map was mounted by integrating a grid of 10,000 particles, regularly distributed in the a, e space. The initial angles were such that $\sigma = 2\lambda_{\rm J} - 2\lambda - \varpi = 0$, $\varpi - \varpi_{\rm J} = 0$ and $\Omega - \Omega_{\rm J} = 0$, and the model considered

perturbations of four major planets[1] . The chaoticity of each initial condition has been quantified by counting the number of peaks in the 1 Myr FFT spectrum of the semi-major axis, and this quantity was translated to a gray-scale.

This map of spectral numbers (Michtchenko and Ferraz-Mello, 2001) allowed to obtain a detailed portrait of the phase space with a relatively low computational cost. Several features can be appreciated in Fig. 1. At the upper right corner there is a huge region of chaos corresponding to the 2:1 resonant space. The "spot " of almost regularity in the middle of that region corresponds to the place where the Zhongguos are located. The border of the resonance is also quite well defined. Outside the resonance, we observe a complex web of weak mean motion resonances (MMRs), which appear as inclined stripes of instability. Most of these are three-body MMRs (Nesvorný and Morbidelli, 1998) involving the orbital periods of Jupiter and Saturn, and some of them are indicated at the bottom of the plot. The dominant ones are the 5:–2:–2 and 7:–2:–3 resonances[2]. Other weaker MMRs, as the stripes in each side of the 5:–2:–2 resonance, corresponds to combinations of the three-body MMR itself with the frequency of the 5:2 Great Inequality between Jupiter and Saturn. At high eccentricities ($e > 0.3$) several narrow MMRs overlap and generate the rather chaotic region observed at the upper left corner of the plot.

The role of these weak resonances is to enhance the chaotic diffusion in the (otherwise stable) neighborhood of the Hecuba gap. An asteroid captured in such resonances will randomly walk along it, being able to excite its eccentricity. In the inner main belt, this mechanism has been proven to be responsible of re-supplying the population of Mars-crossers (Morbidelli and Nesvorný, 1999), and of enhancing the proper element's dispersion of the Flora family (Nesvorný et al., 2001). An interesting feature observed in Fig. 1 is that some weak MMRs touch the border of the 2:1 resonance at a certain eccentricity. In the following, we will discuss whether or not these regions of contact could behave as "gates", allowing an asteroid captured in a narrow MMR to jump inside the 2:1 resonance after exciting its eccentricity.

2.1. Weak mean motion resonances

In order to analyze the efficiency of weak MMRs to inject asteroids in the 2:1 resonance, we performed a simulation of 300 test particles and studied their chaotic diffusion in the proper elements' space. We used the symplectic integrator Swift (Levison and Duncan, 1994), with a time step of 0.05 yr, and taking into account perturbation of four major planets. The simulation spanned 200 Myr. The initial conditions of the test particles were chosen as follows: the eccentricity was

[1] As usual, λ, ϖ and Ω represent the mean, perihelion and node longitudes, respectively, and the index J refers to Jupiter

[2] A three-body resonance of the form $k : -l : -m$ corresponds to a combination of frequencies $kn_{\rm J} - ln_{\rm S} - mn_{\rm A} \simeq 0$, where n refers to the mean motion of the bodies involved.

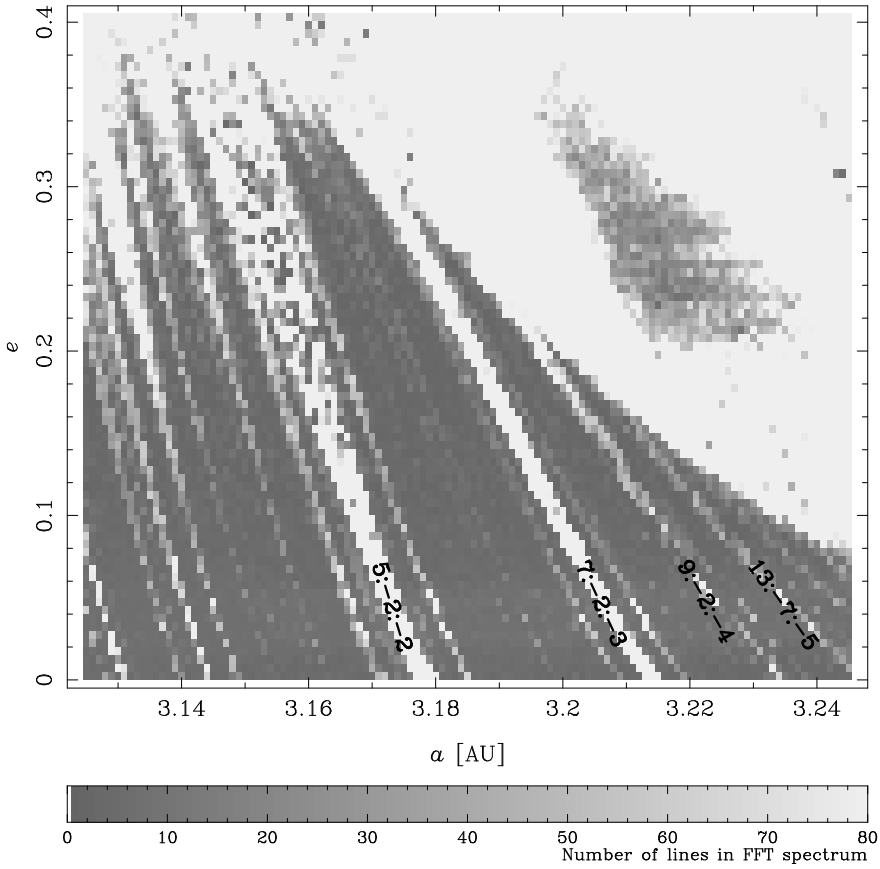

Fig. 1.— Map of spectral numbers (number of peaks in the FFT spectrum) for the left side of the Hecuba gap. The darkest regions are the most stable. The gray-scale is truncated at 80 peaks.

equally spaced in the range $0.05 \leq e \leq 0.4$, $\Delta e = 0.05$; the semi-major axis was also equally spaced in the range $a_{\rm min} \leq a \leq a_{\rm max}$, $\Delta a = 0.003$ AU, where $a_{\rm min}, a_{\rm max}$ depend on the initial eccentricity and varied between 3.10–3.15 and 3.24–3.27 AU, respectively. The remaining elements were chosen such that $\sigma = 0$, $\varpi - \varpi_{\rm J} = 0$, $I = 5°$, and Ω randomly distributed between 0 and 2π. We further divided these initial condition into two sub-sets:

- Set #1 corresponds to 200 initial conditions started the simulation outside the 2:1 resonance.
- Set #2 corresponds to 100 initial conditions that were in the resonance from the very beginning of the simulation (this was verified by looking at the average a and the behavior of σ).

From the results of this simulation, we computed time series of the proper elements a_p, e_p, I_p for each particle. For the particles of Set #1, proper elements were defined as the running averages of a, e, I over 10 Myr, and were sampled every 0.1 Myr. For the particles of Set #2, we followed the same procedure applied in RNF-I, and defined proper elements as the running minima of a and maxima of e, I, also over 10 Myr with 0.1 Myr sampling. It is worth noting that this last definition of proper elements (maxima/minima) can also be applied to the particles of Set #1. In such case, the maximum of the eccentricity has a particular meaning, because it is associated to the condition $\varpi - \varpi_{\rm J} = 0$. This latter set of proper elements are usually referred to as *resonant proper elements*, because they better describe the position of the asteroids with respect to the separatrix of the 2:1 resonance (Morbidelli et al., 1995). Although for Set #1 the averages normally provide proper elements of better quality, we will eventually use at times the maxima/minima to point out some particular dynamical features.

The typical evolution of the particles of Set #1 in the space of proper elements is shown in Fig. 2. In this figure, we plot the averaged values of a and e (sampled every 0.1 Myr) for all particles with initial conditions between $0.2 \leq e \leq 0.4$. It is worth noting that the initial conditions are related to a maximum of e, so the corresponding averaged eccentricities are shifted down by some 0.05. In Fig. 2 we also indicate the approximate location of some MMRs (vertical full lines), and also the curves corresponding to three different values of the invariant

$$N = \sqrt{a}\left(-2 + \sqrt{1-e^2}\cos I\right) \tag{1}$$

which is related to the 2:1 resonance (dashed lines marked N_i).

As we expected, the particles captured in MMRs show diffusive paths in e_p along these resonances. By far, the dominant resonance is 5:–2:–2. These particles also show a significant diffusion in a_p, although it is mostly limited to the width of each MMR. The diffusion in a_p is mainly due to the proper oscillations inside the MMRs and it is larger for larger e_p, because the resonance width increases with eccentricity. However, these proper oscillations have a superimposed forced oscillation, which is induced by the proximity to the 2:1 resonance. This is clearly noted in Fig. 2, where the diffusive paths in a_p are always aligned with the lines of $N = $ const. The particles that are not captured in the narrow MMRs can be identified as the tiny dashes in Fig. 2, mainly at

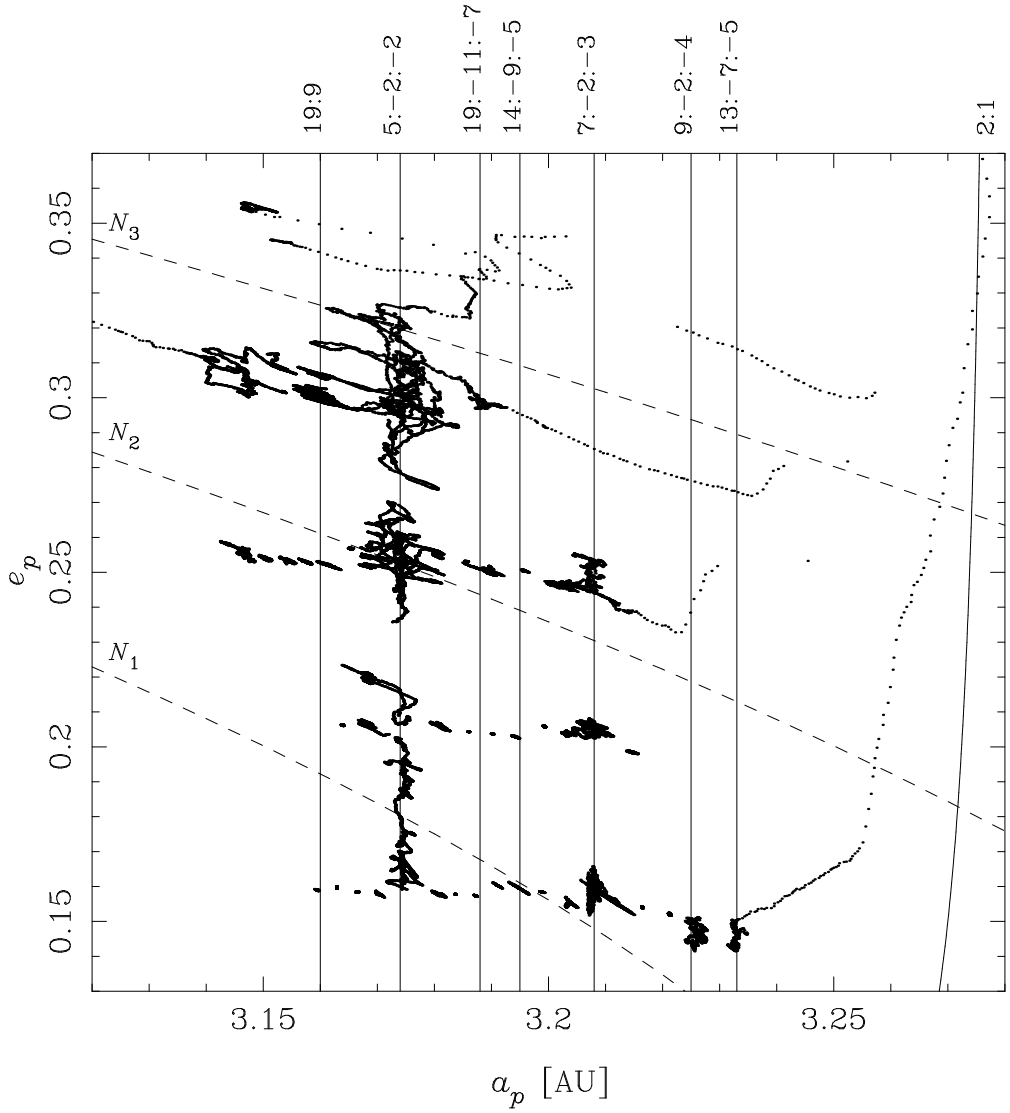

Fig. 2.— The evolution in the proper elements' space of the test particles in Set #1. Only the particles with initial $e \geq 0.2$ are shown. Proper elements are defined as averages over 10 Myr and are sampled every 0.1 Myr. Note that the average eccentricity is shifted down about 0.05 with respect to the initial eccentricity. The location of some MMRs resonance is indicated by full vertical lines, trucated at the approximate border of the 2:1 resonance. Dashed lines correspond to values of the invariant Eq. (1).

$e_p = 0.15$ and 0.20. No significant diffusion is observed in these cases, at least in the time scale of our simulation.

But for our purposes, the most interesting feature observed in Fig. 2 concerns the particles that went injected in the 2:1 resonance. We observe three clear examples at $e_p = 0.15$, 0.25 and 0.30, respectively, but a larger number of injections occurred also at $e_p = 0.35$. These injections happened precisely at the "gates" mentioned above, where the weak MMRs touch the 2:1 resonance border. In Fig. 3 we present the typical behavior of two of these injected particles: one of them had initially $e = 0.20$ (upper panels) and the other $e = 0.30$ (lower panels). For the sake of comparison, we also show in each case the behavior of a neighboring initial condition that was not injected during the simulation (dotted curves). The first case correspond to a particle that started the simulation inside the 13:–7:–5 resonance. The particle chaoticaly evolved there for about 100 Myr until it was pushed to enter the 2:1 resonance. The second case is a particle that started the simulation at the 7:–2:–3 resonance. Even being a stronger resonance, the particle spent more than 100 Myr in it before becoming thrown to the 2:1 resonance. This seems to indicate that the typical diffusion in e_p along the weak MMRs is not actually too large, and opens the question about the efficiency of this mechanism to excite the eccentricities and inject asteroids in the 2:1 resonance. In fact, the examples shown in Fig. 3 were quite lucky (or unlucky) particles, because they started the simulation not only at a weak MMR but also very close to the 2:1 resonance border.

Back to Fig. 2, the apparently large diffusive paths observed at the 5:–2:–2 resonance, for example between $0.15 \leq e_p \leq 0.22$, come in fact from the combined effect of two or more different particles, some of them diffusing upwards from a lower e_p while other diffusing downwards from a higher e_p. In spite of the quite enhanced diffusion at this resonance, it is difficult to imagine how could a particle at $e_p \simeq 0.15$ (for example, a typical Themis family member) be able to excite its eccentricity to much larger values in a time-scale shorter than the age of the Solar System. The dynamics of Themis family members is of the upmost importance, because this family concentrates a large fraction of the asteroidal population at the left side of the 2:1 resonance, and could be the most important reservoir of potential 2:1 resonant objects.

To better quantify the actual diffusion induced by the narrow MMRs at the left side of the Hecuba gap, we computed the diffusion parameters for each proper element, following the same procedure described in RNF-I. In short, given a proper element E, we introduced two different definitions for these parameters: the first one is simply the standard deviation σ_E of the proper element over a given time interval (do not mistake with the critical argument σ); the second is the slope β_E of the linear best-fit for the time series of the proper element. Figure 4 shows the values of $\sigma_a, \sigma_e, \sigma_I$ over 200 Myr, for the initial conditions of Set #1 with $e \leq 0.3$. We can see a correlation between the three quantities, which is related to the evolution at weak MMRs. The initial conditions with $e = 0.4$ were excluded from the plot because they evolve in a regime of overlap of MMRs, and their behavior is totally different from that of the lower e particles, as we will discuss later.

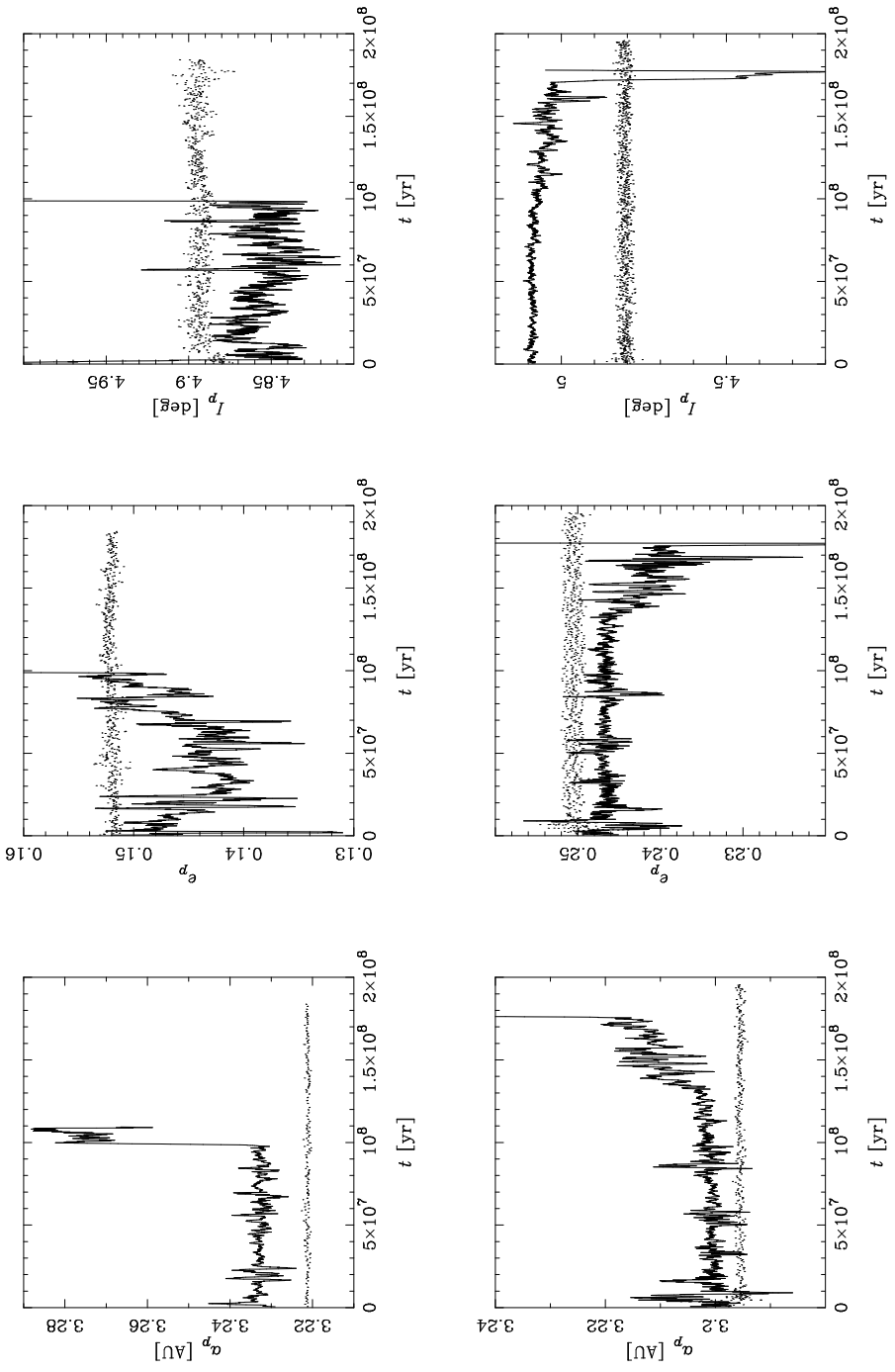

Fig. 3.— Two examples of the evolution of proper elements of particles injected in the 2:1 resonance during our simulation (full lines), and neighboring particles not injected (dotted lines). The upper panels correspond to initial conditions at $e = 0.2$ and the bottom ones, correspond to initial conditions at $e = 0.3$. At variance with Fig. 2, the proper elements shown here are averages over 1 Myr.

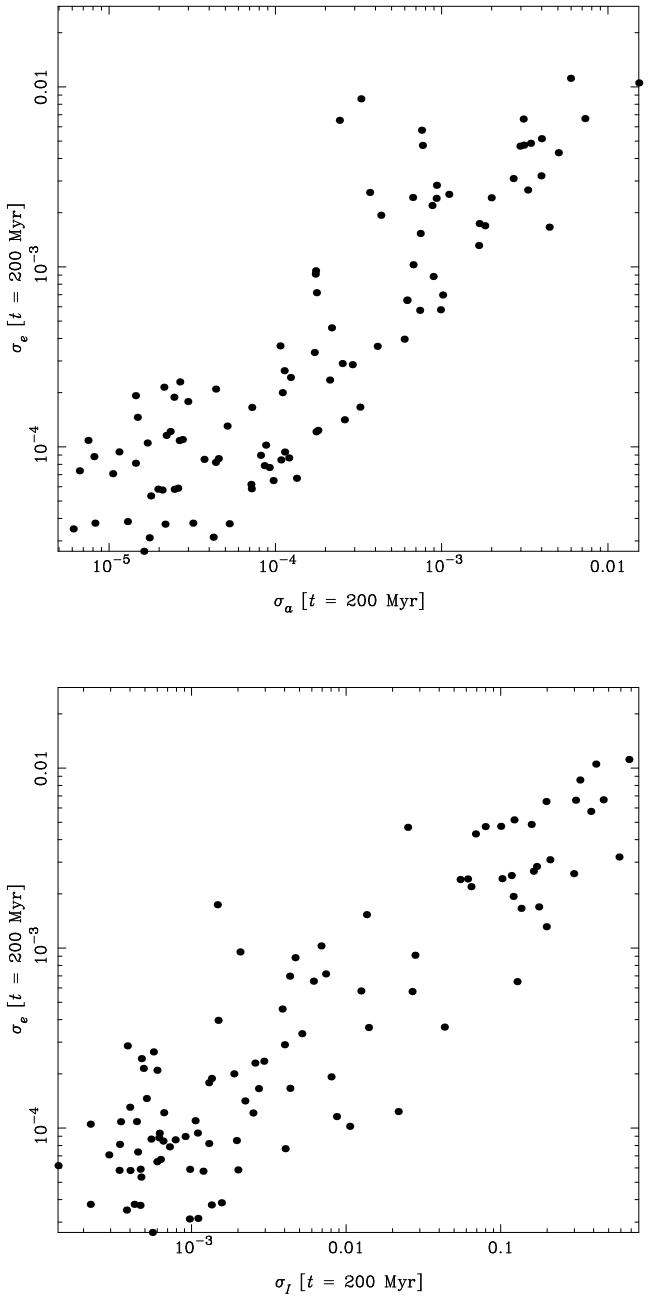

Fig. 4.— Diffusion parameters (standard deviations of proper elements over 200 Myr) for the test particles of Set #1. We are not showing the particles with initial $e = 0.4$. The correlation between the parameters is related to the chaotic diffusion inside the weak MMRs. Units are AU for σ_a, and deg for σ_I.

In Fig. 4 the large values of σ_E correspond to particles captured in weak MMRs. For example, particles at the 5:–2:–2 resonance with $e_p = 0.15$ (typical Themis family members) have values of $\sigma_e \sim 0.005$. This means that, in order to diffuse from their present location up to about $e_p \sim 0.3$ (where they would have a good chance to be thrown to the 2:1 resonance), they would spend some 4–6 Byr. In other words, the narrow MMRs alone seem to be rather inefficient to transport asteroids into the 2:1 resonance in time scales of millions of years, except when the asteroids lie close to the border of the 2:1 resonance from the begining. In such cases, the role of the 9:–2:–4 and 13:–7:–5 resonances to inject members of Themis family in the 2:1 resonance could have some relevance which should be studied with more detail (see Fig. 2).

On the other hand, the overlap of narrow MMRs at $e_p > 0.3$ provides a totally different mechanism to transport asteroids. Due to this overlap, the objects there are able to randomly walk in semi-major axis, virtually jumping between the MMRs, and can be eventually pushed to enter the 2:1 resonance in time scales as shorter as some Myr. These short time scales do not allow to plot their trajectories in the proper elements space (recall that proper elements are averages over 10 Myr). Notwithstanding, about 80% of the initial conditions with $e = 0.4$ in Set #1 ended captured at the 2:1 resonance (at least temporarily) in at most a couple of 10 Myr. We wish to stress that this mobility of a_p at large eccentricities is not related to Jupiter crossing orbits. In fact, the 2:1 resonance induce a forced oscillation of e which reaches its maximum when $\varpi = \varpi_{\rm J}$, so this mechanism is in some sense protecting the particles from having a close approach to Jupiter. Actually, Jupiter crossing orbits at $a \sim 3.15$ AU will happen only for maximum values of $e > 0.55$, even taking into account the 0.35 AU Hill's sphere of that planet. The diffusion cannot be attributed to the perturbation of Mars either, since this planet has not been included in the simulations. However, Mars crossing orbits happen for $e > 0.45$, and this planet should be taken into account in future studies of the dynamics at this high eccentricity region.

The overlap of weak MMRs seems to be a quite efficient way to inject large amounts of objects in the 2:1 resonance in very short time scales. The problem is to find a suitable source of asteroids to feed this mechanism. Unfortunately, the density of observed asteroids near the Hecuba gap has a drastic decay for $e > 0.30$ (see for example, Knežević and Milani, 2001), and most of this high-e asteroids are driven to planet crossing trajectories in time scales smaller than 100 Myr. Maybe the weak MMRs in the neighborhood of the Hecuba gap could be able to feed the region of overlap, by exciting the eccentricity of objects with an already high e (~ 0.3). However, even if this is the case, we would need another mechanism to resupply the weak MMRs themselves. In recent years, the role of non conservative forces (like Yarkovsky effect) and mutual scattering, has been raised as a possible solution to feed the large web of weak MMRs in the asteroid belt, through the introduction of a significant semi-major axis mobility of the asteroids. We will return to this subject later in Sect. 2.3.

Before closing this section, we wish to recall that our present study has been restricted to the very neighborhood of the 2:1 resonance, and to the dynamical effect of a few MMRs. We have not analyzed the possible effect of two important two-body MMRs with Jupiter located in the interval

$3.05 < a < 3.12$ AU, namely 11:5 ($a \simeq 3.07$ AU) and 13:6 ($a \simeq 3.11$ AU). Numerical experiments by Michtchenko (in preparation) show that the diffusion at these resonances is much larger than at the 5:–2:–2 resonance, and they could be able to resupply the high-e overlap region with much better efficiency. Last, but not least, these two resonances could be one of the best possible path to transport material form the region of Themis family to the 2:1 resonance.

2.2. Fate of injected particles

We have shown in the last section that weak MMRs at the left side of the Hecuba gap would be able to inject asteroids into the 2:1 resonance. But, which is the typical fate of these particles after they enter the 2:1 resonant space?

The answer to this question can be found by looking again at Figs. 2 and 3. Once the particles were captured by the 2:1 resonance, they followed a fast diffusion path to Jupiter crossing orbits and were discarded from the simulation after one or several close encounters with this planet. The typical lifetime of injected particles (after the injection) is no longer than 10 Myr, and much smaller in most cases. During this short lifetime, the eccentricity is chaoticaly driven to higher values, while in several cases the inclinations become also excited above 10°. This behavior is related to the presence of a highly chaotic region inside the 2:1 resonance, which is generated by the overlap of several secular and secondary resonances. For $e > 0.20$, the resonant dynamics near the separatrix is dominated by the overlap of secular resonances, mainly ν_5, ν_6 and Kozai resonances (Morbidelli and Moons, 1993). For $0.05 < e < 0.20$, is the overlap of secondary resonances which dominates. A secondary resonance occurs when the period of libration of σ is an integer multiple of the period of circulation of ϖ. Each of these resonances alone does not have a significant effect in the diffusion, but in the case of the 2:1 resonance, the overlap of several $p/1$ secondary resonances ($p \geq 2$) generates an important region of chaos at low eccentricities (Michtchenko and Ferraz-Mello, 1996). This region behaves as a barrier, separating the low eccentricity region from the central region of the 2:1 resonance, where the Zhongguos are found (Ferraz-Mello, 1994). The effect of this barrier is to excite the inclination of the particles there up to values $\sim 30°$ or larger. This excitation is known to happen in relatively short time-scales, and allows to transport particles from the region at $e < 0.1$ to the region at $e > 0.4$ of the 2:1 resonance through a "bridge" at high-inclinations (Henrard et al., 1995).

The actual effect of the barrier of chaos related to the secular and secondary resonances is illustrated in Fig. 5. We show there the evolution in the space of proper a, I of some initial conditions in Sets #1 and #2. The top panel corresponds to the initial conditions at $e = 0.25$, and the bottom one, to those with initial $e = 0.20$. Proper elements were defined here as minimum a and maximum I over 10 Myr. For $e = 0.25$, we clearly distinguish two regions where the particles evolve without exciting their inclinations. One is outside the 2:1 resonance, between 3.15 and 3.18 AU approximately. The other is inside the 2:1 resonance, between 3.21 and 3.23 AU. This last region corresponds more or less to the one where the Zhongguos are located. Both regions are separated

by a "gap" of about 0.03 AU in width, where the inclinations are highly excited. This last region is related to the overlap of secular resonances near the separatrix of the 2:1 resonance, located ~ 3.18 AU. A smaller excitation of the inclinations is also observed for values $a \sim 3.25$ AU, in this case related to the secular resonance ν_{16}. For $e = 0.20$ the situation is slightly different. Still we can see a region outside the resonance, between 3.15 and 3.20 AU, where the proper inclinations remain small. But inside the 2:1 resonance, we observe a region of some 0.05 AU in width where the excitation of inclinations is rather huge. This region is related to the overlap of secondary resonances. Since the density of points in the space of proper elements is a rough indicator of the diffusion speed, we can conclude, by comparing both panels, that the excitation in the region of the separatrix is faster than that in the region of the secondary resonances. We will try in the following to better quantify this diffusion speed.

Following the same recipe applied in RNF-I, we proceeded to mount a map of the residence time in the space of proper elements. In short, we took the space of proper a, e in the range $3.14 \leq a_p \leq 3.28$ AU and $0.025 \leq e_p \leq 0.425$, and we divided it in 28×8 equal cells, each one with $\Delta a = 0.005$ AU and $\Delta e = 0.05$. Then, we use the time series of proper elements of all the particles in Sets #1 and #2 to determine the time that each particle spent in each cell. The time of residence was computed over the 200 Myr interval spanned by our simulation or *until the proper inclination of the particle became larger than* 10°. Since two or more particles can provide different values of residence time for the same cell, in the end we consider their averages. This map of residence times is shown in Fig. 6. The cyan-blue colors correspond to the largest residence times, while the reddish colors correspond to the shortest ones. The blank cells were never occupied by any particle in the simulation. We also show in this plot the approximate locations of the center and separatrix of the 2:1 resonance (calculated analytically), the separatrices of the ν_{16} resonance, the secondary resonances 2/1,...,5/1, and the instability border (IB) which delimits the region of overlap of secular resonances (these latter estimated numerically). To mount this map we have used two sets of proper elements. The first one was defined as the minimum of a and the maxima of e, I over 10 Myr, with a 0.1 Myr sampling. Unfortunately, this set is not able to resolve the residence time in the cells corresponding to region of overlap of secular and secondary resonances. This is because the average residence times there are shorter than 10 Myr. Then, we used a second set of proper elements, defined as the minima/maxima over 1 Myr (also with a 0.1 Myr sampling), to "complete" the cells where the former one failed to provide a residence time.

Several interesting features can be observed in Fig. 6. Outside the 2:1 resonance it is possible to identify a pattern of inclined stripes related to the 5:–2:–2 and 7:–2:–3 resonances. We can also see regions of rather strong stability (darker cells) surrounding these MMRs at low eccentricities. Inside the 2:1 resonance, we observe a region of long residence times between the ν_{16} and the IB line. This is the region where the Zhongguos and Griquas are located (white and black dots, respectively). The residence times there are larger than above the ν_{16} line, in agreement with the results obtained in RNF-I from a different simulation. But the most remarkable feature in Fig. 6 is the wide stripe of short residence times that separates the stable regions outside and inside the 2:1 resonance. The

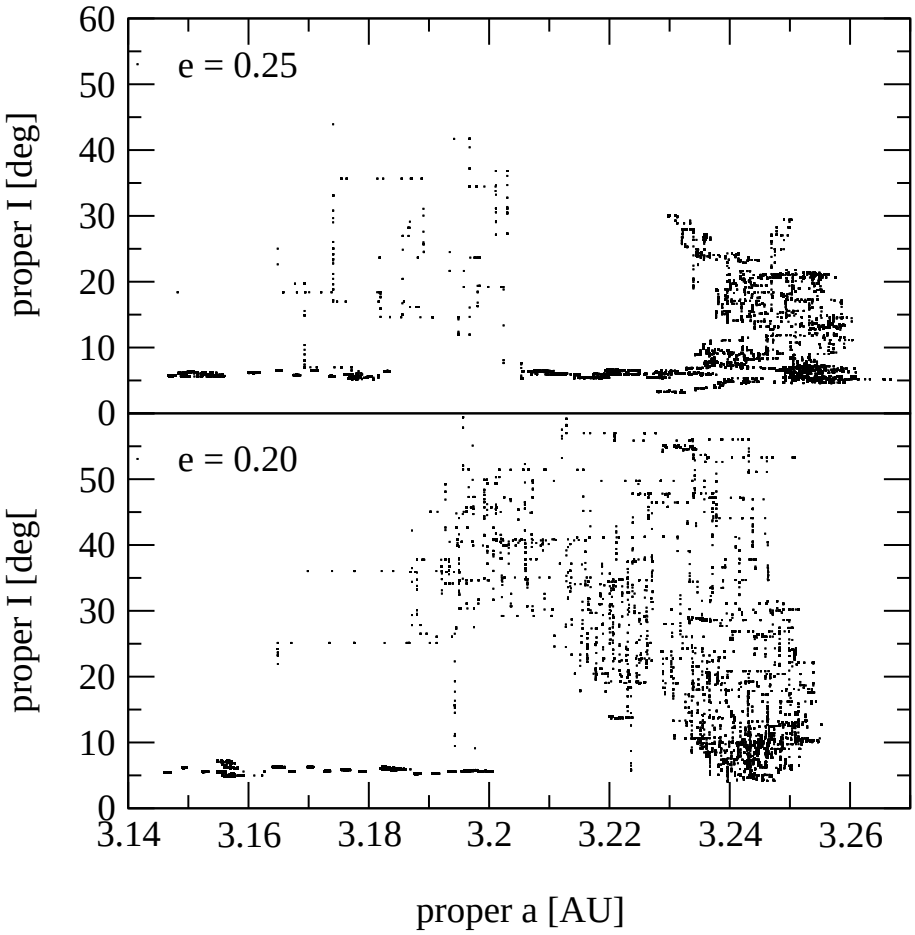

Fig. 5.— Evolution of test particles in the space of proper a, I. The particles correspond to 70 initial conditions in Sets #1 and #2 for two different levels of initial eccentricity (35 particles in each level). Proper elements are defined as maximum of I and minimum of a over 10 Myr, and are sampled every 0.1 Myr. In the top panel, the proper inclinations are excited in the region of overlap of secular resonances, and also at the ν_{16} resonance. In the bottom panel, the excitation correspond to the overlap of secondary resonances.

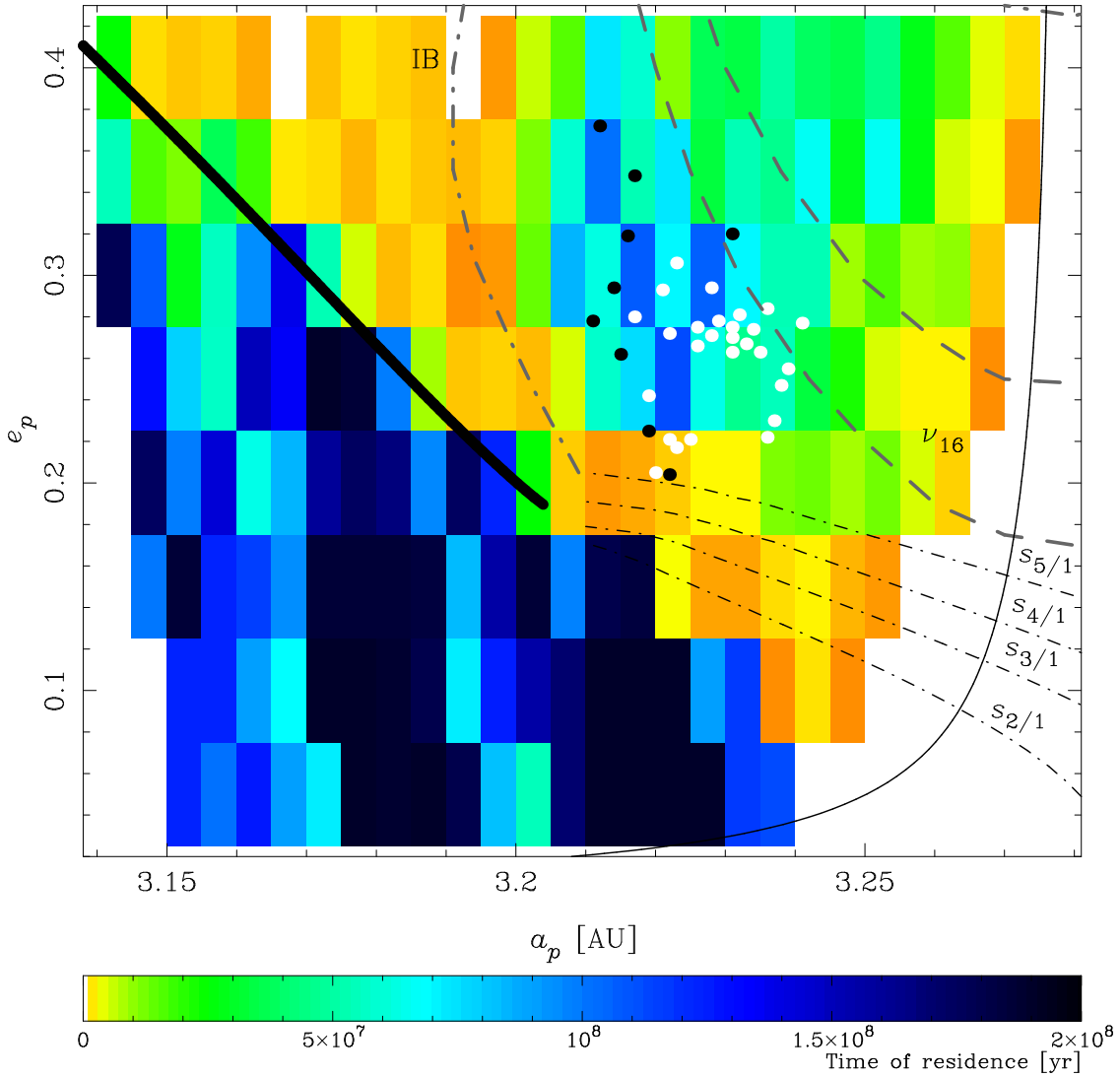

Fig. 6.— Map of residence times, computed from the proper elements in a 200 Myr simulation of test particles outside and inside the 2:1 resonance. We used two sets of proper elements, defined as minimum of a and maxima of e, I over 10 Myr and 1 Myr, respectively. Both sets had a 0.1 Myr sampling. The plot also shows the location of the equilibrium centers of the 2:1 resonance (full thin line), the separatrix (full bold line), the separatrices of the ν_{16} secular resonance (dashed lines), the instability border (IB), and four secondary resonances (dotted-dashed lines marked $s_{k/1}$). The white and black dots represent the real Zhongguos and Griquas, respectively.

typical residence times in this stripe are of the order of 1 Myr or even smaller. It is worth recalling that the residence times in Fig. 6 were computed while $I_p \leq 10°$. Then, they are also likely to represent the time necessary to excite the proper inclinations beyond 10°.

The above results put strong constrains to the possible origin of the resonant population in the Hecuba gap. On one hand, it is clear that the mechanisms of injection analyzed in Sect. 2.1 can help to resupply the population of unstable asteroids in the 2:1 resonance. Their rather high inclinations and short lifetimes are in good agreement with the expected behavior of particles injected into the 2:1 resonance, either by crossing the separatrix or the region of secondary resonances. It is worth noting that inclinations will always be highly excited for particles in the region of secondary resonances. However, inclinations not always become excited when the particles are injected in the region of secular resonances. This is because in that region the diffusion in e_p is much faster than in I_p, then particles can be fastly driven to Jupiter crossing orbits without having enough time to get their inclinations excited. A typical case is shown in Fig. 7, and such mechanism could explain why we presently observe several resonant asteroids having rather low inclinations but very short lifetimes (as the case of (5201) Ferraz-Mello, see Table 1 of RNF-I).

On the other hand, the origin of the Zhongguos cannot be supported under a scenario of "smooth" injection. If we assume that these objects arrived to their present location from outside the 2:1 resonance (for example from Themis family), they had to be able to cross a region of about 0.03 AU in a or 0.05 in e in a time-scale not larger than a couple of Myr (in the most optimistic case), in order to retain their presently observed low inclinations ($I_p \leq 5°$). This is the most important dynamical constrain to the origin of the Zhongguos (the other important constrain is observational, and refers to their size distribution, see RNF-I). The remaining of this paper will be dedicated to analyze some possible mechanisms that could account for the necessary drift to inject the Zhongguos in their present location.

2.3. Yarkovsky orbital drift and mutual scattering

As we already mentioned in Sect. 2.1, non conservative forces and perturbations other than purely planetary ones, could play a non negligible role in the origin of resonant asteroids at the Hecuba gap. Non conservative forces, for example, allow the mobility of the semi-major axes and help to interchange material between regions of regular and chaotic motion. In this section we will discuss the possible role of two mechanisms that favor the mobility of a: (i) Yarkovsky effect and (ii) mutual scattering.

Yarkovsky effect (hereinafter YE) arises from the thermal recoil of a rotating body, which receives the solar radiation from a given direction and re-emits part of it to a different one. There are two variants of the effect: the diurnal, related to the rotation period, and the seasonal, related to the orbital period. The former behaves as a dissipative or anti-dissipative force, depending on the sense of rotation (retrograde or prograde), while the latter is always dissipative (Rubincam, 1995).

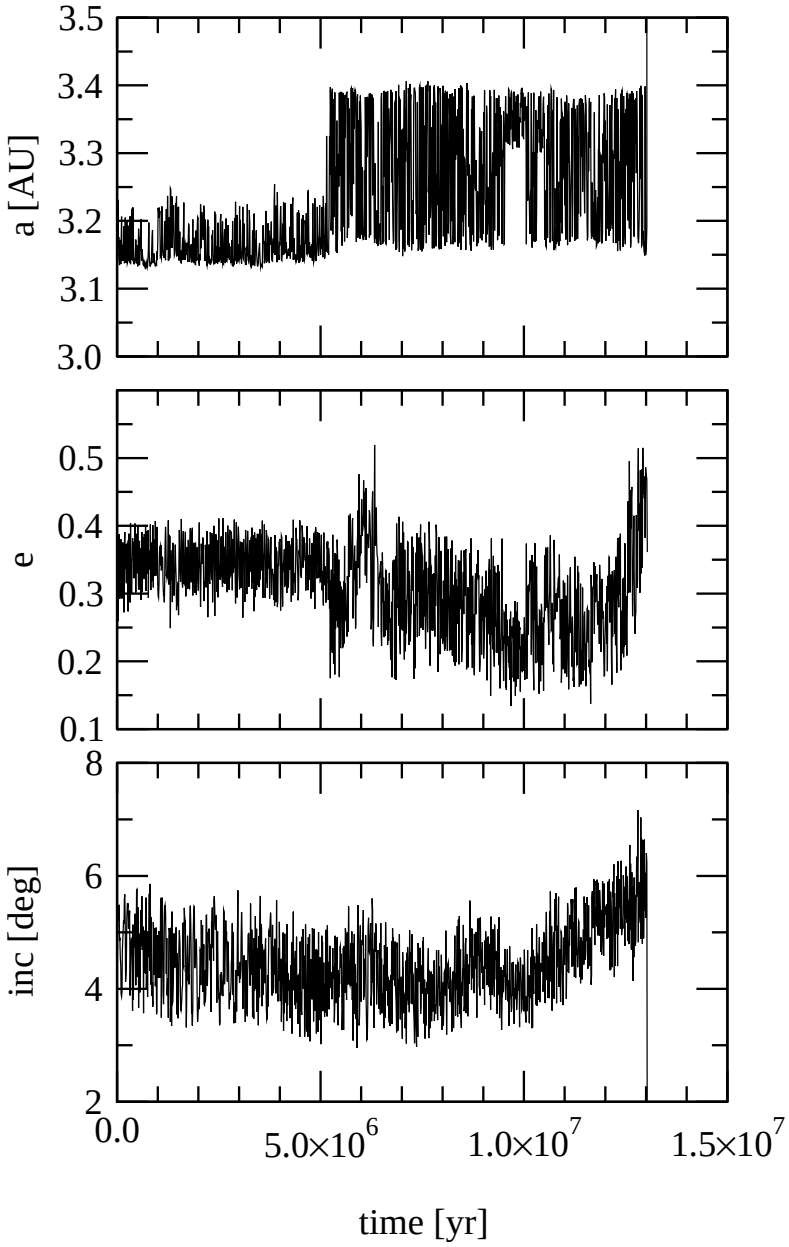

Fig. 7.— Evolution of the osculating elements for a short-lived test particle injected in the 2:1 resonance. The particle was initially at $e = 0.4$. Note that e is largely excited, but the excitation of I is much slower, and the particle escaped while still having a low inclination.

Both effects cause a net drift in proper a which is inversely proportional to the size of the body. In Sect. 3.2 of RNF-I, we have already described simulations with Yarkovsky effect, so we refer the reader to that paper for more details.

To analyze the actual importance of this effect in enhancing the diffusion at the left side of the Hecuba gap, and in favoring the injection of asteroids into the 2:1 resonance, we performed the following simulation. We took 50 initial conditions from Set #1 in the range $0.15 \leq e \leq 0.30$, and integrated them again, this time adding YE to the simulation. We used a version of the Swift integrator that we adapted for this purpose. The YE accelerations were modeled according to Vokrouhlický et al. (2000). The parameters of the model were typical of regolith-covered bodies, with a very low surface conductivity, in order to have a dominant diurnal effect (refer to RNF-I for the precise values of these parameters). We assumed a diameter of 6 km for all the particles, and randomly-oriented prograde spin axes to obtain a net anti-dissipative force. The simulation spanned 100 Myr with a time step of 0.05 yr. We computed proper elements as usual (averages over 10 Myr, with 0.1 Myr sampling), and estimated the diffusion parameters $\sigma_a, \sigma_e, \sigma_I$ and $\beta_a, \beta_e, \beta_I$ as explained in Sect. 2.1 (see also RNF-I). In this case, the parameter β_a has a quite special meaning, because it gives the effective average drift rate induced by YE.

Figure 8 presents the results of this simulation. The abscissas of each plot are the diffusion parameters for each particle in the simulation without YE, while the ordinates are the same parameters in the simulation with YE. In all panels we can appreciate a tendency to larger values of the parameters in the simulation with YE. This is remarkable in the case of proper a, as expected, but is also observed in the case of e_p and (although less evident) in the case of I_p also. We recall that YE by itself should not cause any significant drift of the eccentricities and inclinations. The larger values of diffusion in e_p, I_p observed in the middle and bottom panels of Fig. 8 are rather due to the interaction between YE and the weak MMRs. More precisely, an object near a MMR can be pushed by YE until it reaches the MMR; then it can be driven to enter it or to jump over it. In any case, this causes and excitation of their otherwise stable e_p and I_p. It is worth noting that the inverse process, that is, to extract a body from a MMR with YE, is not so straightforward. In fact, once an object becomes capture in a MMR, it is rather difficult that YE can draw it out. This can be better understood if we recall that non conservative systems tends to configurations of minimum energy, and the MMRs themselves are basins of energy. The interaction between YE and weak MMRs is still not well understood. Unfortunately, the construction of analytical models is quite complex in this case, and the classical models for low order MMRs (see Gomes, 1995, 1997a, and references therein) are not directly applicable.

On the other hand, these classical models are helpful to understand the interaction between YE and the 2:1 resonance, at least in a first approach. We recall that inside the 2:1 resonance, the "natural" effect of any anti-dissipative force will be to excite the eccentricities while keeping constant the amplitude of libration. In other words, consider an ideal 2:1 resonance, with no secular or secondary resonances inside it, and consider a particle approaching to its left border pushed by YE. Then, once the particle enter the resonance, its eccentricity will be excited to higher values and

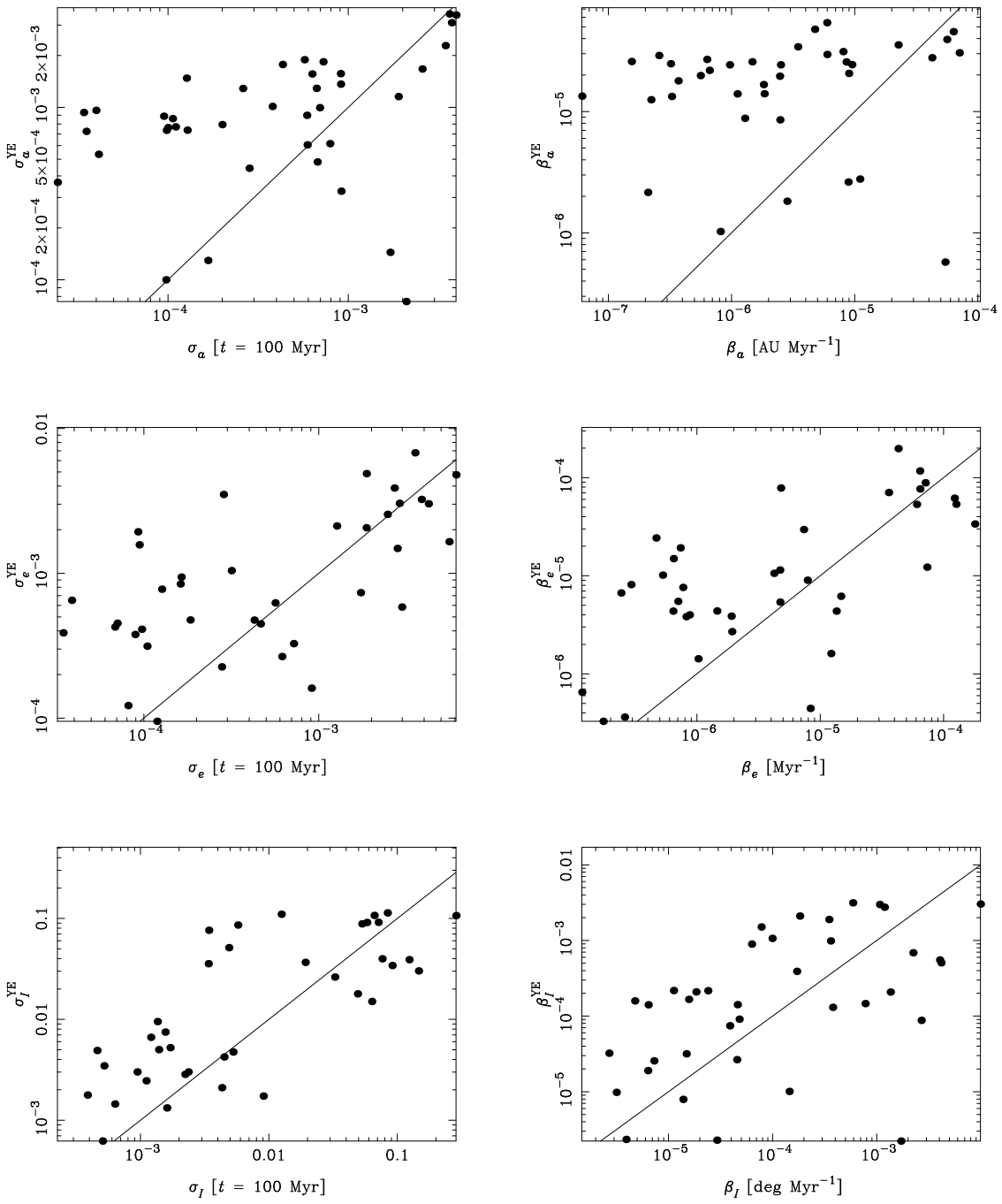

Fig. 8.— Diffusion parameters σ_E and β_E for each proper element E in the simulation without YE (in the abscissas), and comparison with the same quantities in the simulation with YE (in the ordinates). Each dot corresponds to one particle in the simulations. Only particles that survived over 100 Myr in both simulations are shown. The full lines correspond to the identity function.

its amplitude of libration will behave as an adiabatic invariant. This mechanism can make a nearby non resonant asteroid at $e \sim 0.15$ (e.g. a Themis family member), to become a Zhongguo-like asteroid with $e \sim 0.25$. But in the real 2:1 resonance, this implies to cross the region of secondary resonances, where the asteroid will not avoid to excite its inclination, unless it cross sufficiently fast. How fast? The rate of change in a_p which is necessary to achieve a given change in e_p can be easily estimated from Lagrange equations in the averaged circular planar restricted 3-body problem near the 2:1 resonance (see Greenberg and Franklin, 1976). It is given by:

$$\left\langle \frac{da}{dt} \right\rangle = 2 \langle a \rangle \langle e \rangle \left\langle \frac{de}{dt} \right\rangle , \tag{2}$$

where $\langle \ldots \rangle$ stands for the average, and we can consider $\langle a \rangle \equiv a_p$ and $\langle e \rangle \equiv e_p$. Now, according to the results of Sect. 2.2, the particle would need a drift $de_p/dt \sim 0.02$ Myr^{-1} in order to cross the region of secondary resonances without having its inclination excited, which implies $da_p/dt \sim 0.02$ AU Myr^{-1}. From Fig. 8 (top-right panel), it is easy to estimate that the average rate of drift in a_p provided by YE for 6 km bodies at the left side of the Hecuba gap is between $8 \times 10^{-6} \leq \beta_a \leq 5 \times 10^{-5}$ AU Myr^{-1}. This represents about 0.02 AU per Byr, in good agreement with the estimates of Farinella and Vokrouhlický (1999) for regolith bodies. Such rate is enough to keep objects moving around in a_p during the age of the Solar System. But on the other hand, it is too slow to allow a particle to safely cross the region of secondary and/or secular resonances inside the 2:1 resonance, without highly exciting its e_p and I_p. In other words, to inject the observed Zhongguos in their present location, we would require to move objects larger than 6 km at a rate of about 2/100 AU per Myr, which is four orders of magnitude larger than that provided by YE.

In order to confirm these estimates, we took some particles from our simulation, starting very close to the 2:1 resonance border, and extended their integration up to 300 Myr. In Fig. 9, we show the evolution of a_p (averages over 1 Myr, with 0.1 Myr sampling) for three different values of proper eccentricity. After 100 Myr several particles became injected in the 2:1 resonance, but their lifetimes after the injection is not larger than some 10 Myr. In all cases, the injected particles had their proper inclinations excited to values larger than 20° in a few Myr, as expected. Our conclusion is that it would be highly improbable that YE helps to inject the Zhongguos in the 2:1 resonance. However, we want to stress that our simulations were limited, both by the small number of test particles and by the chosen values for the YE parameters, and we believe that more detailed studies would be necessary to draw any definitive conclusion.

The case of mutual scattering is not so different from YE. Mutual scattering arise from the gravitational perturbation of small asteroids between them or by the largest asteroids in the main belt. Recently, it has been proposed by Carruba et al. (2000) that mutual scattering could contribute to the semi-major axis mobility of main belt asteroids. Preliminary studies by these authors show that only the largest asteroids (Ceres, Pallas and Vesta) seem to have a dominant scattering effect throughout the main belt, although this effect would not be large. According to Monte Carlo simulations (Bottke, personal communication), the average dispersion in proper a induced in a typical Themis family member by close encounters with Ceres should be about 1/100 AU per Byr

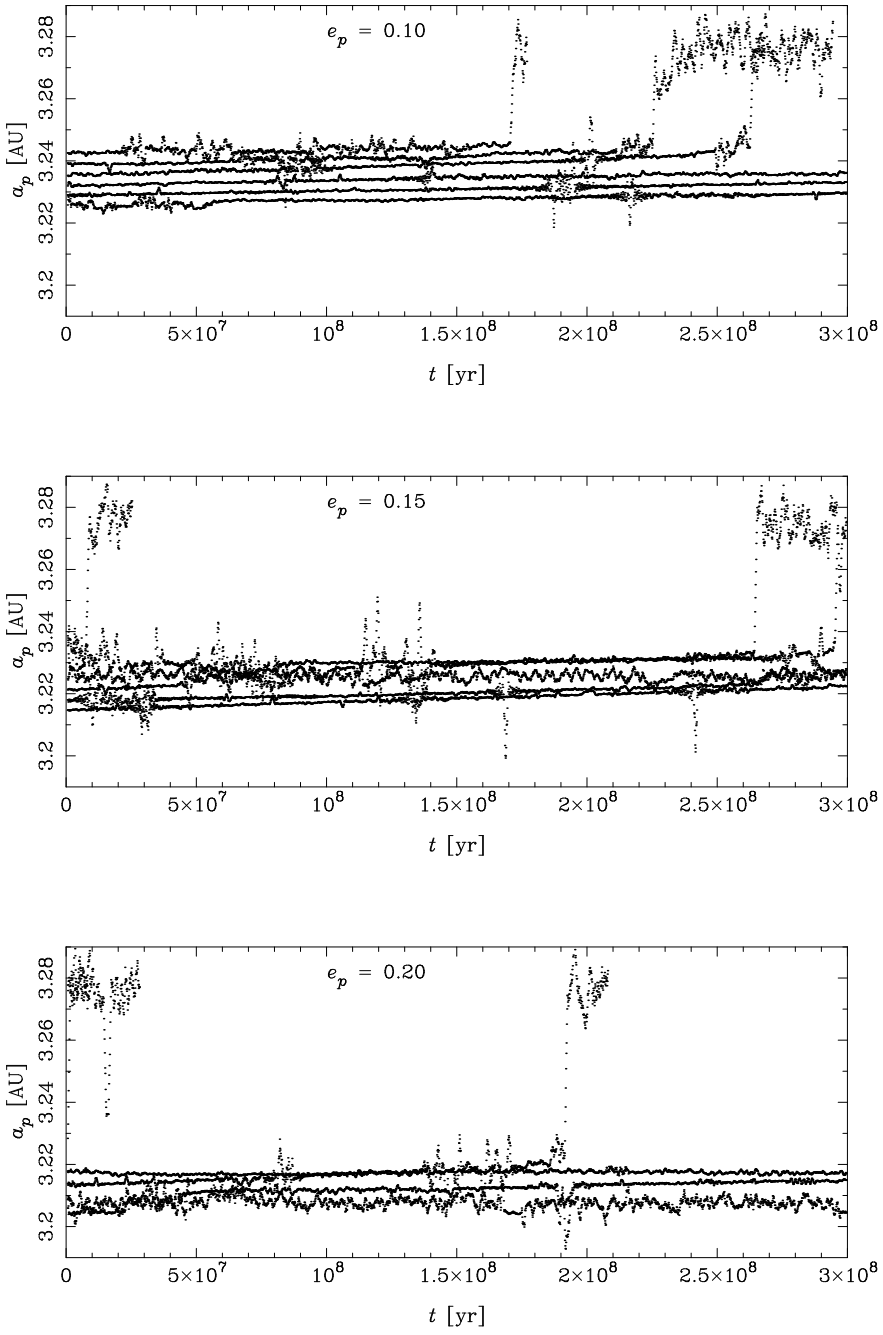

Fig. 9.— The evolution of proper a (averages over 1 Myr) for test particles near the border of the 2:1 resonance under the effect of Yarkovsky forces. All particles have 6 km in diameter and prograde rotation. Their proper eccentricities are indicated in each panel. Some particles are effectively injected in the 2:1 resonance, but they do not survive there for more than some 10 Myr. All the particles injected had their inclinations excited up to 20° or more.

(or maybe less, since Monte Carlo codes tend to overestimate these quantities). This rate of diffusion is even smaller than that of YE, and according to the above considerations we can conclude that mutual scattering is mostly irrelevant to the process of injection of resonant asteroids in the Hecuba gap.

3. Resonant capture due to planetary migration

We will discuss in this section another mechanism to "inject" asteroids in the 2:1 resonance, that is, the capture due to migration of the resonance. It is widely accepted now that the major planets did migrate (changed their semi-major axes) during a certain period of their history (Fernández and Ip, 1984, 1996). This migration arose from the exchange of energy and momentum between the Jovian planets and the swarm of planetesimals that remained in the region beyond 10 AU immediately after the formation of these planets. The planetesimals were scattered by close encounters with all four major planets, but the scattering by Jupiter was much more efficient than that of Saturn, Uranus and Neptune. This caused a net loss of planetesimals, which were presumably ejected to the Oort cloud, and the corresponding energy balance was transferred to the drift in the planetary semi-major axes. Under this scenario, Jupiter migrated inwards, from about 5.4 AU to its present 5.2 AU, while the other planets migrated outwards by some 0.8 AU (Saturn), 3.0 AU (Uranus) and 7.0 AU (Neptune) up to their present positions. It is still under discussion when did this migration take place, but in any case, it should be dated more than 3.8 Byr ago (Levison et al., 2001), and it should have had important consequences in the dynamics of the whole Solar System. One of these consequences was the migration of the MMRs. As the semi-major axis of the planet drifted, it pulled the MMRs and these latter swept the regions where they passed by. When a sweeping MMR reaches an object, it can be either captured in the resonance, or it can jump over the resonance, depending on the type of resonance (inner or outer), the order of the resonance, and the sense of the sweeping.

If we assume the above estimates to be correct, then the 2:1 resonance should have been migrated inwards from 3.40 AU to 3.28 AU, sweeping a region larger than half its width. During this process, we should expect that several asteroids with low eccentricity became captured in the resonance. In fact, the migration of the 2:1 resonance inwards behaves almost in the same way as the application of an anti-dissipative force on the asteroids. For $e < 0.2$ the 2:1 resonance is "open" on the left side (there is no separatrix), and during the sweeping inwards it would pick up asteroids virtually like a "shovel". According to the theory, the captured asteroids would evolve exciting their eccentricities monotonically, while their amplitudes of libration are kept almost constant (adiabatic invariant). The relation between the values of the asteroid's orbital elements before and after the capture, is given approximately by the conservation of the canonical momentum N (Eq. 1). This relation can be used to estimate the final eccentricities of the captured population as a function of the total shift of the resonance in a.

The sweeping of MMRs is believed to have been responsible for the resonant capture of some

groups of minor bodies, like the group of Hilda at the 3:2 resonance with Jupiter (Liou and Malhotra, 1997), and Plutinos at the 2:3 resonance with Neptune (Malhotra, 1995; Gomes, 2000). In the case of the 2:1 resonance, we can guess that a large population of asteroids was indeed captured during the planetary migration, but it was not able to survive until our days due to the global stochasticity of the resonant phase space (Ferraz-Mello et al, 1998b). The question is: could the Zhongguos be the lucky survivors of such presumably captured population of asteroids?

According to their typical dynamical lifetimes (see RNF-I), they could. Unfortunately, this is not enough evidence to conclude that they are. In fact, the resonant capture due to planetary migration is a mechanism much more complex than the simplified view given above. It involves several dynamical processes, like sweeping of secular resonances and planetary inequalities, that would have helped to strongly destabilize the asteroids' orbits. For example, outside the 2:1 resonance, the sweeping of the secular resonance ν_6 was responsible for a huge excitation of the asteroids' e, I throughout the main belt (Gomes, 1997b). Inside the Hecuba gap, slight changes in the value of the Great Inequality (5:2 commensurability) between Jupiter and Saturn were able to largely increase the chaotic diffusion (Ferraz-Mello et al., 1998a). Also, in order to become captured at $e \sim 0.3$, the asteroids needed to pass through the region of secondary resonances at $e \sim 0.15$, with the consequent constrain to their lifetimes (Sect. 2.2). Moreover, we should expect that a non negligible amount of the planetesimals scattered during the migration were thrown towards the inner Solar System (Levison et al., 2001), and contributed to largely perturb the asteroids and to increase the collisions throughout the main belt. In other words, if the origin of the Zhongguos is related to the planetary migration, then they probably needed to pass by several hard tests before being able to remain trapped in a quite small region of the phase space where they could evolve in peace until our days.

To better discuss the viability for capturing the Zhongguos through migration of the resonance, we simulated the evolution of a swarm of 200 test particles under the effect of planetary migration. For each particle, the initial semi-major axis was chosen at random in the interval $3.15 \leq a \leq 3.46$ AU, which was more or less the interval swept by this resonance if Jupiter migrated by 0.2 AU. The initial e, I were also chosen at random, dividing the swarm into two populations of 100 initial conditions each: (i) a "cold" population in the intervals $0 \leq e \leq 0.1$ and $0 \leq I \leq 2.5^\circ$, and a "hot" population, with $0.1 < e \leq 0.2$ and $2.5^\circ < I \leq 5^\circ$. In both cases the remaining initial angles were also chosen at random between $0, 360^\circ$. The total migration time was set to 20 Myr, but the simulation was continued for 2 Myr more after the migration ceased. The migration was included in the model by adding to the planets' accelerations an artificial non conservative term, $\overrightarrow{A}_{\rm nc}$, given by:

$$\overrightarrow{A}_{\rm nc} = \sqrt{GM} C_{\rm nc}\, e^{-(t-t_0)/\tau}\, \frac{\overrightarrow{V}}{|V|} \qquad (3)$$

where G is the gravitational constant, M the solar mass, $\overrightarrow{V}$ the velocity of the planet, t the time, t_0 refers to the time at the beginning of the migration (for our purposes will be $t_0 = 0$), τ is the

characteristic time-scale of the migration (do not confuse with the total migration time), and

$$C_{\rm nc} = \frac{1}{\tau}\left(\frac{1}{\sqrt{a_i}} - \frac{1}{\sqrt{a_f}}\right) \tag{4}$$

is a constant that depends on the initial and final values of the planet's semi-major axis, a_i, a_f (see Malhotra, 1995). We used a modified version of the Swift integrator that we adapted for this purpose[3].

Equation (3) provides an exponential variation of a that converges asymptotically to a_f. For our simulation, we choose a_f equal to the present mean semi-major axes (Bretagnon, 1982), and $a_i = 5.4$ AU for Jupiter, 8.7 for Saturn, 16.3 for Uranus, and 23.2 for Neptune. These values made Jupiter and Saturn migrate in such a way that they started near the mutual 2:1 commensurability and ended near the mutual 5:2 commensurability, but without entering or crossing them (however, they did cross the 7:3 and 9:4 commensurabilities). The characteristic time-scale τ is a critical parameter, because it determines the actual speed of the migration: 63% of the migration happens in that time-scale. In our case it was set to $\tau = 2$ Myr, according to typical values found in the literature. However, recent studies indicate that this time-scale could be up to 10 times larger (Hahn and Malhotra, 1999). Another critical problem concerns the setup of the initial position and velocity of the planets. In our case, we applied a strategy already used by several authors, consisting in integrate the four major planets backwards, starting in their present positions and applying the non conservative forces in the opposite sense[4]. The "final" conditions so obtained could be used as "initial" conditions of the migration, but unfortunately the integrations are not reversible. This is easy to understand if we think that the planets cross several mutual resonances along its migration paths. While in the backwards integration the planets could be able to jump over such mutual resonances, in the forward integration they could be able to be captured in some mutual resonance (and vice-versa). The probability of capture is somehow related to characteristic time-scale τ: the longer the latter, the larger the former. Then, after obtaining our "initial" conditions with the backward integration, we had to perform a series of forward simulations, making a fine tuning of the constants $C_{\rm nc}$ until we arrived to a configuration where the values of the planetary mean semi-major axes were compatible with the present ones.

The results of our simulation with test particles and migrating planets are summarized in Fig. 10. We indicate there the position of the particles in the space of proper elements a_p, e_p and a_p, I_p, for three different times along the simulation. The proper elements were defined as the minimum of a and the maxima of e, I over 1 Myr, with 0.1 Myr sampling. We also indicate the approximate location of the resonance and the separatrices in the a, e plane.

---

[3]Note that this acceleration depends on the velocity, so the leap-frog propagation scheme used by Swift is no longer symplectic. Although this approach has been widely used by many authors, its main disadvantage is that the algorithm slows its efficiency because the accelerations need to be computed twice per time step.

[4]In practice this was accomplished just by setting $t_0 = -20$ Myr and integrating from $t = 0$ to $t = -20$ Myr.

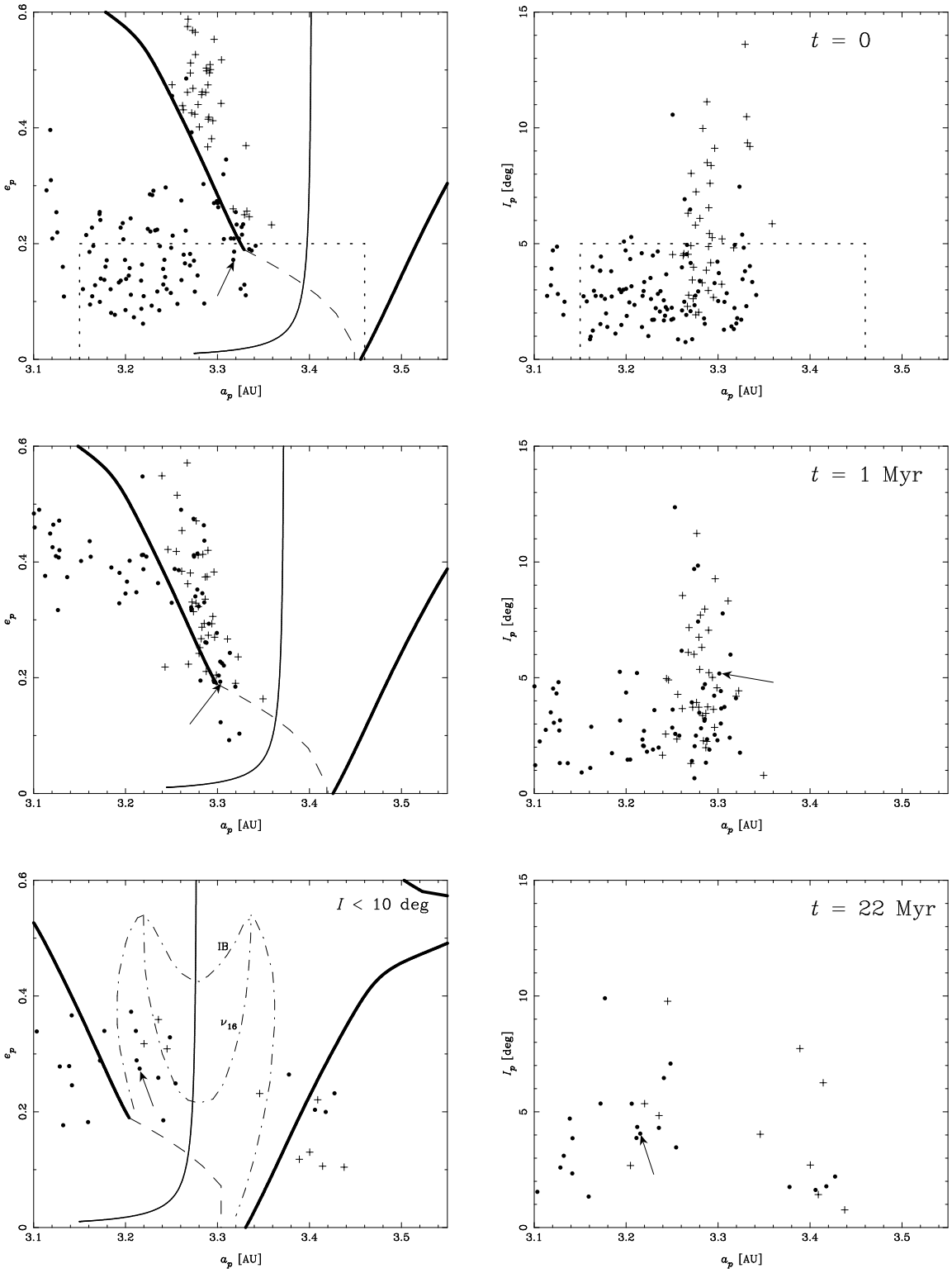

Fig. 10.—

Fig. 10.— Three stages in the simulation of test particles including planetary migration. Top panels: proper elements at the beginning of the simulation; middle panels: status after 1 Myr of migration; bottom panels: final proper elements, 2 Myr after the migration ceased. Proper elements are defined as minimum of a and maxima of e, I over 1 Myr, with 0.1 Myr sampling. Crosses are particles that started the simulation inside the 2:1 resonance, and dots are particles that started outside. The dotted rectangle in the top panels indicates the approximate distribution of the osculating initial conditions of the simulation. In the leftmost panels we indicate the approximate location of the center (full thin line) and the separatrices of the resonance (bold lines). The dashed line indicates the approximate limit between the region of libration and alternation/circulation of σ. In the bottom-left panel, we also plot the location of the ν_{16} resonance and the instability border (IB). Only particles with $I_p < 10^\circ$ are shown in the bottom panels. Finally, the arrow indicates the particle shown in Fig. 11

.

The first two panels show the state of the system at the beginning of the simulation ($t = 0$). Crosses represent particles that are already inside the 2:1 resonance (97 particles), while dots are particles that started the simulation outside the resonance (103 particles). To identify the resonant particles, we integrated the initial conditions of planets and particles over 1 Myr without including migration, and looked at the behavior of the angle σ. This simulation also provided the initial set of proper elements at $t = 0$.

The remaining panels in Fig. 10 show the state of the system after 1 Myr of migration and at the end of the simulation (22 Myr; recall that we ceased the migration at 20 Myr). The last two panels only show those particles that ended with a proper inclination smaller than 10°. Several features can be appreciated in these plots. At $t = 1$ Myr, the particles located at the left side of the resonance have suffered a large excitation of their proper eccentricities (their average e is between 0.2-0.3). This kind of behavior has been already identified by Gomes (1997b) and Levison et al (2001), and was attributed to the sweeping of secular resonances. In our simulation only the eccentricities were excited, while the inclinations remained small. This is most probably related to the sweeping of some strong secular resonance of the perihelion, maybe ν_6. We can also see that, at $t = 1$ Myr, a large part of this e-excited population is entering the 2:1 resonance, jumping through the separatrix. Most of these captured particles remained near the separatrix and did not survive too much inside the resonance, being fastly driven to Jupiter crossing orbits. On the other hand, some particles at the left side of the resonance did not have their eccentricities excited, and became to approach the resonance at $e_p < 0.2$. This is the case of the particle indicate by an arrow in Fig. 10. At $t = 22$ Myr this particle has already entered the resonance and remained in the region of the Zhongguos, with a final proper I less than 5°. The actual behavior of this "baby Zhongguo" during the migration is shown in Fig. 11. We can appreciate there the exact moment when it entered the resonance, between $t = 0.7$ and 1 Myr. After entering the resonance, it took less than 5 Myr to arrive to its final location. Since it ended in the most stable region of the 2:1 resonance, we can

expect that this particle will be able to survive there over the age of the Solar System.

Back to Fig. 10, some other particles were also captured in the resonance at the end of the simulation, keeping their low initial inclinations. From the initial 103 particles starting the simulation outside the resonance (dots), 16% ended captured at $t = 22$, and only 8% did it with $I_p < 10°$. However, the proportion of "cold" and "hot" particles in these statistics is different: 16% of the cold population was captured against 14% of the hot population. But 9% of the hot particles ended captured with $I_p < 10°$, against 6% of the cold ones. This difference could be related to the eventual interaction with secondary resonances during the capture process. From the preservation of the invariant N (Eq. 1), it is easy to show that cold particles take more time to excite their eccentricities during the capture, having more time to interact with the web of secondary resonances. It is true that the secondary resonances themselves will move during the migration, but their net shift should not be large. In fact, the 2:1 resonance itself dictates the proper rate of motion of the asteroids' perihelia inside it, and this rate is less changed by the migration.

Concerning the 97 particles starting the simulation inside the resonance (crosses), only a few amount (4%) were still there after 22 Myr. Some of them also survived at the right side of the resonance, like having been left by the resonance during its migration leftwards.

Our results concerning the capture of Zhongguo-type objects due to migration provide the first evidence of a mechanism able to inject such objects inside the 2:1 resonance. However, as we already mentioned, resonant capture due to migration involves many different dynamical processes that interact between them in a complex way. Our simulation considered a quite small number of test particles, which does not allow to make a good statistical analysis of the results. Moreover, we only tested a very particular model of migration (exponential) with a very particular value of the characteristic time-scale. Would we obtain similar results, for example, if we use a value of τ ten times larger? The answer to this and to other similar questions is beyond the scope of this work, and the problem is still open for future, more detailed, studies. In the next section we will discuss another mechanism to inject objects inside a resonance, related to the breakup of asteroids in the neighborhood of the resonance.

4. Catastrophic injection

It has been proposed (Morbidelli et al., 1995; Moons et al., 1998) that the Zhongguos could be the resonant counterpart of the Themis family. That is, the breakup of Themis near the 2:1 resonance would have probably injected a lot of asteroids inside the resonance, and the Zhongguos would be the remnants of this injected swarm. The basic arguments to support this hypothesis are three: (i) The proper eccentricity of (3789) Zhongguo is very similar to the typical proper eccentricity of the Themis family members, that is $e_p \sim 0.2$. In this case, e_p is understood as the maximum of e. (ii) The distribution of Themis family in proper semi-major axis (i.e., minimum of a) has a cutoff at the separatrix of the 2:1 resonance, but (3789) Zhongguo seem to be at the

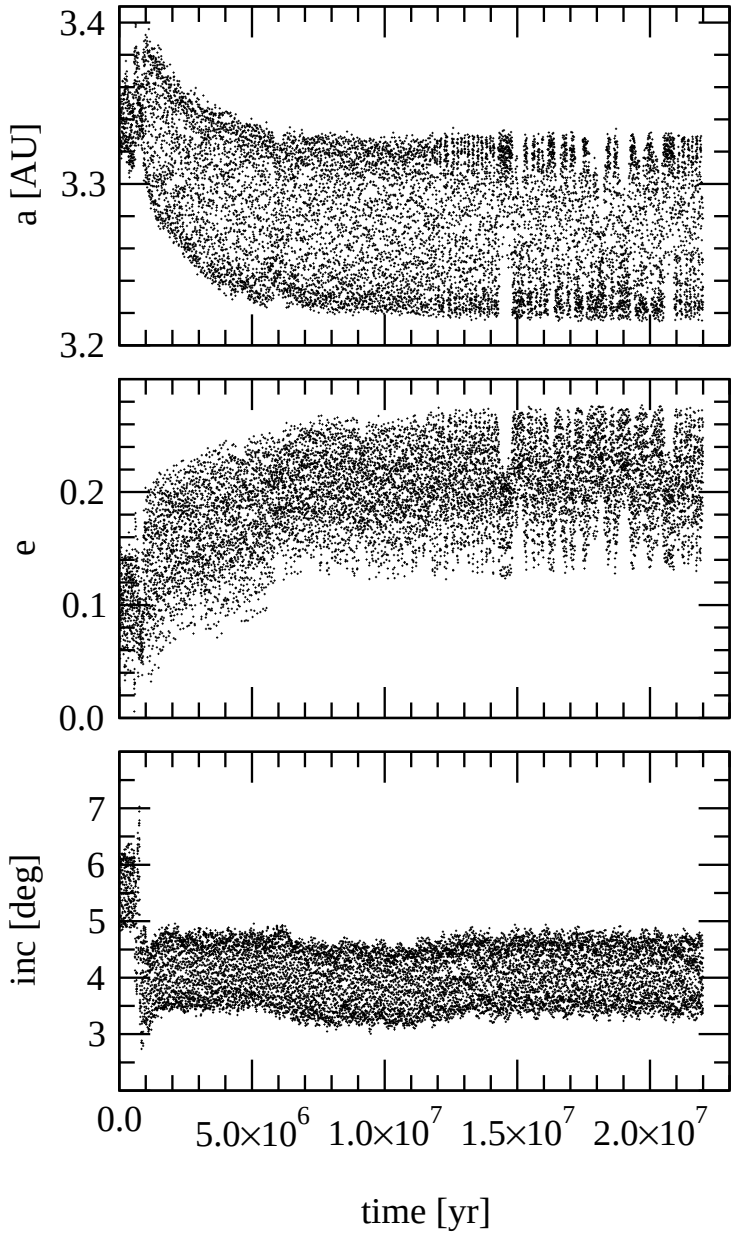

Fig. 11.— The evolution of osculating elements for the particle indicated by an arrow in Fig. 10. The particle ended captured in the region of Zhongguos.

tail of the "natural" prolongation of the distribution inside the resonance. (iii) The Zhongguos are very small objects (less than 15 km) and their collisional lifetimes should be smaller than the age of the Solar System ($\sim 1 - -2$ Byr). Then, it is difficult to assume that they have actually been in the resonance for the last 4.5 Byr. Arguments (i) and (ii) are not very strong indeed, because they require that the breakup occurred at a very particular configuration, when the parent body was at its maximum excursion in eccentricity. Moreover, they are based on the present observed distribution of Themis family members, and they do not take into account that the original distribution (after the breakup) could have been much more compact. In fact, the present distribution can be the result of the dynamical diffusion at the left side of the Hecuba gap (weak MMRs, Yarkovsky, etc.), similar to the case of the Flora family in the inner belt (Nesvorný et al, 2001). On the other hand, argument (iii) is one of the strongest arguments in favor of the catastrophic injection of the Zhongguos. We have already discussed this problem in RNF-I, so we refer the reader to that paper for more details.

In this section, we are going to present some simple simulations aiming to determine under which conditions a breakup of a Themis-like parent body can eject fragments with the necessary velocity to reach the region of Zhongguos inside the 2:1 resonance. For this purpose, we are going to use a very simple model of breakup with isotropic ejection of fragments, as we explain in the following.

The kinetic energy of the fragments after the breakup event can be written as

$$\sum_i \frac{1}{2} m_i v_i^2 = M Q_{\rm D}^* f_{\rm KE} \tag{5}$$

(see Petit and Farinella, 1993) where m_i and v_i are the masses and velocities of the fragments, $M = \sum_i m_i$ is the mass of the parent body, $Q_{\rm D}^*$ is the specific energy of the impact, and $f_{\rm KE}$ is the so-called parameter of *anelasticity*, and represents the fraction of the kinetic energy of the projectile that is transferred to the kinetic energy of the fragments. For a parent body of radius $R_{\rm PB}$ and density $\rho_{\rm PB}$ the specific energy can be estimated as:

$$Q_{\rm D}^* = B\, \rho_p \left(\frac{R_p}{1{\rm cm}} \right)^b \tag{6}$$

where B, b are parameters that depend on the chemical properties of the parent body. According to Benz and Asphaug (1999; see also Love and Ahrens, 1996) typical values for stony bodies are $B = 0.3 - 0.5$ erg cm^3 g^{-2}(we will use 0.4) and $b = 1.36$. The parameter $f_{\rm KE}$ is the most critical one, because it determines the actual dispersion of the fragments after the breakup: the smaller the $f_{\rm KE}$ the more compact the family formed. Unfortunately, this parameter is poorly known. Recent studies using hydrocode models estimate values of $f_{\rm KE}$ between 0.065 to 0.10 for S-type bodies (P. Michel, personal communication), and smaller values (~ 0.01) should be expected for C-type objects (like Themis) since, according to laboratory experiments, they should absorb much more energy.

The first assumption in our model is that the distribution of ejection velocities $N(v_{ej})$ can be

modeled by a Maxwellian, with mean velocity $\overline{v}_{ej}$. given by:

$$\overline{v}_{ej}^2 = \frac{\sum_i m_i v_i^2}{\sum_i m_i} \tag{7}$$

We further assume that the ejection velocity is independent of the mass of the fragments. Although this assumption is consistent with the results of Giblin et al. (1998), there exist evidence of a possible velocity-size relationship between the members of asteroidal families (Cellino et al., 1999). But our model is not aimed to reproduce the actual shape of the observed families, and the above assumption can be considered more than adequate for our purposes. Finally, we also assume that the ejection is isotropic, in agreement with the results of Zappalà et al. (1996) for most asteroidal families. Following Petit and Farinella (1993), we estimate the escape velocity as:

$$v_{esc}^2 = 1.64 G \frac{4}{3} \pi \rho_{\rm PB} R_{\rm PB}^2 \tag{8}$$

where G is the gravitational constant. Only the fragments with $v_{ej} > v_{esc}$ are able to escape, with a relative velocity "at infinity" $v_\infty^2 = v_{ej}^2 - v_{esc}^2$. From $N(v_{ej})$, we obtain the correlated distribution $N(v_\infty)$, and we further assume that it has an upper cutoff at a speed $v_{cut} = 1000$ m s^{-1}. The distribution $N(v_\infty)$ is then decomposed in the distributions tangential to the orbit $N(v_T)$, radial $N(v_R)$, and normal $N(v_W)$. Finally, the orbital elements a, e, I of the fragments relative to the parent body are computed using Gauss equations, while for λ, ϖ, Ω we assume the same values of the parent body. It is worth recalling that, to compute Gauss equations, we need to assume the values of the true anomaly f and the argument of perihelion ω at the moment of the breakup. Following the considerations in Morbidelli et al. (1995), we choose here $f = 90°$ and $f + \omega = 45°$.

Using this model of isotropic ejection, we simulated the formation of synthetic Themis families for different values of the parameter $f_{\rm KE}$. We considered a Themis-like parent body with $\rho_{\rm PB} = 1300$ kg m^{-3} (typical of C-type bodies) and $R_{\rm PB} = 200$ km. This radius was estimated by simply adding the mass of all the presently known members of the family (1850 asteroids, as determined in RNF-I), but it is also in good agreement with the estimates of Tanga et al. (1999). The orbital elements of the parent body were taken from a numerical integration of Themis itself: $a = 3.124$ AU, $e = 0.203$, $I = 1.13°$, $\sigma \simeq 0$, $\varpi - \varpi_{\rm J} \simeq 0$ and $\Omega - \Omega_{\rm J} \simeq 0$. With these values, the parent body is at a maximum of eccentricity at the moment of the breakup. The advantage of this choice is twofold: (i) it puts the parent body in its nearest approach to the 2:1 resonance border (Morbidelli et al., 1995); (ii) the resulting osculating elements a, e, I of the fragments, obtained from Gauss equations, are equivalent to their resonant proper elements a_p, e_p, I_p (recall that all fragments will have $\sigma \simeq 0$, $\varpi \simeq \varpi_{\rm J}$ and $\Omega \simeq \Omega_{\rm J}$).

In Fig.12, the shaded histogram represents the distribution in proper a of a synthetic Themis family (2000 fragments) generated with $f_{\rm KE} = 0.01$. The outlined histogram is the actual distribution of Themis family, and the small histogram at the lower-right edge corresponds to the observed Zhongguos (see Table 3 on RNF-I). As expected, the distribution of Themis family shows a sudden cutoff at the border of the 2:1 resonance (Sx). If we extrapolate this distribution inside the resonance, the Zhongguos appear to effectively lie in the tail the distribution. On the other hand, the

synthetic family shows a very narrow distribution, and the fragments were not able to reach the border of the 2:1 resonance. The difference between the synthetic and the real family is notorious, If we assume that our model of fragmentation is essentially correct, then the rather flat distribution of the real family can be related to: (i) an already flat initial distribution after the breakup, or (ii) the subsequent dynamical dispersion of the family due to weak MMRs, Yarkovsky, etc. The former option is quite improbable, because to obtain such initial flat distribution we should consider values of $f_{\rm KE} \sim 1$ or larger. Then, we believe that the second option is the actual responsible of the presently observed distribution.

On the other hand, it is worth noting that we do not need to consider very high values of $f_{\rm KE}$ to inject asteroids in the resonance. In fact, with values as small as 0.03 some fragments are already able to reach the resonance border. The actual implications of this mechanism in the origin of the Zhongguos can be better appreciated in Fig. 13. We plot there the distribution in the space of proper elements of the ejected fragments (black dots) from three simulations, using $f_{\rm KE} = 0.01$, 0.05 and 0.10, respectively. The top panels correspond to the same simulation shown in Fig. 12. The grey dots are the actual Themis family, and the open circles are the Zhongguos. The circle indicated by an arrow is Zhongguo itself. This asteroid, together with the small cluster of 1975 SX (see Fig. 7 of RNF-I), seem to be the natural extension of Themis family inside the resonance, as Morbidelli et al. (1995) already pointed out. However, the cluster of resonant asteroids that really matters is that of 1994 UD1, located at $e_p \sim 0.27$. As we showed in RNF-I, this cluster lies in the most stable region of the 2:1 resonance, and concentrates almost 70% of the stable population. According to Fig. 13, this cluster is far from the region where the possible Themis outcomes would be eventually injected, and its origin seems unlikely to be related to the breakup of Themis. However, we cannot totally rule out this possibility because there could exist some unknown dynamical mechanism inside the 2:1 resonance able to transport the injected fragments to the region of 1994 UD1. Moreover, if we consider a very energetic impact, (bottom panels of Fig. 13), some fragments can reach the resonant space at the right side of the resonance center. Due to the symmetry of the resonant motion along the lines of $N = \text{const.}$ (Eq. 1), these fragments will be actually in the region of 1994 UD1 at the left side of the resonance center. Notwithstanding, we must recall that the value $f_{\rm KE} = 0.1$ is very much larger than that we should expect in the breakup of a typical C-type body. Then, we believe that the scenario shown in the bottom panels of Fig. 13 would never hold at all.

5. Conclusions

In this paper we have analyzed different hypothesis for the origin of the asteroids in the 2:1 resonance with Jupiter (Hecuba gap). All these hypothesis are related to the idea of the injection of asteroids in the 2:1 resonance from the neighbouring regions. We have concentrated our attention on the left side of the Hecuba gap, which accounts for a huge population of asteroids, most of them related to Themis family.

We have discussed three possible mechanisms to inject asteroids in the 2:1 resonance: (i) chaotic

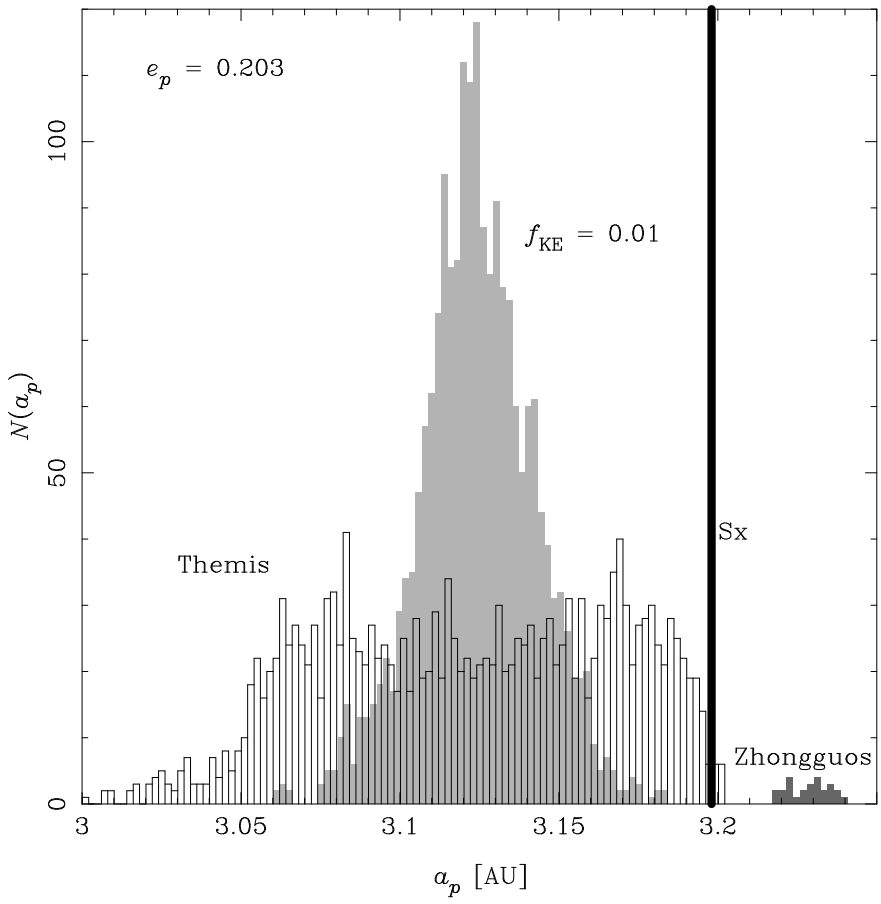

Fig. 12.— The shaded histogram represents the distribution in resonant proper semi-major axis of a synthetic Themis family, with 2000 fragments generated with our model of isotropic ejection using $f_{\rm KE} = 0.01$. The outlined histogram is the actual distribution of 1850 Themis family members. The bold vertical line indicates the location of the separatrix of the 2:1 resonance. The small histogram at the right side of the separatrix corresponds to the 61 known Zhongguos. All the histograms are projected in the plane $e_p = 0.203$.

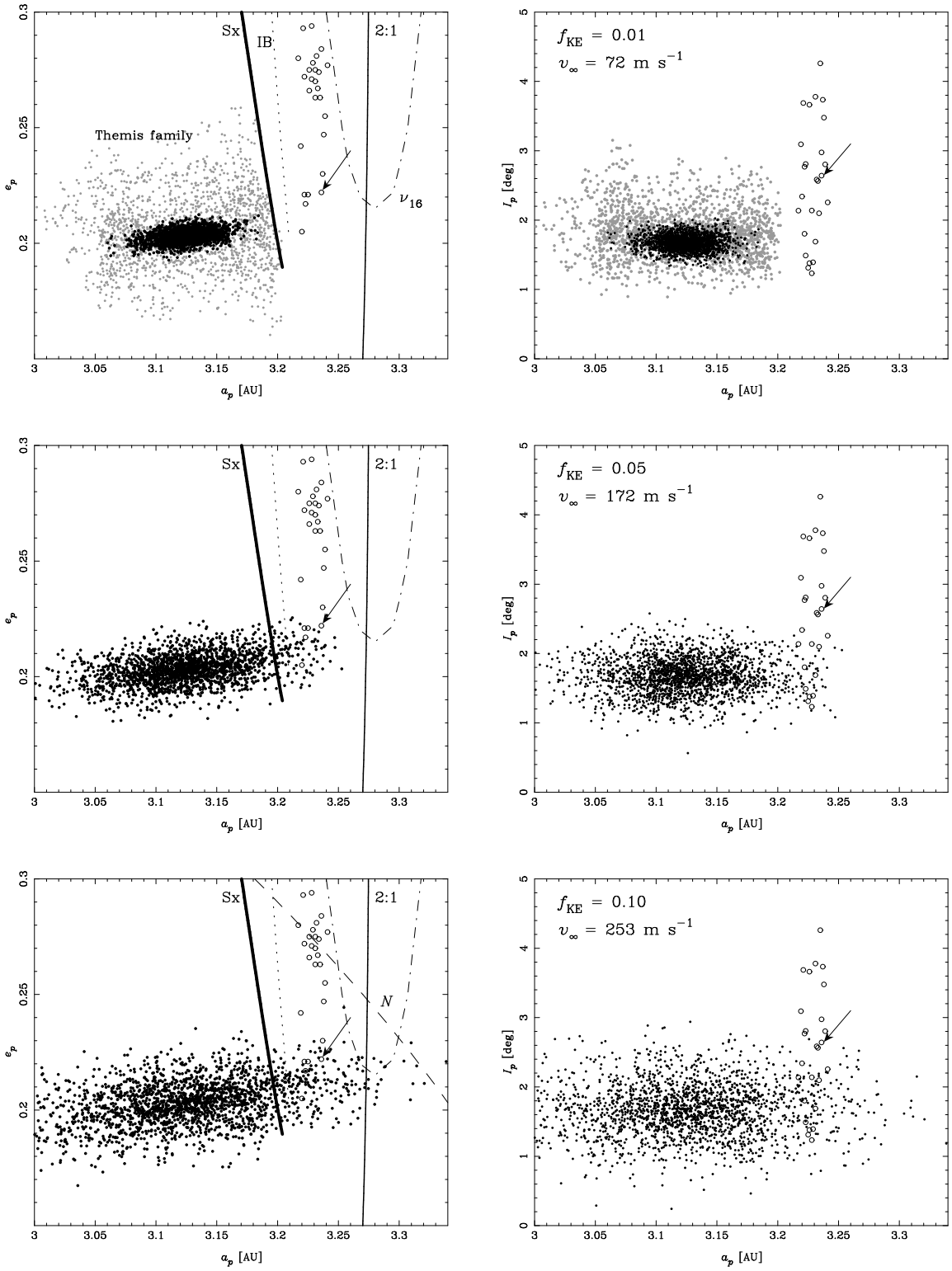
Sx
IB
2:1
Themis family
ν_{16}
f_{KE} = 0.01
v_∞ = 72 m s^{-1}
f_{KE} = 0.05
v_∞ = 172 m s^{-1}
f_{KE} = 0.10
v_∞ = 253 m s^{-1}
N
a_p [AU]
e_p
I_p [deg]

Fig. 13.—

Fig. 13.— Top to bottom: Three different simulations of the breakup of a Themis-like parent body, using different values of $f_{\rm KE}$. The black dots represent the distribution of the fragments in the space of resonant proper a, e (left) and $a.I$ (right).We generated 2000 fragments in each simulation. The average value of v_∞ is indicated in each case. The open circles are the stable resonant asteroids. The asteroid indicated by an arrow is (3789) Zhongguo. The cluster of resonant asteroids at $e_p \sim 0.27$ is the group of 1994 UD1 (see RNF-I). The gray dots in the top panels correspond to the actual Themis family. We also show the location of the resonance center (full thin line), separatrix (bold line), instability border (dotted line marked IB) and ν_{16} resonance (dotted-dashed line). In the lower-left panel, we also plot the curve of $N = \text{const.}$ (dashed line) that passes through the cluster of 1994 UD1. Recall that the motion of the resonant asteroids is symmetric with respect to the center of the resonance along this curve.

diffusion in the neighborhood of the resonance, (ii) capture due to migration of the resonance, and (iii) breakup of a Themis-like asteroid.

We have found that the dynamics at the left neighborhood of the resonance is dominated by several weak mean motion resonances, most of them involving the orbital periods of Jupiter and Saturn simultaneously. Asteroids captured in these resonances have their eccentricities excited and can reach the border of the 2:1 resonance, being then injected. This mechanism proved to be efficient over time scales of some 100 Myr, but only for asteroids that are close to the resonance border. On the other hand, the overlap of weak mean motion resonances at high eccentricities ($e > 0.35$) allows asteroids to randomly walk over large intervals of semi-major axis (~ 0.1 AU). This overlap could help to inject objects in the 2:1 resonance in an even shorter time scale (some 10 Myr).

The particles injected by these mechanisms arrive to the most unstable region of the resonant phase space, and do not survive in the resonance for more than 10 Myr, at most. Then, these mechanisms provides a flux that could help to keep the population of unstable resonant asteroids in a steady state. But it cannot account for the origin of marginally unstable (Griquas) and stable (Zhongguos) populations.

We have also discussed the possible role of Yarkovsky effect and mutual scattering by main belt asteroids in enhancing the flux of injected asteroids. For bodies larger than 5 km, Yarkovsky effect accounts for a net drift in semi-major axis of about 1/200 AU per Byr or less. Then, Yarkovsky effect can contribute to the flux of unstable resonant asteroids, but the provided drift is not enough to inject objects in the most stable places of the resonant phase space. The main constraint is related to the huge excitation of the inclinations occuring when the asteroids cross the resonance border, which is not compatible with the rather low inclinations of the observed Zhongguos. Similar considerations hold for the effects of mutual scattering.

We have investigated the possibility of resonant capture due to migration of the 2:1 resonance. If planetary migration happened during the early history of the Solar System, it caused the decay of Jupiter's semi-major axis by some 0.2 AU, with the consequent drift of the 2:1 resonance inwards.

According to our simulations, this drift could favor the capture of low-eccentricity non resonant asteroids by the 2:1 resonance. We simulated an exponential migration with a charateristic time scale of 2 Myr, and found evidence that such mechanism could create a primordial population of resonant asteroids, with dynamical properties compatible with the observed Zhongguos. However, our results need to be confirmed by more detailed studies, using more reliable models of planetary migration.

Finally, we have discussed the origin of the 2:1 resonant asteroids in the framework of the breakup that originated Themis family. We simulated a fragmentation of a Themis-like parent body using a simple model where the ejection velocity is assumed to be independent of the fragments' masses. We have found that, for small values of the anelasticity parameter $f_{\rm KE}$, typical of C-type bodies, it is not possible to inject fragments into the 2:1 resonance. For larger values, the injection is possible, but the fragments arrive to a region of the resonant phase space which is not compatible with the presently observed distribution of Zhongguos. Although we cannot rule out this mechanism of injection, a relation between the breakup of Themis and the origin of Zhongguos seems unlikely.

F. Roig wish to thank the São Paulo State Science Foundation (FAPESP) for giving financial support to this work through PhD scholarship 97/5806-9. The Department of Space Studies of the Southwest Research Institute at Boulder, Colorado, is highly acknowledge for hosting the four month visit of F. Roig during the final stages of this work. Fruitful discussions with W. Bottke, A. Morbidelli and R. Gomes helped to improve the contents of this paper, and are highly appreciated.

REFERENCES

Benz, W., and Asphaug, E.: 1999. Catastrophic disruptions revisited. *Icarus* **142**, 5–20.

Bretagnon, P.: 1982. Théorie du mouvements de l'ensemble des planètes, Solution VSOP82. *Astron. Astrophys.* **114**, 278–288.

Carruba, V., Burns, J., Bottke, W., and Morbidelli, A.: 2000. Asteroid mobility due to encounters with Ceres, Vesta, Pallas: Monte Carlo codes *vs.* direct numerical integrations. *DPS Meeting #32*, 14.06

Cellino, A., Michel, P., Tanga, P., Zappalá, V., Paolicchi, P., and Dell'Oro, A.: 1999. The velocity-size relationship for members of asteroid families and implications for the physics of catastrophic collisions. *Icarus* **141**, 79–95.

Farinella, P., and Vokrouhlický, D.: 1999. Semi-major axis mobility of asteroidal fragments. *Sci.* **283**, 1507–1510.

Fernández, J.A., and Ip, W.H.: 1984. Some dynamical aspects of the accretion of Uranus and Neptune. The exchange of orbital angular momentum with planetesimals. *Icarus* **58**, 109–120.

Fernández, J.A., and Ip, W.H.: 1996. Orbital expansion and resonant trapping during the late accretion stages of the outer planets. *Planet. Space Sci.* **44**, 431–439.

Ferraz-Mello, S.: 1994. Dynamics of the asteroidal 2/1 resonance. *Astron. J.* **108**, 2330–2337.

Ferraz-Mello, S., Michtchenko, T.A., and Roig, F.: 1998a. The determinant role of Jupiter's Great Inequality in the depletion of the Hecuba gap. *Astron. J.* **116**, 1491–1500.

Ferraz-Mello, S., Michtchenko, T.A., Nesvorný, D., Roig, F., and Simula, A.: 1998b. The depletion of the Hecuba gap *vs.* the long lasting Hilda group. *Planet. Space Sci.* **46**, 1425–1432.

Giblin, I., Martelli, G., Farinella, P., Paolicchi, P., Di Martino, M., and Smith, P.N.: 1998. The properties of fragments from catastrophic disruption events. *Icarus* **134**, 77–112.

Gomes, R.: 1995. The effect of non-conservative forces on resonance lock: Stability and instability. *Icarus* **115**, 47–59.

Gomes, R.: 1997a. Orbital evolution in resonance lock I. The restricted 3-body problem. *Astron. J.* **114**, 2166–2176.

Gomes, R.: 1997b. Dynamical effects of planetary migration on the primordial asteroid belt. *Astron. J.* **114**, 396–401.

Gomes, R.: 2000. Planetary migration and Plutino orbital inclinations. *Astron. J.* **120**, 2695–2707.

Greenberg, R., and Franklin, F.: 1976. Coupled librations in the motion of asteroids near the 2:1 resonance. *MNRAS* **173**, 1–8.

Hahn, J.M., and Malhotra, R.: 1999. Orbital evolution of planets embedded in a planetesimal disk. *Astron. J.* **117**, 3041–3053.

Henrard, J., Watanabe, N., and Moons, M.: 1995. A bridge between secondary and secular resonances inside the Hecuba gap. *Icarus* **115**, 336–346.

Knežević, Z., and Milani, A.: 2001. Synthetic proper elements for outer main belt asteroids. Submitted to *Cel. Mech. Dyn. Astr.*

Levison, H.F., and Duncan, M.J.: 1994. The long-term dynamical behavior of short-period comets. *Icarus* **108**, 18–36.

Levison, H.F., Dones, L., Chapman, C., Stern, S.A., Duncan, M.J., and Zahnle, K.: 2001. Could the Lunar "Late Heavy Bombardment" have been triggered by the formation of Uranus and Neptune? *Icarus* **151**, 286–306.

Liou, J.C., and Malhotra, R.: 1997. Depletion of the outer asteroid belt. *Science* **275**, 375–377.

Love, S.G., and Ahrens, T.J.: 1996. Catastrophic impacts on gravity dominated asteroids. *Icarus* **124**, 141–155.

Malhotra, R.: 1995. The origin of Pluto's orbit: Implications for the Solar System beyond Neptune. *Astron. J.* **110**, 420–429.

Michtchenko, T.A., and Ferraz-Mello, S.: 1996. Comparative study of the asteroidal motion in the 3:2 and 2:1 resonances with Jupiter II. Three-dimensional model. *Astron. Astrophys.* **310**, 1021–1035.

Michtchenko, T.A., and Ferraz-Mello, S.: 2001. Resonant structure of the outer Solar System in the neighborhood of the planets. *Astron. J.* **122**, 474–481.

Moons, M., Morbidelli, A., and Migliorini, F.: 1998. Dynamical structure of the 2/1 commensurability with Jupiter and the origin of the resonant asteroids. *Icarus* **135**, 458–468.

Morbidelli, A., and Moons, M.: 1993. Secular resonances inside mean motion commensurabilities. The 2/1 and 3/2 cases. *Icarus* **103**, 99–108.

Morbidelli, A., and Nesvorný, D.: 1999. Numerous weak mean motion resonances drive asteroids toward terrestial planets orbits. *Icarus* **139**, 295–308.

Morbidelli, A., Zappalà, V., Moons, M., Cellino, A., and Gonczi, R.: 1995. Asteroid families close to mean motion resonances: Dynamical effects and physical implications. *Icarus* **118**, 132–154.

Nesvorný, D., and Morbidelli, A.: 1998. An analytic model of three-body mean motion resonances. *Cel. Mech. Dyn. Astr.* **71**, 243–271.

Nesvorný, D., Morbidelli, A., Vokrouhlický, D., and Brož, M.: 2001. The Flora family: A case of the dynamically dispersed collisional swarm? Submitted to *Icarus*.

Petit, J.M., and Farinella, P.: 1993. Modeling the outcomes of high-velocity impacts between small solar system bodies. *Cel. Mech. Dyn. Astr.* **57**, 1–28.

Roig, F., Nesvorný, D., and Ferraz-Mello, S.: 2001. The asteroidal population in the Hecuba gap. Part I: Dynamics and size distribution of the resonant asteroids **(RNF-I)**. In preparation.

Rubincam, D.P.: 1995. Asteroid orbit evolution due to thermal drag. *J. Geophys. Res.* **100**, 1585–1594.

Tanga, P., Cellino, A., Michel, P., Zappalá, V., Paolicchi, P., and Dell'Oro, A.: 1999. On the size distribution of asteroid families: The role of geometry. *Icarus* **141**, 65–78.

Vokrouhlický, D., Milani, A., and Chesley, S.: 2000. Yarkovsky effect on small near-Earth asteroids: Mathematical formulation and examples. *Icarus* **148**, 118–138.

Zappalá, V., Cellino, A., Dell'Oro, A., Migliorini, F., and Paolicchi, P.: 1996. Reconstructing the original ejection velocity field of asteroid families. *Icarus* **124**, 156–180.